

AD\_\_\_\_\_

Award Number: DAMD17-01-1-0123

TITLE: Taxol Resistance and Microtubule Dynamics in Breast  
Cancer

PRINCIPAL INVESTIGATOR: George A. Orr, Ph.D.

CONTRACTING ORGANIZATION: Albert Einstein College of Medicine  
Bronx, New York 10461

REPORT DATE: June 2004

TYPE OF REPORT: Final

PREPARED FOR: U.S. Army Medical Research and Materiel Command  
Fort Detrick, Maryland 21702-5012

DISTRIBUTION STATEMENT: Approved for Public Release;  
Distribution Unlimited

The views, opinions and/or findings contained in this report are those of the author(s) and should not be construed as an official Department of the Army position, policy or decision unless so designated by other documentation.

**BEST AVAILABLE COPY**

**20040901 125**

**REPORT DOCUMENTATION PAGE**Form Approved  
OMB No. 074-0188

Public reporting burden for this collection of information is estimated to average 1 hour per response, including the time for reviewing instructions, searching existing data sources, gathering and maintaining the data needed, and completing and reviewing this collection of information. Send comments regarding this burden estimate or any other aspect of this collection of information, including suggestions for reducing this burden to Washington Headquarters Services, Directorate for Information Operations and Reports, 1215 Jefferson Davis Highway, Suite 1204, Arlington, VA 22202-4302, and to the Office of Management and Budget, Paperwork Reduction Project (0704-0188), Washington, DC 20503

<b>1. AGENCY USE ONLY</b> (Leave blank)		<b>2. REPORT DATE</b> June 2004	<b>3. REPORT TYPE AND DATES COVERED</b> Final (15 May 2001 - 14 May 2004)	
<b>4. TITLE AND SUBTITLE</b> Taxol Resistance and Microtubule Dynamics in Breast Cancer			<b>5. FUNDING NUMBERS</b> DAMD17-01-1-0123	
<b>6. AUTHOR(S)</b> George A. Orr, Ph.D.				
<b>7. PERFORMING ORGANIZATION NAME(S) AND ADDRESS(ES)</b> Albert Einstein College of Medicine Bronx, New York 10461  <i>E-Mail:</i> orr@aecom.yu.edu			<b>8. PERFORMING ORGANIZATION REPORT NUMBER</b>	
<b>9. SPONSORING / MONITORING AGENCY NAME(S) AND ADDRESS(ES)</b> U.S. Army Medical Research and Materiel Command Fort Detrick, Maryland 21702-5012			<b>10. SPONSORING / MONITORING AGENCY REPORT NUMBER</b>	
<b>11. SUPPLEMENTARY NOTES</b>				
<b>12a. DISTRIBUTION / AVAILABILITY STATEMENT</b> Approved for Public Release; Distribution Unlimited				<b>12b. DISTRIBUTION CODE</b>
<b>13. ABSTRACT (Maximum 200 Words)</b> <p>Alterations to microtubule dynamics, leading to a less stable polymer, may be a crucial determinant in the development of resistance towards Taxol, and other drugs with a binding site on the microtubule polymer. We propose that two potential mechanisms by which breast cancer cells could alter their microtubule dynamics are by (1) differential expression of the several <math>\alpha</math> and <math>\beta</math> tubulin isoforms and (2) differential binding of endogenous regulators of microtubule assembly to the cytoskeleton as a result of posttranslational modifications to these tubulin isoforms. The overall goal of this proposal is to develop rapid and innovative protein-based technologies for both quantitating the <math>\alpha</math>- and <math>\beta</math>-tubulin isoform composition in drug-sensitive and -resistant human breast cell lines, and for characterizing the posttranslational modifications to these isoforms. It is only by thoroughly understanding Taxol resistance in human breast cancer cells that we will be able to develop ways to overcome Taxol resistance in breast cancer.</p>				
<b>14. SUBJECT TERMS</b> No Subject Terms Provided.				<b>15. NUMBER OF PAGES</b> 53
				<b>16. PRICE CODE</b>
<b>17. SECURITY CLASSIFICATION OF REPORT</b> Unclassified	<b>18. SECURITY CLASSIFICATION OF THIS PAGE</b> Unclassified	<b>19. SECURITY CLASSIFICATION OF ABSTRACT</b> Unclassified	<b>20. LIMITATION OF ABSTRACT</b> Unlimited	

## Table of Contents

Cover.....	1
SF 298.....	2
Table of Contents.....	3
Introduction.....	4
Body.....	4
Key Research Accomplishments.....	10
Conclusions.....	10
Reportable Outcomes.....	11
References.....	12
Appendices.....	14

## INTRODUCTION

Alterations to microtubule dynamics, leading to a less stable polymer, may be a crucial determinant in the development of resistance towards Taxol, and other drugs with a binding site on the microtubule polymer. We propose that two potential mechanisms by which breast cancer cells could alter their microtubule dynamics are by (1) differential expression of the several  $\alpha$ - and  $\beta$  tubulin isotypes and (2) differential binding of endogenous regulators of microtubule assembly to the cytoskeleton as a result of posttranslational modifications to these tubulin isoforms (Orr et al, 2003). Currently, there is no reliable method for quantitating the complete  $\alpha/\beta$ -tubulin protein isotype composition in human cells. Moreover, no precise structural information exists on the structural diversity of  $\alpha$ - and  $\beta$ -tubulin isoforms in human tumors, tissue, or cell lines. The overall goal of this proposal was to develop rapid and innovative protein-based technologies for both quantitating the  $\alpha$ - and  $\beta$  tubulin isotype composition in drug-sensitive and -resistant human breast cell lines, and for characterizing the posttranslational modifications to these isoforms. The C-terminal 20 amino acid domain of  $\alpha$ - and  $\beta$ -tubulins represents the isotype-defining region and is also the site for the majority of the posttranslational modifications.

## BODY

### Task 1 - To Develop Quantitative MALDI-MS Procedures to Determine Tubulin Isotype Composition.

- *Synthesize and purify the C-terminal tubulin peptides including  $^{15}\text{N}$ -labeled  $\alpha 1/\beta 1$ -peptides.*
- *Establish linear standard curves for each peptide against the  $^{15}\text{N}$ -labeled  $\alpha 1/\beta 1$ -peptides.*

Peptides corresponding to the C-terminal CNBr fragments of human  $\alpha$ - and  $\beta$ -tubulins found in the MDA-MB-231 breast cell line, including  $\kappa\alpha 1$ ,  $\alpha^*$ ,  $\beta 1$ ,  $\beta \text{II}$  and  $\beta \text{IVb}$ , were synthesized on an Applied Biosystems 433A Peptide Synthesizer using Fmoc-based chemistry. All peptides were prepared on a 0.1 mmol scale. We also prepared detyrosinated  $\kappa\alpha 1$  and the phosphorylated and non-phosphorylated forms of  $\beta \text{III}$ . The peptides were purified by preparative (1 x 22 cm) C8 reverse phase chromatography using acetonitrile/ 0.1% TFA gradients. MALDI MS was used to authenticate the structure of each peptide. Figure 1 is a representative analytical C 8 reverse phase chromatogram of selected purified peptides. The  $^{15}\text{N}$ -labeled analogs of  $\kappa\alpha 1$  and its detyrosinated counterpart were also synthesized and purified.  $^{15}\text{N}$ -labeled amino acids were incorporated at the underlined/bold residues, thus increasing the mass of both peptides by 4 daltons.

$\text{A}_{426}$ **ALEKDYEEVGVDSVEGE****EEEEGEE** $\pm$ /-Y

The MALDI-MS spectrum of the  $^{14}\text{N}$ - and  $^{15}\text{N}$ -labeled detyrosinated  $\kappa\alpha 1$  peptide is shown in figure 2. Note the ~4 dalton difference between the largest peaks in the two ion

clusters. The  $^{14}\text{N}$  labeled peptide has a predicted monoisotopic mass of  $m/z$  2698.1, a difference of 0.3  $m/z$  from the observed MALDI-TOF data. This peptide has a predicted isotope cluster as follows:

<u><math>m/z</math></u>	<u>% Relative Intensity</u>
2698.1	72.3
2699.1	100.0
2700.1	76.3
2701.2	41.8
2702.2	18.2

The observed ions starting at  $m/z$  2701.8 corresponds to  $^{15}\text{N}$ - labeled peptide. The observed isotopic cluster for this  $^{15}\text{N}$  peptide agrees with the predicted isotopic cluster.

**Task 2 - To optimize conditions for the CNBr release of C-terminal tubulin peptides.**

- *Establish the conditions for radiolabeling bovine brain tubulins with  $^3\text{H}$  and  $^{32}\text{P}$  using tubulin tyrosine ligase and casein kinase, respectively.*
- *Optimize cell lysis, SDS-Page, electroblotting and CNBr digestion conditions for maximal recovery of tubulin peptides from cell extracts.*

We proposed originally to radiolabeling bovine brain tubulin with  $^3\text{H}$  and  $^{32}\text{P}$  using tubulin tyrosine ligase and casein kinase, respectively, to use as standards for optimizing CNBr digestions conditions for the maximal recovery of tubulin C-terminal peptides. We have found, however, that we could avoid the need for radiolabeling of tubulin by using an antibody-based detection system. A rabbit polyclonal antibody prepared against a synthetic peptide corresponding to the final 12 amino acids of human  $\alpha\text{1}$  was used to follow the release of the CNBr C-terminal fragment. Under our published digestion conditions (Rao et al, 2001), i.e. CNBr (150 mg/ml) in 70 % formic acid for 3.5 hr at room temperature, no immunoreactivity remained on the nitrocellulose filter after the incubation period. This result was in agreement with our previous studies indicating that these digestion conditions also resulted in the quantitative cleavage of brain tubulin in solution.

**Tasks 3 & 4 - To characterize and quantify the tubulin isotype composition in the parental drug-sensitive MDA MB 231 and MCF-7 breast carcinoma cell lines .**

- *C-terminal peptides will be isolated by the optimized conditions established in Task 2. Individual peptides will be isolated by reverse phase HPLC and identified by CID/PSD-MALDI-MS.*
- *Quantitative MALDI-MS analysis using the  $^{15}\text{N}$ -labeled  $\beta\text{1}$  peptide will be performed to establish the absolute isotype composition for each parental cell line.*

- *Currently over 30 cloned MDA-MB 231 and MCF-7 cell lines have been selected for varying levels of resistance to either Taxol, epothilone B, eleutherobin or discodermolide. All cell lines will be characterized for their tubulin isotype profiles.*

**1. Reported Detection of  $\beta$ II tubulin in the MDA-MB 231 Breast Carcinoma Cell Line** - Two abstracts presented at the "French-American Colloquium on the Cytoskeleton and Human Disease" in Marseille (April 2001) suggested that the  $\beta$ II-tubulin isotype was a major component of the tubulin cytoskeleton in the MDA-MB 231 breast cell line (Lobert et al, 2001; Xu and Luduena, 2001). In both cases, the identification was by immunological-based methods. Our mass spectrometry-based method, which measures isotype composition based on the CNBr-release of the highly divergent C-terminal peptides, found that the  $\beta$ II isotype was below the level of detection in this cell line (Rao et al, 2001). Since we could detect  $\beta$ II tubulin in bovine brain microtubule preparations, we did not believe that our inability to detect the  $\beta$ II isoform in this cell line was a problem inherent to our MS-based method. Nevertheless, we decided that it was important to confirm the tubulin isotype composition in MDA-MB 231 breast cell line.

**2. Ion Suppression Effects in MALDI-TOF MS Analysis of C-terminal Tubulin Peptides** - Ion suppression effects can be a significant problem in MALDI-TOF MS analysis. Our MALDI-TOF MS analysis of tubulin CNBr C-terminal peptides from total cell extracts may have under represented certain tubulin isotypes due to these ion suppression effects (Rao et al., 2001). In that study, the C-terminal peptides of  $\beta$ II-,  $\beta$ III and  $\beta$ IVa were not observed and the  $\beta$ IVb peptide ion was minor compared to  $\beta$ I. Ions for minor tubulin species could have been suppressed by the presence of the more highly abundant tubulin C-terminal peptides and/or because of differential ionization efficiencies of the various peptides. We reevaluated this approach by reducing the complexity of the sample prior to CNBr digestion (Verdier-Pinard et al., 2003a). Tubulin was purified by the Taxol-based polymerization method from MDA-MB231 cell extracts followed by the separation of  $\alpha$ -tubulin and  $\beta$ -tubulin on SDS-PAGE gels prior to transfer to the nitrocellulose membrane. The region of the blot containing either  $\alpha$ -tubulin or  $\beta$ -tubulin was CNBr-digested and MALDI-TOF MS analysis was performed. The m/z peaks intensities corresponding to  $\beta$ IVb and monoglutamylated  $\beta$ I-tubulin C-terminal peptides were increased significantly compared to those obtained from total cell extracts (see Rao et al., 2001). Very low levels of the C-terminal peptide of tyrosinated  $\alpha$ 4-tubulin were also detected. However, the  $\beta$ II C-terminal peptide was still undetectable (Verdier-Pinard et al., 2003a).

It could be argued that the Taxol-dependent polymerization process selectively enriched for specific  $\beta$ -tubulin isotypes. For this reason, immunoblot analysis was used to follow the isotype composition during the tubulin isolation step. Our data established that the

isotype composition of the final Taxol-stabilized microtubule pellet was representative of the cellular tubulin composition (Verdier-Pinard et al., 2003a).

**3. Analysis of Tubulin Isoypes by combined Isoelectric Focusing and Mass Spectrometry** - Due to the ion suppression effects noted above, it was necessary to modify our experimental protocol. The isolation of tubulin from cell extracts using the Taxol-driven polymerization coupled to high resolution isoelectric focusing enabled us to easily visualize and analyze the different tubulin isoforms present in cancer cell lines. The position of each tubulin band on the IPG strip was definitely assigned by performing in-gel trypsin digestion followed by MALDI-TOF MS analysis. After tryptic digestion of each excised band, mass analysis detected several isotype- specific tryptic peptides that confirmed the assignment of each band to an individual tubulin isotype class based on the sequence derived pI values (Verdier-Pinard et al., 2003a). We confirmed the presence of the tubulin isotypes in the MDA-MB-231 and A549 cell lines identified previously by MALDI-TOF mass spectrometry analysis of C-terminal tubulin peptides (Rao et al., 2001). Because the C-terminal sequence obtained previously by MS/MS for  $\alpha^*$ -tubulin matches the C-terminal sequence of the recently described human  $\alpha 6$ -tubulin, and because in the present study a protein having the pI value predicted for human  $\alpha 6$ -tubulin was detected and confirmed as being  $\alpha 6$ -tubulin by peptide mapping, we consider them to be identical. An increase in  $\beta$ III-tubulin expression was detected in resistant compared to sensitive cells. A minor  $\beta$ III-tubulin species that corresponded most likely to monoglutamylated or phosphorylated  $\beta$ III-tubulin was also detected.

The potential ion suppression effects are overcome in the present isoelectrofocusing/mass spectrometry approach since the total amount of each tubulin isotype is analyzed directly, giving a better appreciation of isotype ratios. Interestingly, the ratios of  $K\alpha 1$ -tubulin:  $\beta$ I-tubulin and  $\alpha 6$ -tubulin:  $\beta$ IVb-tubulin are close to one in the cell lines examined so far. This trend suggests that there could be a specific pairing of a particular  $\alpha$ -tubulin isotype with a particular  $\beta$ -tubulin isotype. The most striking difference between our analysis of tubulin isotype expression at the protein level (Rao et al., 2001; Verdier-Pinard et al., 2003a) and previous studies at the mRNA level (Kavallaris et al., 1997) is the absence of detectable  $\beta$ IVa- and  $\beta$ II-tubulin expression in both sensitive and resistant cell lines. Since our data established that tubulin was quantitatively recovered from cells by Taxol-driven polymerization (Verdier-Pinard et al., 2003), either there is an unknown bias in the RT-PCR results or there is a still unknown silencing mechanism of  $\beta$ II- and  $\beta$ IVa-tubulin mRNA translation. Increased  $\beta$ III-tubulin expression levels have been repeatedly confirmed at the protein level using a variety of methods in cell lines resistant to Taxol (Nicoletti et al., 2001; Ranganathan et al., 1998a; Ranganathan et al., 1998b). Together with this present study, these observations strongly suggest that only  $\beta$ III-tubulin levels correlate with sensitivity towards Taxol (Nicoletti et al., 2001; Ranganathan et al., 1998a; Ranganathan et al., 1998b) and that the regulation of  $\beta$ -tubulin expression is even more complex than the autoregulatory mechanism described by Cleveland and colleagues (Cleveland and Sullivan, 1985).

**4. Evaluation of Tubulin Isotype-specific Antibodies** – The ability to resolve and identify each tubulin isotype on isoelectric focusing gels allowed us to evaluate the specificity of a panel of tubulin isotype-specific antibodies (Verdier-Pinard et al., 2003a). The anti- $\beta$ -tubulin isotype monoclonal antibodies produced and characterized by Dr. Luduena and coworkers (Banerjee et al, 1990; Luduena, 1998) represent valuable tools that have helped to unravel the functional significance of the different tubulin isotypes. No cross-reactivity of the anti- $\beta$ I-,  $\beta$ III-, and  $\beta$ IV- tubulin antibodies was observed in the present study. This is contrary to what has been published for non-denaturing immunoaffinity isolation of  $\alpha/\beta$ -tubulin heterodimers enriched in  $\beta$ I-,  $\beta$ II-,  $\beta$ III- or  $\beta$ IV- tubulin isotypes (Banerjee et al., 1992; Luduena, 1998). Therefore, the presence of contaminating  $\beta$ -tubulin isotypes of a different class in these fractions is more likely due to heterodimer-heterodimer interactions in residual small oligomers than to cross-reactivity of these antibodies with multiple isotypes. However, extensive cross-reactivity of the anti- $\beta$ II-tubulin antibody with  $\beta$ I-tubulin was detected. This cross-reactivity is the likely reason that  $\beta$ II has been reported to be present in the MDA-MB 231 (Verdier-Pinard et al., 2003a).

**5. Analysis of Tubulin isotypes by LC-MS** - For these studies, microtubules were isolated from MDA-MB 231 cell extracts using either Taxol dependent polymerization or the glutamate-based purification of Sackett. Both methods yielded ~100-200  $\mu$ g of tubulin from ten 100 mm culture dishes of cells. For LC/ESI-MS studies, 10  $\mu$ g of tubulin sample in 70% formic acid was loaded onto a 1 mm x 15 cm Vydac C4 column (Vydac, Hesperia, CA). A HP 1100 high-performance liquid chromatography (HPLC) equipped with a degasser and a binary pump was used to degas the solvents and pump the solvents to generate acetonitrile gradients at a flow rate of 50  $\mu$ l/min. Solvent A was deionized water containing 5% acetonitrile and 0.1% trifluoroacetic acid and solvent B was 95% (v/v) acetonitrile containing 0.1% trifluoroacetic acid. The sample was desalted at 5%B for 45 min and separated by a 3 min 5%B-40%B gradient followed by a 100 min 40%B-60%B and 7 min 60%B-95%B gradients and washing at 95%B for 10 min. The column effluent was delivered directly to a LCQ quadrupole ion trap mass spectrometer (ThermoFinnigan, Riviera Beach, FL) without flow splitting.

Figure 4 (top panel) is a representative chromatogram showing the total ion current of a typical human microtubule preparation. All the masses in the range of human tubulins were found between 44 and 60 min of the gradient, which includes the largest ion peak (Verdier-Pinard et al, 2003b). This result was expected, as tubulin represented the major protein component in the Taxol-stabilized microtubule pellets. After averaging the scans between 44 and 60 min, we obtained overall profiles of the deconvoluted mass peaks for the different tubulin proteins in both cell lines (Fig. 1B and Fig. 2B). The observed masses matched closely those of  $\beta$ I-,  $\beta$ IVb-,  $\alpha$ 6-,  $\text{tyr}\alpha$ 4-,  $\text{K}\alpha$ 1-,  $\text{glu-K}\alpha$ 1- and  $\beta$ III-tubulin, respectively (Verdier-Pinard et al, 2003b).



To confirm the identity of these tubulin isotypes, tryptic mass mapping of the C4-resolved isotypes present in A549 tubulins was performed. For these experiments, tubulin isotypes were separated using a 0.05%/min solvent B gradient to increase the separation between tubulin isotypes and the column effluent was split for fraction collection and for delivery to the ion trap mass spectrometer. The total ion current was deconvoluted in one min segments across the gradient and fractions that contained the same protein masses were pooled. After removal of solvents, tryptic digestion was performed and the resulting peptides were analyzed by MALDI-TOF MS searching for tubulin isotype-specific tryptic peptides (Verdier-Pinard et al, 2003b). Importantly, no peaks of significant intensity are observed in the regions expected for the  $\beta$ II tubulins. Thus the data obtained from the analysis of native, full length tubulins are in complete agreement with the isotype composition data obtained by analysis of the C-terminal tubulin peptides released by CNBr. All of our MS-based methods show that the  $\beta$ II is not a major tubulin isotype in the MDA-MB 231 breast carcinoma cell line.

## 6. Quantitation of Tubulin Isotype Expression by SILAC

We have used stable isotope-containing amino acids in cell culture (SILAC) to differentially label proteins in Taxol-sensitive- and resistant cell lines (Ong et al, 2003). In the SILAC method, two cell lines are cultured for several generations in media containing either deuterated leucine ( $d_3$ -Leu) or normal leucine ( $d_0$ -Leu). Figure 5 shows the incorporation of  $d_3$ -Leu into tubulin. After 5 days (equivalent to 5 doubling), all of the "light" tubulin has been replaced by its "heavy" counterpart. For relative quantitation of protein expression, equal amounts of total cytosolic proteins from each cell line were mixed and tubulins were isolated by Taxol-induced polymerization. For relative quantitation of total  $\alpha$ - and  $\beta$ -tubulin levels, the region containing tubulin was excised from a SDS-PAGE gel and subjected to trypsin digestion followed by MALDI-TOF mass spectrometry. Depending on the number of leucine residues contained in a tryptic peptide, this peptide was represented by two m/z peaks separated by a multiple of 3 Da in the mass spectra. In Figure 5, the masses of the peptides differ by 6 Da since the peptide contains two leucines. The signal intensity of each peak in these doublets was used to calculate the relative abundance of a given isotype within the two cell lines. We compared the tubulin content of MDA-MB-231 cell line and MDA-MB-231.K20T, a Taxol-resistant cell line bearing a Glu198Gly mutation in  $\alpha$ I-tubulin. Our data indicated that total  $\alpha$ - and  $\beta$ -tubulin expression increased about 2-fold in drug-resistant MDA-MB-231.K20T cell line. For relative quantitation of individual tubulin isotype levels, samples were separated by IEF and gel bands containing a particular isotype were analyzed by tryptic mass mapping. In MDA-MB-231.K20T,  $\beta$ III-tubulin was increased by 2-fold,  $\beta$ IVb decreased by 0.7-fold,  $\alpha$ 1 increased by 2-fold and  $\alpha$ 6 increased by 1.3-fold. In the case of  $\alpha$ I, a small amount of wild type protein was detected in MDA-MB-231.K20T (2.5-fold less than in MDA-MB-231), whereas most of this isotype was represented by the more basic mutated protein. The SILAC-MS technology is a powerful tool for analyzing tubulin isotype expression in cell lines, and also the differential expression of proteins associated with the microtubule cytoskeleton. Such quantitative

proteomic studies will highlight those changes in cellular microtubule composition that may be related to Taxol resistance.

## KEY RESEARCH ACCOMPLISHMENTS

- Synthesis and purification of the highly divergent C-terminal peptides of the human tubulin isotypes including,  $\kappa\alpha 1$ , detyrosinated  $\kappa\alpha 1$ ,  $\alpha^*$ ,  $\beta 1$ ,  $\beta II$ ,  $\beta IVb$ , and phospho- and dephospho- $\beta III$ .
- Synthesis and purification of  $^{15}N$ -labeled  $\kappa\alpha 1$  and detyrosinated  $\kappa\alpha 1$ .
- Demonstration that the  $^{14}N$ - and  $^{15}N$ -labeled peptides are clearly resolvable by MALDI MS.
- Establish that the CNBr digestion conditions are optimal for the release of the C-terminal tubulin peptides from nitrocellulose.
- Developed a combined high resolution isoelectric focusing/mass spectrometry-based method for the analysis of tubulin isotypes, posttranslational modifications, and mutations from Taxol-resistant human cell lines.
- The method was used to establish the specificity of the anti- $\beta 1$ ,  $\beta II$ ,  $\beta III$  and  $\beta IV$  monoclonal antibodies.
- Developed LC-ESI-MS for the analysis of mutations and posttranslational modifications to intact tubulins.
- Characterization of the tubulin isotype composition of the MDA-MB 231 breast carcinoma cell line by 3 independent mass spectrometry-based methods.
- The absence of  $\beta II$  and  $\beta IVa$  tubulins in the MDA-MB-231 breast carcinoma cell line has been confirmed by all three methods.
- Developed the combined SILAC-MS approach for the relative quantitation of tubulin isotype expression in human cell lines.

## REPORTABLE OUTCOMES

Rao, S, Åberg, F, Deng, H., Nieves, E., Horwitz, S.B., and Orr, G.A. (2001) Analysis of tubulin isotype composition in human breast and lung carcinoma cell lines and tissue by mass spectrometry. Abstract presented at Fifth International Symposium of Mass

Spectrometry in the Health and Life Sciences: Molecular and Cellular Proteomics, San Francisco, August 2001.

Verdier-Pinard, P., Martello, L., Wang, F., Orr, G.A., and Horwitz, S. B. Analysis of  $\alpha$ - and  $\beta$  tubulin content by LC-MS and IEF in human cancer cells sensitive and resistant to microtubule stabilizing drugs. Abstract presented at the American Association for Cancer Research meeting, San Francisco, 2002

Verdier-Pinard, P., Wang, F., Martello, L.A., Horwitz, S.B. And Orr, G.A (2002) Mass Spectrometry-based Analysis of Tubulin Isoforms in Taxol® Sensitive- and Resistant-Human Cancer Cell Lines. Abstract presented at the first annual HUPO meeting, Versaille, France November 2002.

Verdier-Pinard, P., Wang, F., Martello, L.A., Burd, B., Orr, G.A. and Horwitz, S.B. (2003) Analysis of Tubulin Isotypes and Mutations from Taxol-resistant Cells by Combined Isoelectrofocusing and Mass Spectrometry. *Biochemistry* **42**, 5349-5357.

Orr, G.A., Verdier-Pinard, P., McDaid, H., He, L. and Horwitz, S.B. (2003) Mechanisms of Taxol resistance related to microtubules. (2003) *Oncogene*, **22**, 7280-7295.

Verdier-Pinard, P., Wang, F., Burd, B., Angeletti, R.H., Horwitz, S.B., and Orr GA. (2003) Direct analysis of tubulin expression in cancer cell lines by electrospray ionization mass spectrometry. *Biochemistry*. **42**, 12019-12027.

Verdier-Pinard, P., Burd, B., Horwitz, S.B., and Orr GA. Quantitative proteomics of  $\alpha$ - and  $\beta$ -tubulin isotype expression in human cancer cells. Abstract presented at the American Association for Cancer Research meeting, Orlando, 2004.

## PERSONNEL INVOLVED

Dr. George A. Orr  
Dr. Susan B. Horwitz  
Ms. Berta Burd

## CONCLUSIONS

An emerging theme in studies of Taxol resistance is that alterations to microtubule dynamics may be a crucial factor in the development of resistance. Microtubule assembly can be potentially altered by differential expression and/or posttranslational modifications to tubulin isotypes. Although PCR- and microarray-based technologies can be used to measure mRNA expression levels for tubulins, there is a need for the development of rapid and sensitive protein-based methods for determining the tubulin protein isotype composition, and characterizing posttranslational modifications to these isotypes, in drug-sensitive and resistant cell lines. The data presented in this progress report demonstrate

that mass spectrometry is a powerful approach for the compositional analysis of tubulins expressed in drug-sensitive and resistant cell lines. Importantly, our studies confirm an increased expression of  $\beta$ III-tubulin in resistant cells indicating that this tubulin isotype is a unique marker of resistance. The information gained from these experiments will provide a greater understanding of the modifications that occur to microtubules when human breast tumors become resistant to Taxol.

## REFERENCES

- Banerjee, A., Roach, M.C., Trcka, P. and Luduena, R.F. (1990) Increased microtubule assembly in bovine brain tubulin lacking the type III isotype of beta-tubulin. *J Biol Chem* **265**:1794-9.
- Banerjee, A., Roach, M.C., Trcka, P. and Luduena, R.F. (1992) Preparation of a monoclonal antibody specific for the class IV isotype of beta-tubulin. Purification and assembly of alpha beta II, alpha beta III, and alpha beta IV tubulin dimers from bovine brain. *J Biol Chem* **267**:5625-30.
- Cleveland, D.W. and Sullivan, K.F. (1985) Molecular biology and genetics of tubulin. *Annu Rev Biochem* **54**:331-65.
- Kavallaris, M., Kuo, D.Y., Burkhart, C.A., Regl, D.L., Norris, M.D., Haber, M. and Horwitz, S.B. (1997) Taxol-resistant epithelial ovarian tumors are associated with altered expression of specific beta-tubulin isotypes. *J Clin Invest* **100**:1282-93.
- Lobert, S., Dozier, J.H., Frankfurter, A., and Correia, J.J. Beta II tubulin is the predominant tubulin isotype in normal and tumor breast tissue. Abstract PB13, French-American Colloquium on the Cytoskeleton and Human Disease. April, 2001, Marseille, France.
- Luduena, R.F. (1998) Multiple forms of tubulin: different gene products and covalent modifications. *Int Rev Cytol* **178**:207-75.
- Nicoletti, M.I., Valoti, G., Giannakakou, P., Zhan, Z., Kim, J.H., Lucchini, V., Landoni, F., Mayo, J.G., Giavazzi, R. and Fojo, T. (2001) Expression of beta-tubulin isotypes in human ovarian carcinoma xenografts and in a sub-panel of human cancer cell lines from the NCI Anticancer Drug Screen: correlation with sensitivity to microtubule active agents. *Clin Cancer Res* **7**:2912-22.
- Ong, S.E., Blagoev, B., Kratchmarova, I., Kristensen, D.B., Steen, H., Pandey, A., and Mann, M. (2002) Stable isotope labeling by amino acids in cell culture, SILAC, as a simple and accurate approach to expression proteomics. *Mol Cell Proteomics* **1**, 376-86.
- Orr, G.A., Verdier-Pinard, P., McDaid, H., He, L. and Horwitz, S.B. (2003) Mechanisms of Taxol resistance related to microtubules. (2003) *Oncogene*, **22**, 7280-7295.
- Ranganathan S, Benetatos CA, Colarusso PJ, Dexter DW and Hudes GR (1998a) Altered beta tubulin isotype expression in paclitaxel-resistant human prostate carcinoma cells. *Br J Cancer* **77**:562-6.
- Ranganathan, S., Dexter, D.W., Benetatos, C.A. and Hudes, G.R. (1998b) Cloning and sequencing of human betaIII-tubulin cDNA: induction of betaIII isotype in human prostate carcinoma cells by acute exposure to antimicrotubule agents. *Biochim Biophys Acta* **1395**:237-45.

- Rao, S., Aberg F., Nieves, E., Horwitz, B.S. and Orr, G.A. (2001) Identification by mass spectrometry of a new alpha-tubulin isotype expressed in human breast and lung carcinoma cell lines. *Biochemistry* **40**:2096-103.
- Sackett, D. L. (1995) Rapid purification of tubulin from tissue and tissue culture cells using solid-phase ion exchange. *Anal Biochem* **228**, 343-8.
- Verdier-Pinard, P., Wang, F., Martello, L., Burd, B., Orr, G.A. and Horwitz, S.B. (2003a) Analysis of tubulin isotypes and mutations from taxol-resistant cells by combined isoelectrofocusing and mass spectrometry. *Biochemistry* **42**:5349-57.
- Verdier-Pinard, P., Wang, F., Burd, B., Angeletti, R.H., Horwitz, S.B., and Orr GA. (2003b) Direct analysis of tubulin expression in cancer cell lines by electrospray ionization mass spectrometry. *Biochemistry* **42**, 12019-12027.
- Xu, K. And Ludueña, R. F. Effect of Taxol on the  $\beta$ II isotype of tubulin in the nuclei of cancer cells. Abstract PB14, French-American Colloquium on the Cytoskeleton and Human Disease. April, 2001, Marseille, France.

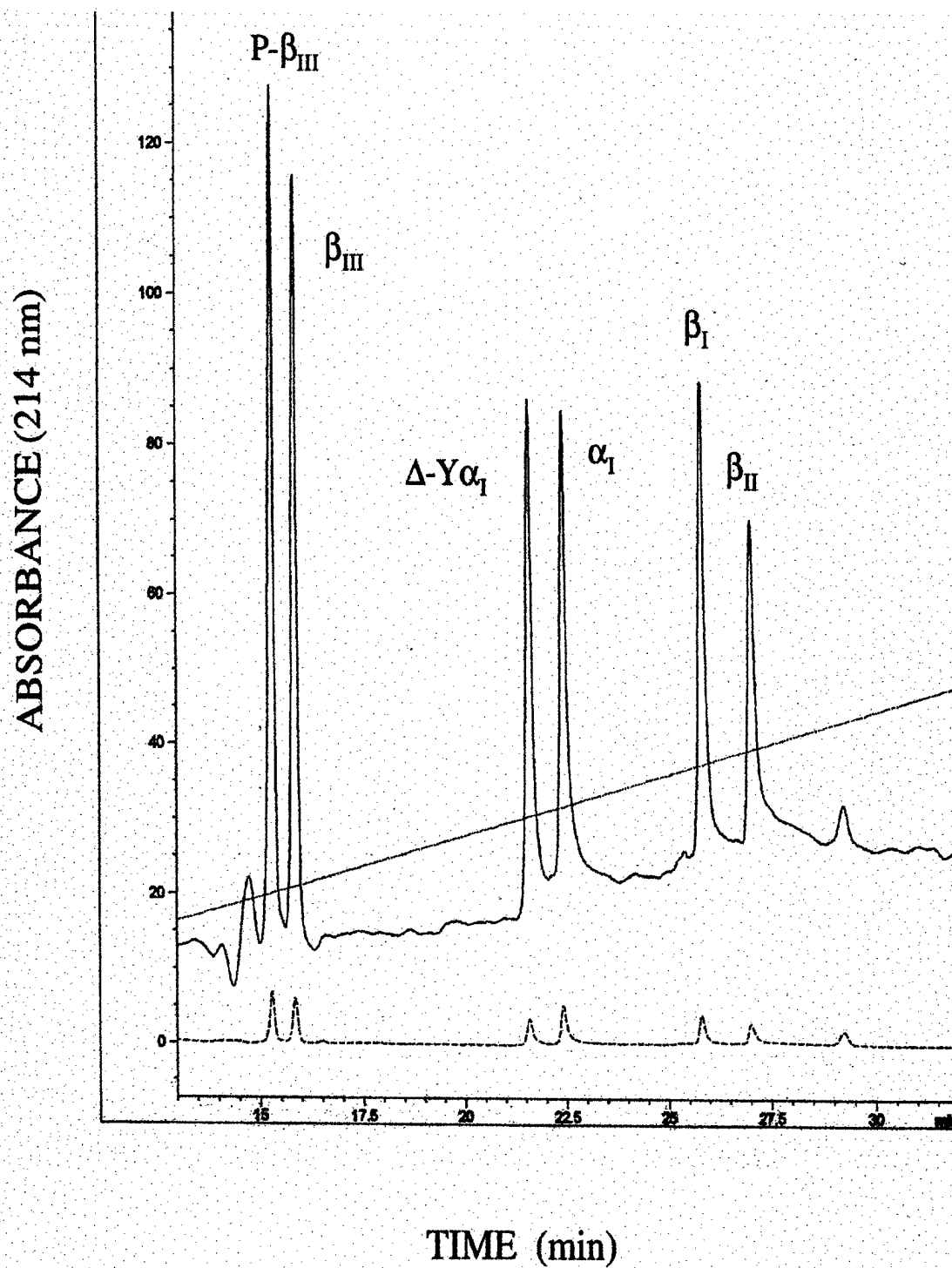


**Figure 1. C-18 reverse phase HPLC of synthetic peptides corresponding to C-terminal CNBr fragments of selected human tubulins**

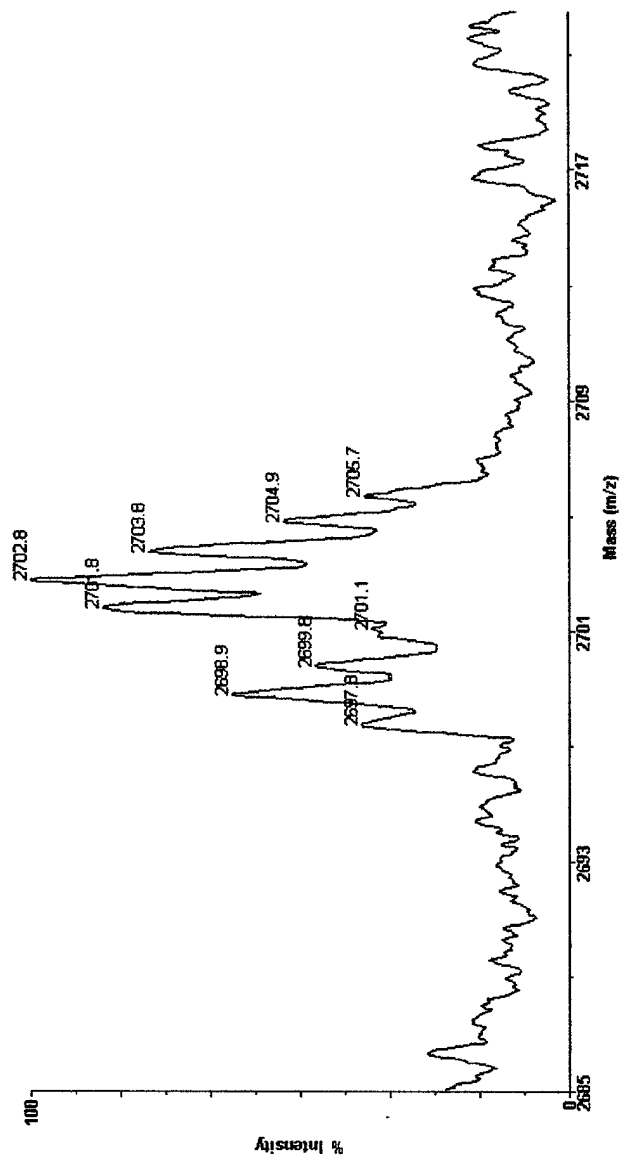


Figure 2. MALDI TOF-MS of the  $^{14}\text{N}$  and  $^{15}\text{N}$ -labeled synthetic deetyrosinated k- $\alpha$ 1 peptides (AALEKDYEEVGVDSEGEVEEGEE).

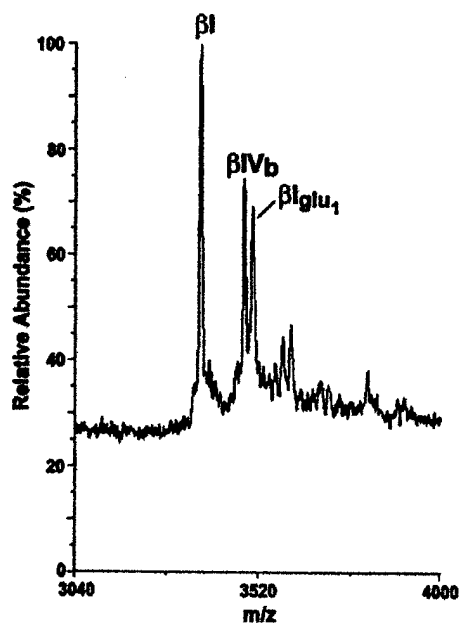
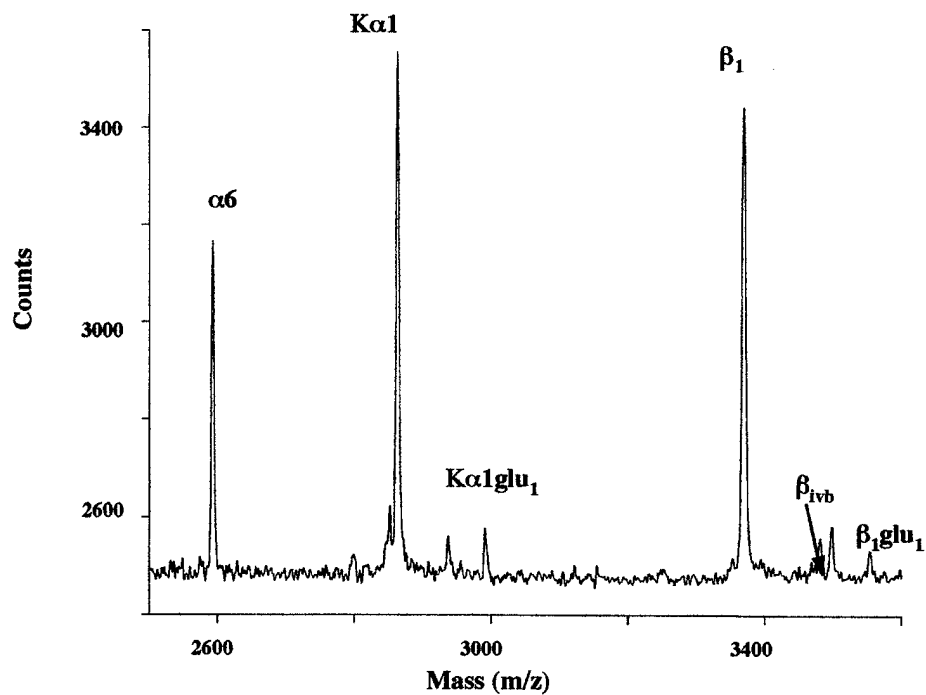


Figure 3. Negative ion MALDI-TOF MS analysis of Human Tubulins.  
(Upper Panel, Total cellular extracts; Lower panel, Taxol-stabilized microtubules)



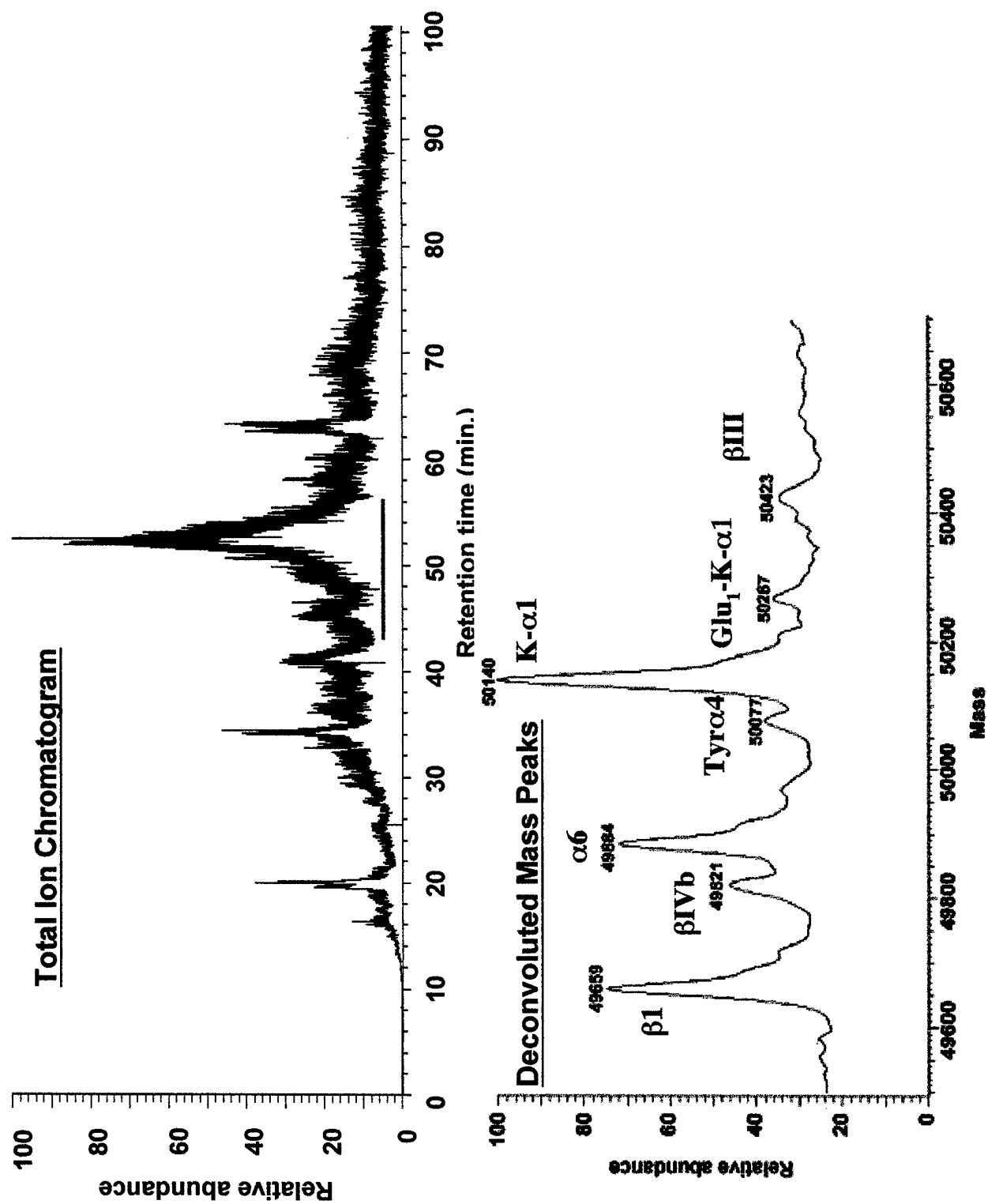
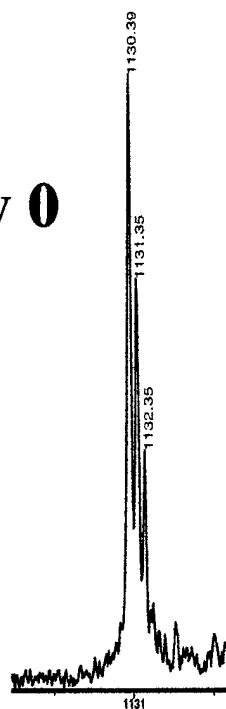


Figure 4. LC-ESI-MS analysis of Taxol-stabilized microtubules from human cell line

Tubulin Isotypes  
resolved by high  
resolution IEF  
prior to tryptic  
mass mapping.

**Day 0**



$\beta_{242}\text{FPQLNAELR}_{251}$

(common  $\beta$ -tubulin  
tryptic peptide)

**Day 5**

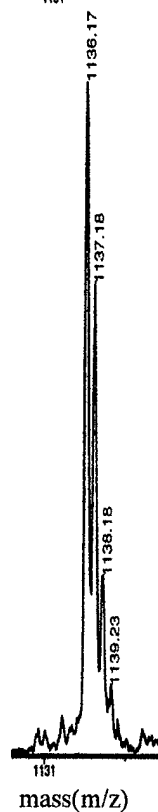


Figure 5. Incorporation of  $d_3$ -Leucine into  $\beta 1$ -tubulin

# Analysis of Tubulin Isotypes and Mutations from Taxol-Resistant Cells by Combined Isoelectrofocusing and Mass Spectrometry<sup>†</sup>

Pascal Verdier-Pinard,<sup>‡</sup> Fang Wang,<sup>§</sup> Laura Martello,<sup>‡,||</sup> Berta Burd,<sup>‡</sup> George A. Orr,<sup>‡</sup> and Susan Band Horwitz<sup>\*,‡</sup>

Department of Molecular Pharmacology, Albert Einstein College of Medicine, Bronx, New York 10461, and Laboratory for Macromolecular Analysis and Proteomics, Albert Einstein College of Medicine, Bronx, New York 10461

Received December 4, 2002; Revised Manuscript Received March 6, 2003

**ABSTRACT:** Six human  $\alpha$ -tubulin and seven human  $\beta$ -tubulin isotypes, each of which can undergo posttranslational modifications, have been detected by the reverse transcriptase–polymerase chain reaction. This repertoire of tubulin isotypes plays a role in development and in the building of specialized microtubule-based structures. In cell lines, the relationship between resistance to microtubule-interacting drugs and altered tubulin isotype expression profiles is often established by quantitation of cDNA and/or Western blot analysis. Tubulin mutations in major isotypes are detected by sequencing cDNA, but more analysis of expression of tubulin mutations at the protein level, to assess their role in drug resistance, is needed. We utilized a Taxol-based purification and high-resolution isoelectrofocusing combined with a mass spectrometry-based analysis of tubulin. This approach has allowed the separation and relative quantitation of tubulin isotypes having a difference in isoelectric point values of 0.01, without the need for two-dimensional gel electrophoresis. The specificity of tubulin isotype antibodies also has been established. In cell lines resistant to microtubule-stabilizing drugs that express heterozygous tubulin mutations, the relative amount of mutant tubulin expression has been determined. In these cell lines, the absence of  $\beta$ II- and  $\beta$ IVa-tubulin has been demonstrated, and an increased level of expression of  $\beta$ III-tubulin in resistant cells has been confirmed, indicating that this tubulin isotype is a unique marker of resistance.

Studies on the microtubule cytoskeleton reveal a spectrum of activities from structural to mechanical to signal transduction processes (1). Mitosis is a microtubule-dependent process, and inhibition of mitotic spindle function represents the mode of action of major anticancer drugs, i.e., the taxanes and vinca alkaloids. Microtubules are built upon the assembly of  $\alpha$ / $\beta$ -tubulin heterodimers. In human tissues, the expression of six  $\alpha$ - and seven  $\beta$ -tubulin isotypes has been detected (Table 1). Additionally, tubulin undergoes posttranslational modifications, and complex patterns of tubulin isoform expression can be observed, especially in the central nervous system (2).

The existence of multiple tubulin species raises the question of the physiological relevance of such diversity (3). The greatest sequence divergence among tubulin isotypes resides in their C-termini (Table 1), sites that are exposed at the surface of microtubules and interact with microtubule-associated proteins and undergo posttranslational modifica-

tions. Specific tubulin isotypes are constituents of specialized microtubules (2). Moreover, alterations in tubulin isotype expression profiles and tubulin mutations have been reported in cell lines resistant to antimetabolic agents (4–8).

The expression of a given tubulin isotype in a cell line or tissue is usually detected by quantification and sequencing of RT-PCR<sup>1</sup> products. Using this method, mutations in tubulin have been detected in cell lines resistant to Taxol and the epothilones (5–8). Despite the convenience of this approach, it does not give direct access to the corresponding protein expression levels. This is particularly relevant to  $\beta$ -tubulin mRNA because it appears to be autoregulated by the level of the free  $\beta$ -tubulin pool in cells (9). Similarly, heterozygous transcriptional expression of a tubulin mutation does not indicate that both wild-type and mutant tubulin proteins are expressed and, if so, at what ratio. Antibodies directed against the C-terminus of each tubulin isotype and against some of their posttranslational modifications provide useful tools for evaluating their respective levels of expression. However, possible cross-reactivity of these antibodies against different tubulin isotypes may introduce some quantitation bias, because of the lack of resolution of the different tubulin isoforms by SDS–PAGE.

<sup>†</sup> This work was supported in part by U.S. Public Health Service Grants CA 39821 and CA 77263, Grant A149749 from the National Foundation for Cancer Research (S.B.H.), Grant DAMD17-01-0123 from the Department of Defense Breast Cancer Research Program (G.A.O.), and Grant 5T32 GM07260 from the National Institute of General Medical Services Training Program in Pharmacological Sciences (L.M.).

<sup>\*</sup> To whom correspondence should be addressed. Phone: (718) 430-2163. Fax: (718) 430-8959. E-mail: shorwitz@aecom.yu.edu.

<sup>‡</sup> Department of Molecular Pharmacology.

<sup>§</sup> Laboratory for Macromolecular Analysis and Proteomics.

<sup>||</sup> Present address: Department of Pathology, New York University School of Medicine, New York, NY 10016.

<sup>1</sup> Abbreviations: RT-PCR, reverse transcriptase–polymerase chain reaction; SDS–PAGE, sodium dodecyl sulfate–polyacrylamide gel electrophoresis; PBS, phosphate-buffered saline; DTT, dithiothreitol; IPG, immobilized pH gradient; IEF, isoelectric focusing; HRP, horseradish peroxidase; MALDI-TOF, matrix-assisted laser desorption ionization time-of-flight; LC–MS, liquid chromatography coupled to mass spectrometry; 2D, two-dimensional; pI, isoelectric point.

Table 1: Human Tubulin Isotypes

Isotype (accession #)	Human gene	C-terminus sequence <sup>a</sup>	Tissue expression	pI <sup>b</sup>
<b>α-TUBULINS</b>				
1 (I77403)	TUBA1/k-α1	MAALEKDYEEVGVDSEGESEEGEEY	Widely expressed	4.94
1 (CAA25855)	TUBA3/b-α1	MAALEKDYEEVGVSVEGESEEGEEY	Mainly in brain	5.02
3 (Q13748)	TUBA2	MAALEKDYEEVGVDSEGESEEGEEY	Testis-specific	4.98
4 (A25873)	TUBA4	MAALEKDYEEVGVDSEGESEEGEEY	Brain, muscle	4.95
6 (Q9BQE3)	TUBA6	MAALEKDYEEVGVDSEGESEEGEEY	Widely expressed	4.96
8 (Q9NY65)	TUBA8	MAALEKDYEEVGVDSEGESEEGEEY	Heart, muscle, testis	4.94
<b>β-TUBULINS</b>				
I (AAD33873)	HM40/TUBB	YQDATAEEEEDFGEEAEEEA	Constitutive	4.78
II (AAH01352)	Hβ9/TUBB2	YQDATADEQGEFEEEGEDEA	Major neuronal, lung	4.78
III (AAH00748)	Hβ4/TUBB4	YQDATAEEEGEMYEDDEEESEAQGP	Minor neuronal, testis	4.83
IVa <sup>c</sup> (P04350) (NP_006078)	Hβ5/TUBB5	YQDATAEEQGEFEEEAEEVA YQDATAEEQGEFEEEAEEVA	Brain specific	4.81 4.78
IVb (P05217)	Hβ2	YQDATAEEQGEFEEEAEEVA	Major testis	4.79
V (NP_115914)	5-beta/Beta V	YQDATAANDGEFAFDEEEEIDG	Uterine adenocarcinoma	4.77
VI (NP_110400)	Hβ1/TUBB1	YQDAKAVLEEDDEEVTEEAEMEPEDKGH	Blood	5.05

<sup>a</sup> Amino acids differing from isotype 1 (Kα1) for α-tubulins or from isotype I (HM40/TUBB) for β-tubulins are highlighted in black. <sup>b</sup> The isoelectric points were calculated on the basis of the tubulin primary sequences found in the NCBI protein database (accession numbers given in first column) using the ExPaSy Compute pI/MW tool. <sup>c</sup> Two βIVa-tubulin sequences with distinct C-termini were found in the NCBI protein database. The top C-terminus sequence was found in human brain, and the bottom sequence was found in a human oligodendroglioma and in mouse brain.

We sought to perform both qualitative and quantitative analysis of tubulin content in cancer cell lines where tubulin represents ~3–4% of the total protein (10–12). Here we present a method based on Taxol-driven polymerization of total soluble tubulin from cell lysates. The resulting Taxol-stabilized microtubule pellets were analyzed by high-resolution isoelectrofocusing on immobilized pH gradient strips. Mass spectrometry analysis of in-gel tryptic digests definitively assigned each major tubulin species to a tubulin isotype class. Western blotting of these strips further established the specificity of tubulin isotype-specific antibodies. This methodology allowed us to evaluate the percentage of each tubulin isotype in cancer cell lines and to detect the expression of charge-altering mutations in tubulin from both Taxol- and epothilone-resistant cell lines. Additionally, the apparent absence of detectable βII- and βIVa-tubulin protein in cell lines where these isotypes were detected at the mRNA level demonstrated that RT-PCR-based analysis of tubulin isotype expression has to be interpreted cautiously. The increase in the level of βIII-tubulin expression in cell lines resistant to microtubule-interacting drugs may represent a significant tubulin isotype-related marker.

## MATERIALS AND METHODS

**Chemicals.** Taxol was obtained from the Drug Development Branch of the National Cancer Institute (Bethesda, MD), dissolved in sterile dimethyl sulfoxide, and stored at –20 °C. Trypsin was obtained from Promega (Madison, WI).

All other chemicals were obtained from Sigma (St. Louis, MO) except where noted.

**Cell Culture.** The human A549 lung, MDA-MB-231 breast, HeLa cervical carcinoma, and CA46 Burkitt lymphoma cell lines were maintained as described previously (10, 13, 14).

**Isolation of Tubulin from Cell Lines.** Subconfluent cultures of cells from seven to ten 100 mm dishes were washed once with PBS and scraped in 1 mL of PBS. For CA46 cells, 250 mL of suspension culture at a cell density of 10<sup>6</sup> cells/mL was centrifuged and the cell pellets were washed with PBS. Pellets of 0.3–0.4 mL of packed cells were obtained. One and one-half volumes of MME buffer [0.1 M 2-(N-morpholino)ethanesulfonic acid (pH 6.9), 1 mM MgCl<sub>2</sub>, and 1 mM EGTA] was used to resuspend the cell pellets. The resulting cell suspensions were frozen in liquid nitrogen. Upon use, cell suspensions were rapidly thawed, and 1/10 volume of a 10-fold stock solution of protease inhibitor cocktail (Boehringer Mannheim) in MME buffer and 1 mM DTT were added. Cell suspensions were sonicated with a microtip probe (Ultrasonics) seven times for 30 s with 30 s rest intervals on melted ice. Cell lysates were centrifuged at 120000g (Beckman TLA100.3 rotor) for 1 h at 4 °C. Cytosolic supernatants (SI) were transferred to new tubes, and the DNA and cell debris pellets (PI) were discarded.

Taxol-stabilized microtubule pellets were isolated by following the method of Vallee (15). In brief, cytosolic supernatants were incubated at 37 °C in the presence of 10

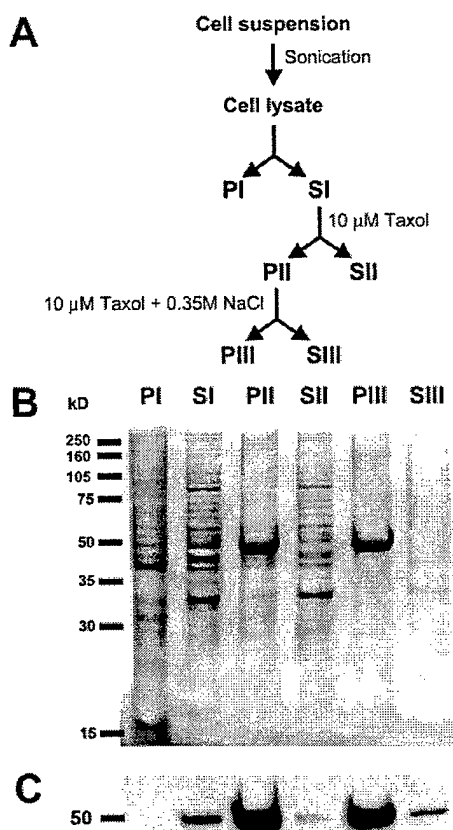


FIGURE 1: Taxol-based purification of tubulin from A549 cells. (A) Tubulin purification scheme (see Materials and Methods for details): PI, DNA and cell debris pellet; SI, cytosolic extract; PII, Taxol-stabilized microtubule pellet; SII, supernatant II; PIII, washed Taxol-stabilized microtubule pellet; SIII, supernatant III. (B) The different fractions were analyzed by SDS-PAGE (10% acrylamide gel, MW markers indicated on the left), and the gel was stained with Coomassie blue. (C) After SDS-PAGE of the same fractions, proteins were transferred to a nitrocellulose membrane that was probed with a pan  $\alpha$ -tubulin antibody.

$\mu$ M Taxol and 1 mM GTP for 20 min. Reaction mixtures were layered on a 0.1 mL cushion containing 5% sucrose in MME, 10  $\mu$ M Taxol, and 1 mM GTP. Samples were centrifuged at 80000g (Beckman TLA100.3 rotor) for 30 min at 37 °C. Microtubule pellets (PII) were washed and resuspended in 0.1 mL of MME buffer containing 0.35 M NaCl and 10  $\mu$ M Taxol. After centrifugation at 80000g for 30 min at 37 °C, microtubule pellets (PIII) were frozen on dry ice and kept at -70 °C until they were used. The Taxol-based purification of tubulin from A549 cells was monitored by SDS-PAGE and Western blot analyses (Figure 1) using either DM1A, a pan  $\alpha$ -tubulin antibody, or DM1B, a pan  $\beta$ -tubulin antibody (Biogenex, San Ramon, CA), and pure bovine brain tubulin as a standard (Cytoskeleton Inc., Denver, CO).

**Isoelectric Focusing.** Microtubule pellets (containing approximately 100–200  $\mu$ g of protein) were resuspended in 350  $\mu$ L of solubilization buffer {7 M urea, 2 M thiourea, 4% 3-[(3-cholamidopropyl)dimethylammonio]-1-propanesulfonate, 0.5% Triton X-100, 0.5% ampholyte-containing buffer (pH 4.5–5.5), 20 mM DTT, and bromophenol blue}, loaded onto 18 cm IPG strips at pH 4.5–5.5 (Amersham Pharmacia Biotech), and run on an IPGphor IEF system for

a total of 70 000 Vh. IPG strips were then stored at -20 °C. Prior to use, IPG strips were incubated in equilibration buffer [125 mM Tris-HCl (pH 6.8), 5%  $\beta$ -mercaptoethanol, and 1% SDS] for 2  $\times$  20 min each, and then incubated in IPG strip transfer buffer [25 mM Tris-HCl (pH 8.3) and 192 mM glycine] for 20 min.

**Coomassie Blue Staining.** IPG strips were fixed in a 50% methanol/20% trichloroacetic acid mixture for 30 min, stained with 0.1% R250 Coomassie blue in a 50% methanol/10% acetic acid mixture, destained in a 35% methanol/10% acetic acid mixture, incubated for 30 min in 2% glycerol, layered on filter paper with the plastic backing facing the paper, covered with a piece of transparent plastic sheet, and air-dried prior to scanning. IPG strips were scanned and bands quantitated using Image Quant (Amersham).

**Western Blotting of IPG Strips.** IPG strips were electrotransferred onto nitrocellulose membranes with the gel facing the membrane (without removing the plastic backing from the strip) and transferred for approximately 20 h at 100 mA. Only a partial transfer of proteins was achieved, and after being transferred, strips were directly fixed and stained with Coomassie blue stain (see above) so that the blots and gel could be aligned.

The  $\beta$ -tubulin isotype content was examined using a panel of mouse monoclonal antibodies directed against the C-terminus of  $\beta$ I-,  $\beta$ II-,  $\beta$ III-, and  $\beta$ IV-tubulins originally produced by R. F. Ludueña and co-workers. The anti- $\beta$ I-tubulin antibody (generous gift from R. F. Ludueña) was used at a 1:10000 dilution; the anti- $\beta$ II-,  $\beta$ III-, and  $\beta$ IV-tubulin antibodies (Biogenex) were used at a 1:250 dilution, and a goat anti-mouse HRP-linked IgG was used as the secondary antibody (1:2000 dilution, Transduction Laboratories, San Jose, CA).

Membranes were probed for  $\alpha$ -tubulin isotypes with an anti-K $\alpha$ 1-tubulin rabbit polyclonal antibody (SRa1) at a 1:20000 dilution or an anti- $\alpha$ 6-tubulin rabbit polyclonal antibody (SRa6) at a 1:5000 dilution. A donkey anti-rabbit HRP-linked IgG was used as the secondary antibody (1:2000 dilution, Amersham). Antibodies SRa1 and SRa6 were prepared using synthetic C-terminus peptides GVDSVEGEGEE and GADSADGEDEG as antigens, respectively. A Cys residue was added at the N-terminus of these peptides for their conjugation to maleimide-activated keyhole limpet (Pierce, Rockford, IL). The conjugated peptides were injected into rabbits, and bleeds were analyzed by an enzyme-linked immunosorbent assay using the same K $\alpha$ 1- and  $\alpha$ 6-tubulin C-terminus peptides conjugated to maleimide-activated bovine serum albumin (Pierce). All blots were visualized using an enhanced chemiluminescence detection system (Amersham).

The only major non-tubulin proteins in the salt-extracted microtubule pellets (PIII) were  $\gamma$ - and  $\beta$ -actin, whose pIs are more basic than those of the tubulins. Blots were probed with a monoclonal anti-actin antibody (1:1000 dilution, clone AC-40, Sigma), allowing precise alignment of the different blots and the corresponding transferred Coomassie blue-stained gel. Membranes were first probed with a tubulin isotype-specific antibody and then with the anti-actin antibody, and finally, they were stripped before another tubulin isotype-specific antibody was used.

**IPG Strip in-Gel Trypsin Digestion.** IPG strips were stained with imidazole and zinc salts according to the

procedure of Castellanos-Serra et al. (16). Tubulin binds zinc, and positively stained tubulin bands appeared. The bands were cut with the plastic backing using scissors, washed with 1 mL of water (2 × 5 min, 1 × 10 min), and dehydrated in 90% aqueous acetonitrile (0.5 mL, 2 min). After centrifugal evaporation of residual acetonitrile, 25  $\mu$ L of 12.5 ng/ $\mu$ L trypsin in 20 mM ammonium bicarbonate buffer (pH 8.3) containing 80 mM glycine was added to each tube. Trypsin digestion was performed at 37 °C overnight with constant shaking. The supernatant was desalted on a Millipore C18 ZipTip, and the tryptic peptides were eluted from the ZipTip with 4.0  $\mu$ L of a 50% acetonitrile/H<sub>2</sub>O mixture containing 0.1% trifluoroacetic acid.

**Protein Identification.** One microliter of a tryptic peptide mixture was mixed with 1  $\mu$ L of a saturated  $\alpha$ -cyano-4-hydroxycinnamic acid solution in a 50% acetonitrile solution containing 0.1% TFA, and 1  $\mu$ L of the resulting solution was deposited on a clean mass spectrometer probe surface. Mass spectra were recorded in the positive or negative mode on a Voyager-DE STR MALDI-TOF mass spectrometer (PerSeptive Biosystems, Framingham, MA) equipped with a 2.0 m flight tube and a 337 nm nitrogen laser. Protein identification was accomplished through a database search (Swiss-Prot and NCBI) using MS-Fit and ProFound programs (*Homo sapiens*/*Mus musculus*, mass measurement error within 1 Da, partially oxidized methionine, average and/or monoisotopic masses, and two maximum miscleavages). The isoelectric point for each tubulin was calculated using the Compute MW/pI tool from the ExPaSy Web site.

## RESULTS

**Taxol-Based Purification of Tubulin from Cell Lines.** Taxol microtubule pellets were isolated from cell lines using the method of Vallee (15). A representative preparation of tubulin from A549 cells is presented in Figure 1. There was no detectable tubulin in the first pellet (PI) containing cell debris and DNA, indicating that essentially all tubulin in the cell lysate (SI) was present in a soluble form. Tubulin polymerization by Taxol was quantitative as 98% of the tubulin present in SI was recovered in the Taxol-stabilized microtubule pellet (PII). The Taxol-stabilized microtubule pellet was washed with NaCl to release microtubule-associated proteins (MAPs). The resulting pellet (PIII) was highly enriched in tubulin, but a significant presence of tubulin was observed in SIII. Nevertheless, this loss from PIII was random regarding tubulin isotypes (data not shown) and most likely represented denatured tubulin. Therefore, the final microtubule pellet, PIII, was representative of cellular tubulin composition. We estimated that ~0.3 mg of tubulin was obtained from each preparation. Tubulin represented ~2% of total protein and approximately 5% of total soluble proteins in A549 cells.

**Separation of Tubulin Isotypes by Isoelectric Focusing.** IPG plates (pH 4.5–5.4) and IPG strips (pH 4–7) have been previously used to separate tubulin isoforms (17–19), but as indicated in Table 1, differences in pI values between two isotypes can be as small as 0.01. Only narrow-range IPG gels (pH 4.5–5.5) can resolve tubulin isotypes with such small differences in pI values. The length of the IPG gel and the shape of the pH gradient are also factors that increase the maximum separation of proteins. Therefore, we used 18

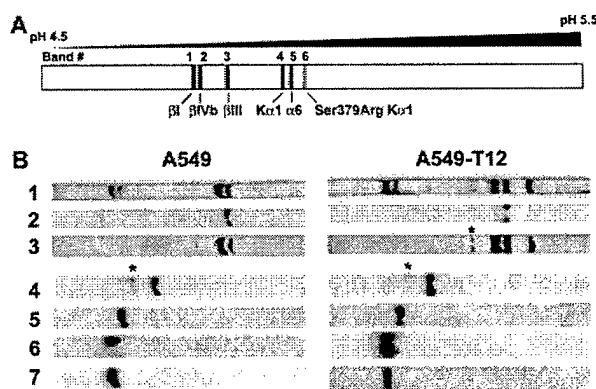


**FIGURE 2:** IEF-based analysis of tubulin isotypes in A549 and A549-T12 cells. (A) Schematic representation of an IPG strip (pH 4.5–5.5). Predicted positions of tubulin isotypes present in A549 cells are depicted as vertical black bands. A gray band indicates the predicted position of the mutant K $\alpha$ 1-tubulin present in A549-T12 cells. Bands were numbered from the most acidic to the most basic pI value. (B) Tubulin isotypes present in Taxol-stabilized microtubule pellets from A549 (left) or A549-T12 (right) cells were separated by IEF on 18 cm IPG strips and electrotransferred to nitrocellulose membranes: lane 1, IPG strips stained with Coomassie blue after electrotransfer; lane 2, blots probed with anti- $\alpha$ 6-tubulin antibody; lane 3, blots probed with anti-K $\alpha$ 1-tubulin antibody; lane 4, blots probed with anti- $\beta$ III-tubulin antibody; lane 5, blots probed with anti- $\beta$ IV-tubulin antibody; lane 6, blots probed with anti- $\beta$ I-tubulin antibody; lane 7, blots probed with anti- $\beta$ II antibody. Asterisks denote minor acidic isoforms (see the Results).

**Table 2: pI Differences between Tubulins**

$\Delta$ pI	calculated	measured <sup>a</sup>
$\alpha 6 - K\alpha 1$	+0.020	+0.017
mutant K $\alpha 1 - K\alpha 1$	+0.040	+0.044
$\beta III - \beta I$	+0.050	+0.055
$\beta IVb - \beta I$	+0.010	+0.011
glu K $\alpha 1 - K\alpha 1$	-0.030	-0.033
glu $\beta III - \beta III$	-0.030	-0.027

<sup>a</sup> Based on distances between bands (linear pH gradient).

cm IPG strips with a linear pH gradient from 4.5 to 5.5, on which tubulin bands having a pI difference of only 0.01 could be separated from each other by 2 mm. To visualize tubulin isotypes, tubulin in cell extracts was purified and concentrated by Taxol-driven polymerization. This approach allowed us to use Coomassie blue staining of the IPG strips. On the basis of our previous studies in A549 non-small cell lung carcinoma cells (13, 14), we expected to find the following tubulin isotypes from acidic to basic pI:  $\beta$ I-,  $\beta$ IVb-,  $\beta$ III-, K $\alpha$ 1-, and  $\alpha$ 6-tubulin. Lane 1 in Figure 2B shows that we effectively separated four major protein bands contained in Taxol-stabilized microtubules from A549 cells. Two bands were in the pI range expected for most  $\beta$ -tubulins, and two bands were in the pI range for  $\alpha$ -tubulins (Table 1 and Figure 2A). In A549-T12 cells, an A549 Taxol-resistant cell line containing a Ser to Arg substitution at residue 379 in K $\alpha$ 1-tubulin, an additional major band in the pI range for  $\alpha$ -tubulins and a minor band with an intermediate pI between those of  $\alpha$ - and  $\beta$ -tubulins were observed. The differences in pI observed between each band on the IPG strips stained with Coomassie blue matched the calculated pI differences between  $\beta$ I-,  $\beta$ IVb-, and  $\beta$ III-tubulin and between K $\alpha$ 1- and  $\alpha$ 6-tubulin (Table 2). The minor band in A549-T12 matched the expected position for  $\beta$ III-tubulin, and the major ad-

Table 3: Analysis of Tryptic Digests from IEF Gel Bands by MALDI-TOF Mass Spectrometry

IEF gel piece <sup>a</sup>	tubulin isotype-specific peptide <sup>b</sup>	measured mass of peptide (Da)	calculated mass of peptide (Da)	$\Delta$ mass (Da)	protein determination <sup>c</sup>
band 1	47ISVYYNEATGGK <sub>58</sub>	1300.7	1300.6	-0.1	$\beta$ I-tubulin
	283ALTVPELTQQVFDK <sub>297</sub>	1658.6	1658.9	0.3	55% sequence coverage
	363MAVTFIGNSTAIQELFK <sub>379</sub>	1869.2	1869.0	-0.2	
band 2	63AVLDLEPGTMDSVR <sub>77</sub>	1600.7	1600.8	0.1	$\beta$ IVb-tubulin
	20FWEVISDEHGIDPTGTGTYHGSDQLQLER <sub>46</sub>	3115.6	3115.4	-0.2	49% sequence coverage
band 3	155VREEYPDR <sub>162</sub>	1062.7	1062.5	-0.2	$\beta$ III-tubulin
	310YLTVAIVFR <sub>318</sub>	1068.8	1068.6	-0.2	42% sequence coverage
	47ISVYYNEASSHK <sub>58</sub>	1396.6	1396.7	0.1	
	363MSSTFIGNSTAIQELFK <sub>379</sub>	1872.6	1872.0	-0.6	60% sequence coverage
	217LATPTYGDLNHLVSATMSGVTTSLR <sub>241</sub>	2604.7	2604.3	-0.4	
	217LATPTYGDLNHLVSATMSGVTTSLR <sub>241</sub> (MSO)	2620.5	2620.3	-0.2	
	20FWEVISDEHGIDPSGNYVGSDQLQLER <sub>46</sub>	3076.8	3076.4	-0.4	
band 4	340SIQFVDWCPTGFK <sub>352</sub>	1527.5	1527.7	0.2	K $\alpha$ 1-tubulin
	281AYHEQLSVADITNACFEPANQMVK <sub>304</sub> (MSO)	2694.0	2694.2	-0.2	60% sequence coverage
	423EDMAALEKDYEEVGVDSEGEDEGEY <sub>451</sub> <sup>d</sup>	3235.4	3235.3	-0.1	
band 5	431DYEEVGADSDADGEDEGEY <sub>449</sub> <sup>d</sup>	2077.8	2077.7	-0.1	$\alpha$ 6-tubulin
	281AYHEQLTVAEITNACFEPANQMVK <sub>304</sub> (MSO)	2706.5	2706.3	-0.2	56% sequence coverage
	423EDMAALEKDYEEVGADSDADGEDEGEY <sub>449</sub> <sup>d</sup>	2964.9	2965.1	0.2	

<sup>a</sup> IEF gel pieces were numbered from the most acidic to the most basic protein band (see Figure 2A). <sup>b</sup> Identified peptides and combinations of peptides specific for a tubulin isotype. MSO represents oxidized methionine. <sup>c</sup> Sequence coverage was calculated on the basis of all the matched tryptic peptides, i.e., tubulin isotype-specific and shared peptides detected. <sup>d</sup> Detection of these peptides was greatly improved in the negative mode.

ditional band, with the most basic pI, matched the position of K $\alpha$ 1-tubulin harboring the Ser379Arg mutation (20). The Coomassie blue-stained IPG strips shown in Figure 2 (lane 1) were stained after electrotransfer onto nitrocellulose membranes, indicating that only a small portion of the proteins in each band was effectively transferred.

**Validation of Tubulin Isotype Positions on IPG Strips by MALDI-TOF Mass Spectrometry.** The position of each tubulin band on the IPG strips was definitively assigned by performing in-gel trypsin digestion followed by analysis of the respective tryptic digests by MALDI-TOF MS (Table 3). The major tubulin species were assigned numbers from 1 to 6 from the most to the least acidic tubulin, i.e., from  $\beta$ I-tubulin to the mutant K $\alpha$ 1-tubulin present in A549-T12 microtubules (Figure 2A). After tryptic digestion of each excised band, mass analysis detected several isotype-specific tryptic peptides that confirmed the assignment of each band to an individual tubulin isotype class based on the sequence-derived pI values (see above). For band 6, corresponding to the mutant K $\alpha$ 1-tubulin, the tryptic peptide profile was identical to the wild-type K $\alpha$ 1-tubulin peptide profile, except that the ion with an  $m/z$  ratio of 1808.5, corresponding to the peptide 374–390, was not detected, whereas an additional ion with an  $m/z$  ratio of 1203.5 was present (data not shown). The Ser379Arg replacement in the mutant K $\alpha$ 1-tubulin introduces an additional trypsin cleavage site in the wild-type peptide 374–390 ( $m/z$  ratio of 1808.1), resulting in two new tryptic peptides, peptide 374–379 ( $m/z$  ratio of 691.9) that was not detected and peptide 380–390 ( $m/z$  ratio of 1203.3) that was detected.

**Probing of IEF Western Blots with Tubulin Isotype-Specific Antibodies.** A polyclonal anti- $\alpha$ 6-tubulin antibody recognized one band at the position corresponding to  $\alpha$ 6-tubulin (Figure 2B, lane 2). Our anti-K $\alpha$ 1-tubulin antibody was apparently also reacting with the  $\alpha$ 6-tubulin band and labeled the band corresponding to the mutant K $\alpha$ 1-tubulin from A549-T12 (lane 3). A minor  $\alpha$ -tubulin species, having

a pI more acidic than that of K $\alpha$ 1-tubulin, was also labeled with this antibody and corresponded most likely to monoglutamylated K $\alpha$ 1-tubulin (Table 2) (14). The anti- $\beta$ III-, anti- $\beta$ IV-, and anti- $\beta$ I-tubulin antibodies (Figure 2B, lanes 4–6, respectively) were remarkably specific, each of them labeling only the respective band for  $\beta$ III-,  $\beta$ IV-, and  $\beta$ I-tubulin. In the case of  $\beta$ III-tubulin, a second minor band was labeled and could correspond to either monoglutamylated or phosphorylated  $\beta$ III-tubulin (Table 2; see the Discussion). The anti- $\beta$ IV-tubulin antibody labeled one band corresponding to  $\beta$ IVb-tubulin. No labeling occurred at positions expected for either of the two possible  $\beta$ IVa-tubulin isotype sequences (Table 1). As expected, the anti- $\beta$ II-tubulin antibody and the anti- $\beta$ I-tubulin antibody labeled the same band because these two tubulin isotypes have the same pI value (Figure 2B, lane 7). Because of the previously mentioned potential cross-reactivity of this antibody with  $\beta$ I-tubulin (21) and the reported presence of  $\beta$ II-tubulin mRNA in these cells (13), we further examined the reactivity of this antibody (see below). The fact that none of the nine  $\beta$ II-tubulin-specific peptides were found in the tryptic digest of the  $\beta$ I-tubulin band (Table 3) strongly suggested that the anti- $\beta$ II-tubulin antibody was cross-reacting with  $\beta$ I-tubulin.

**Relative Quantitation of Tubulin Isotypes in A549 and A549-T12 Cells.** We evaluated the amount of total  $\alpha$ -tubulin and total  $\beta$ -tubulin by Western blot analysis after complete transfer of tubulin from a SDS-PAGE gel loaded with the different fractions presented in Figure 1. Using a standard curve with bovine brain tubulin and a pan  $\alpha$ - or a pan  $\beta$ -tubulin antibody, we obtained an  $\alpha$ : $\beta$  tubulin ratio of  $1.1 \pm 0.12$ . This ratio is close to the theoretical ratio of 1, considering that microtubules are formed of tubulin  $\alpha$ / $\beta$  heterodimers. However, the same evaluation of total  $\alpha$ -tubulin and total  $\beta$ -tubulin by Western blot analysis, after transferring IEF gels to nitrocellulose, was not possible because, as mentioned above, only a portion of the tubulin contained in each band transferred to the membrane.

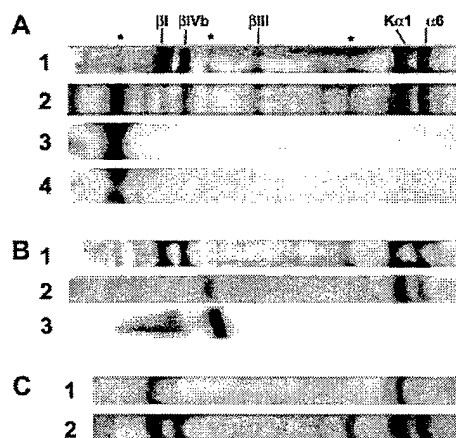


FIGURE 3: Tubulin isotypes in human cancer cell lines. Tubulin was isolated from parental and drug-resistant cell lines and analyzed by IEF. (A) Lane 1, A549 tubulin isotypes stained with Coomassie blue; lane 2, A549-EpoB40 tubulin isotypes stained with Coomassie blue; lane 3, A549-EpoB40 tubulin isotypes blotted on a nitrocellulose membrane that was probed with anti- $\beta$ I-tubulin antibody; lane 4, A549-EpoB40 tubulin isotypes blotted on a nitrocellulose membrane that was probed with anti- $\beta$ II-tubulin antibody. Asterisks denote minor acidic isoforms. (B) Lane 1, MDA-MB-231 tubulin isotypes stained with Coomassie blue; lane 2, MDA-MB-231-K20T tubulin isotypes stained with Coomassie blue; lane 3, MDA-MB-231-K20T tubulin isotypes blotted on a nitrocellulose membrane that was probed with anti- $\beta$ I-tubulin antibody. (C) CA46 (lane 1) and HeLa (lane 2) tubulin isoforms were stained with Coomassie blue.

Therefore, we stained the IEF gels with Coomassie blue and quantified each tubulin band, and when we summed all the signals from the  $\alpha$ -tubulin bands or all the signals from  $\beta$ -tubulin bands, the resulting ratio of total  $\alpha$ -tubulin to total  $\beta$ -tubulin was greater than 1 ( $1.4 \pm 0.45$  for A549  $1.5 \pm 0.33$  for A549-T12). This ratio was dependent on tubulin concentration, and the ratio decreased to 1.1 when the IEF gels were loaded with a larger amount ( $>200 \mu\text{g}$  of protein) of tubulin (see Figure 3A, lane 1). When Fast green was used as the stain in place of Coomassie blue, the same differential staining between  $\alpha$ - and  $\beta$ -tubulin was observed (data not shown). It would appear that this excess of  $\alpha$ -tubulin over  $\beta$ -tubulin is only apparent and is due to differential staining of  $\alpha$ - and  $\beta$ -tubulin by Coomassie blue. For this reason, on Coomassie blue-stained IEF gels, the relative amount of a particular  $\alpha$ -tubulin or a particular  $\beta$ -tubulin isotype was calculated as a percentage of the total  $\alpha$ -tubulin or total  $\beta$ -tubulin, respectively. From at least three independent measurements,  $\beta$ I- and  $\beta$ IVb-tubulin in A549 microtubules represented  $66 \pm 10.3$  and  $29 \pm 1.2\%$  of total  $\beta$ -tubulin, respectively. In most samples,  $\beta$ III could not be detected by Coomassie blue staining except when a larger amount of protein was loaded on the IEF gel (Figure 3A, lane 1). K $\alpha$ 1- and  $\alpha$ 6-tubulin in A549 represented  $66 \pm 1.4$  and  $34 \pm 1.3\%$  of the total  $\alpha$ -tubulin, respectively. In A549-T12,  $\beta$ I-,  $\beta$ IVb-, and  $\beta$ III-tubulin represented  $56 \pm 5.0$ ,  $38 \pm 4.0$ , and  $6 \pm 4.0\%$  of the total  $\beta$ -tubulin, respectively. K $\alpha$ 1-tubulin,  $\alpha$ 6-tubulin, and the mutant K $\alpha$ 1-tubulin represented  $41 \pm 3.6$ ,  $28 \pm 6.0$ , and  $30 \pm 2.4\%$  of the total  $\alpha$ -tubulin, respectively. These relative percentages of the different tubulin isotypes were similar regardless of the amount of protein loaded on the IEF gel or whether Coomassie blue or Fast green was used as a stain.

**Expression of Tubulin Isoforms and of  $\beta$ I-Tubulin Mutations in Cell Lines.** We have examined the tubulin isotype composition in other cell lines. Some of these cell lines were resistant to Taxol or epothilones and harbored pI-altering mutations in  $\beta$ I-tubulin. The A549-derived epothilone B-resistant cell line, A549-EpoB40, has a  $\beta$ I Gln292Glu mutation (5), and we observed the expected shift of  $\beta$ I-tubulin to a more acidic pI with no change in the pIs of other tubulins. However, an apparent decrease in the amount of  $\beta$ IVb-tubulin was noted (Figure 3A, lane 2). Western blotting with the anti- $\beta$ I-tubulin antibody confirmed that the  $\beta$ I-tubulin shifted to a more acidic pI and demonstrated that only the mutant  $\beta$ I-tubulin, but not the wild type, was expressed in this cell line (lane 3; see the Discussion). When the anti- $\beta$ II-tubulin antibody was used, the same labeling pattern was obtained as with the anti- $\beta$ I-tubulin antibody. Importantly, there was no labeling at the position corresponding to  $\beta$ II-tubulin or wild-type  $\beta$ I-tubulin, confirming the cross-reactivity of the anti- $\beta$ II-tubulin antibody with  $\beta$ I-tubulin (lane 4). The tubulin expression profile in MDA-MB-231 breast cancer cells was not significantly different from the A549 tubulin profile (Figure 3B, lane 1). The MDA-MB-231-K20T cell line has a  $\beta$ I Glu198Gly mutation (22), and we observed the expected shift of  $\beta$ I-tubulin to a more basic pI (lane 2). Western blotting with the anti- $\beta$ I-tubulin antibody confirmed that the  $\beta$ I-tubulin shifted to a more basic pI and demonstrated that most of the  $\beta$ I-tubulin consisted of mutant protein with possibly a trace of wild-type protein (lane 3; see the Discussion). The same labeling pattern was observed with the anti- $\beta$ II antibody (data not shown). Moreover, in this resistant cell line,  $\beta$ IVb-tubulin, when observed, appeared only as a faint band by Coomassie blue staining compared to the parental cell line. These observations were in agreement with RT-PCR quantitative results on this cell line.<sup>2</sup> In the Burkitt's lymphoma cell line CA46, we observed only two major tubulins,  $\beta$ I- and K $\alpha$ 1-tubulin, and two minor tubulins,  $\beta$ IVb- and  $\alpha$ 6-tubulin (Figure 3C, lane 1). In HeLa cells, the tubulin profile was very similar to A549 and MDA-MB-231 profiles except that there was an apparent increase in the level of monoglutamylated K $\alpha$ 1 and possibly monoglutamylated  $\beta$ I-tubulin (lane 2).

## DISCUSSION

Alterations in tubulin isotype expression and introduction of point mutations into one or both alleles of specific tubulin genes have been associated with resistance to microtubule-stabilizing agents. RT-PCR analysis, although useful for RNA quantitation and sequencing, does not provide insight into the levels of protein expression. With the advent of proteomic-based approaches, it becomes clear that there can be a discrepancy between mRNA transcripts and corresponding protein levels (23, 24).

The isolation of tubulin from cell extracts using Taxol-driven polymerization coupled to high-resolution IEF enabled us to easily visualize and analyze the different tubulin isoforms present in cancer cell lines. We confirmed the presence of the tubulin isotypes in A549 and MDA-MB-231 cell lines identified previously by MALDI-TOF mass spectrometry analysis of C-terminal tubulin peptides (14).

<sup>2</sup> K. Wiesen, unpublished observations.



Because the C-terminal sequence obtained previously by MS/MS for  $\alpha^*$ -tubulin (14) matches the C-terminal sequence of the recently described human  $\alpha 6$ -tubulin, and because in the study presented here a protein having the pI value predicted for human  $\alpha 6$ -tubulin was detected and confirmed as being  $\alpha 6$ -tubulin by peptide mapping, we consider them to be identical. An increase in the level of  $\beta$ III-tubulin was detected in A549-T12 cells compared to the parental A549 cells, which is in agreement with previous immunofluorescence studies (13). A minor  $\beta$ III-tubulin species that corresponded most likely to monoglutamylated or phosphorylated  $\beta$ III-tubulin was also detected. Only monoglutamylated  $\beta$ I-tubulin, identified previously by MALDI-TOF mass spectrometry analysis of C-terminal tubulin peptides (14), was not readily detected by Western blotting (14). In all the IPG strips stained with Coomassie blue, we generally observed a barely detectable band at the position of monoglutamylated  $\beta$ I-tubulin, whereas a band at the position of monoglutamylated K $\alpha$ 1-tubulin was clearly visible and was detected by the anti-K $\alpha$ 1-tubulin antibody. Non-neuronal polyglutamylases generate these isoforms (25), but the process that limits the glutamylation to only one residue is unclear. The higher percentage of stable microtubules in the brain may favor extensive polyglutamylation, and conversely, the greater dynamicity of cancer cell microtubules (26) may limit polyglutamylase activity. Noticeably, known posttranslational modifications of tubulin are predicted to induce a shift in pI values. This is exemplified with the highly modified brain tubulin that appears as multiple bands on IPG strips and gels (17, 18).

In our previous approach, C-terminal peptides were not separated prior to MALDI-TOF mass spectrometry analysis (14).  $\beta$ III-Tubulin was not detected, and  $\beta$ IVb-tubulin represented a very small amount of C-terminal peptide. In this case, ions for minor tubulin species such as  $\beta$ III-tubulin or  $\beta$ IVb-tubulin could have been suppressed by the presence of the more highly abundant tubulin C-terminal peptides and/or because of differential ionization efficiencies of the various peptides. These technical limitations are overcome in the present isoelectrofocusing/mass spectrometry approach where the total amount of each tubulin isotype is analyzed directly, giving a better appreciation of isotype ratios. Our quantitation of Coomassie blue-stained IEF gels is still only relative. Nevertheless, when LC-MS was used to analyze the same Taxol-stabilized microtubule pellet from A549 and the deconvoluted mass peaks corresponding to each tubulin isotype were integrated, similar relative percentages were obtained.<sup>3</sup> Interestingly, the ratios of K $\alpha$ 1-tubulin to  $\beta$ I-tubulin and  $\alpha 6$ -tubulin to  $\beta$ IVb-tubulin are close to 1 in the cell lines that have been examined so far. In CA46 Burkitt's lymphoma,  $\alpha 6$ - and  $\beta$ IVb-tubulin are both minor species. This trend suggests that there could be a specific pairing of a particular  $\alpha$ -tubulin isotype with a particular  $\beta$ -tubulin isotype, and we plan to investigate the possibility of such  $\alpha/\beta$  subunit sorting.

The most striking difference between our analysis of tubulin isotype expression at the protein level (ref 14 and this study) and previous studies at the mRNA level (13) is the absence of detectable  $\beta$ IVa- and  $\beta$ II-tubulin expression

in both sensitive and resistant cell lines. In A549,  $\beta$ III-,  $\beta$ II-,  $\beta$ IVa-, and  $\beta$ IVb-tubulin mRNA were present at low and similar levels (RT-PCR tubulin isotype: $\beta$ 2-microglobulin ratio of  $\sim 0.15$ ) that were approximately 10 times lower than that of  $\beta$ I-tubulin mRNA (RT-PCR ratio of  $\sim 1.5$ ). A 2-fold increase in  $\beta$ III-,  $\beta$ II-, and  $\beta$ IVa-tubulin mRNA levels was observed in A549-T12 (13). In agreement with the results presented here, both  $\beta$ II- and  $\beta$ IVa-tubulin isotypes could not be detected by MALDI-TOF mass spectrometry of C-terminal peptides derived from total A549 cell extracts (14). The reasons for the discrepancy between tubulin isotype mRNA and protein expression levels are not clear, but such differences have been observed for other proteins (23, 24). Since our data established that tubulin was quantitatively recovered from cells by Taxol-driven polymerization (Figure 1), either there is an unknown bias in the RT-PCR results or there is a still unknown silencing mechanism of  $\beta$ II- and  $\beta$ IVa-tubulin mRNA translation. Increased  $\beta$ III-tubulin expression levels have been repeatedly confirmed at the protein level using a variety of methods in cell lines resistant to Taxol (13, 27–30). Together with the study presented here, these observations strongly suggest that only  $\beta$ III-tubulin levels correlate with sensitivity toward Taxol (13, 27–30) and that the regulation of  $\beta$ -tubulin expression is even more complex than the autoregulatory mechanism described by Cleveland and colleagues (9).

Mutations that produce a change in charge are likely to have a significant effect on protein function and/or drug binding. In the case of tubulin, we and others have obtained such mutations in cell lines selected for resistance to microtubule-stabilizing drugs (5–8). When analyzed by two-dimensional gel electrophoresis, the wide pH range used in the first dimension resulted in a poor resolution of the spots corresponding to wild-type and mutant proteins and prevented quantitation. Like the expression of a particular isotype, the detection of wild-type and mutant mRNA of a specific tubulin does not indicate that it is translated and, if so, at what ratio. Most likely, mutations affect only one allele (8), and it is expected that both tubulin isoforms would be produced in equal amounts. We found that situation in A549-T12, where the percentage of wild-type K $\alpha$ 1-tubulin decreased at the expense of mutant K $\alpha$ 1-tubulin ( $\sim 30\%$  of the total  $\alpha$ -tubulin). But in two cell lines, MDA-MB-231-K20T and A549-EpoB40, the wild-type  $\beta$ I-tubulin mRNA was not detected by RT-PCR (5, 22) and only the mutant protein was detected in these cells. The heterozygous status would need to be checked at the DNA level, and if confirmed, it would imply a silencing mechanism of the wild-type allele (8). If a mutation in tubulin plays a role in resistance to microtubule-interacting agents, the ratio of mutant tubulin to wild-type tubulin in a cell should influence the degree of resistance. In fact, when equal amounts of wild-type and mutant tubulin are expressed, the level of resistance to Taxol tends to be lower than when only the mutant tubulin is expressed (5, 8, 13).

The anti- $\beta$ -tubulin isotype monoclonal antibodies produced and characterized by R. F. Ludueña and co-workers (31–33) represent valuable tools that have helped to unravel the functional significance of the different  $\beta$ -tubulin isotypes. No cross-reactivity of the anti- $\beta$ I-, anti- $\beta$ III-, and anti- $\beta$ IV-tubulin antibodies was observed in this study. This is contrary

<sup>3</sup> P. Verdier-Pinard, manuscript in preparation.

to what has been published for nondenaturing immunoaffinity isolation of  $\alpha/\beta$ -tubulin heterodimers enriched in  $\beta$ I-,  $\beta$ II-,  $\beta$ III-, or  $\beta$ IV-tubulin isotypes (21, 31, 34, 35). Therefore, the presence of contaminating  $\beta$ -tubulin isotypes of a different class in these fractions is more likely due to heterodimer-heterodimer interactions in residual small oligomers than to cross-reactivity of these antibodies with multiple isotypes. However, extensive cross-reactivity of the anti- $\beta$ II-tubulin antibody with  $\beta$ I-tubulin was confirmed. The peptide EGEDEEA that was used to generate the anti- $\beta$ II-tubulin antibody is from the C-terminal sequence of chicken  $\beta$ II-tubulin (EEGEDEEA in humans; see Table 1) (21). The human  $\beta$ I-tubulin C-terminus contains the sequence GEEAEEEA, so it is possible that the anti- $\beta$ II-tubulin recognizes the GEE sequence present in the  $\beta$ I-tubulin C-terminus. Recently, Arai et al. (36) described an anti- $\beta$ II-tubulin polyclonal antibody that specifically recognized the EEEEGED sequence of the human  $\beta$ II-tubulin C-terminus and did not cross-react with C-terminal peptides of other  $\beta$ -tubulin isotypes. The peptide EAEEVEA that is common to  $\beta$ IVa and  $\beta$ IVb was used to generate the anti- $\beta$ IV-tubulin antibody (34). Thus, both isotypes, with clearly distinct pIs, can be labeled with this antibody. However, we have observed only the presence of  $\beta$ IVb-tubulin in the cell lines examined so far.

There are fewer  $\alpha$ -tubulin isotype-specific antibodies available (37). A rabbit polyclonal antibody against human  $\alpha$ 6-tubulin, made in our laboratory by S. Rao, did not cross-react with  $\alpha$ 1-tubulin. However, the anti- $\alpha$ 1-tubulin polyclonal antibody cross-reacted with  $\alpha$ 6-tubulin. Further testing of these antibodies on samples containing different  $\alpha$ -tubulin isotypes will permit a more extensive definition of their specificity. Altogether, our approach provides a method for screening the specificity of antibodies directed against tubulin isotypes and establishes that the anti- $\beta$ I-, anti- $\beta$ III-, anti- $\beta$ IV-tubulin antibodies are highly specific.

A similar analysis of tubulin isotypes at the protein level in human tumor biopsies would provide an alternative to RT-PCR for investigating the clinical relevance of differential expression of tubulin isotypes in relation to the responsiveness of patients to microtubule-interacting drugs. Recent clinical data from non-small cell lung cancer patients indicated that both  $\beta$ III-tubulin mRNA levels (38) and  $\beta$ III-tubulin protein levels (39) were higher in tumors that did not respond to taxane-based treatment. Finally, the microtubule cytoskeleton appears to be increasingly involved in several neurodegenerative diseases (40–45), and comparative analysis of tubulin protein expression with normal tissue would provide greater insight into these pathologies.

## ACKNOWLEDGMENT

We thank Dr. Srinivasa Rao for generating the SRa1 and SRa2 antibodies and Ms. Linda Siconolfi-Baez for assistance with the IEF procedure.

## REFERENCES

- Gundersen, G. G., and Cook, T. A. (1999) *Curr. Opin. Cell Biol.* 11, 81–94.
- Ludueña, R. F. (1998) *Int. Rev. Cytol.* 178, 207–275.
- Ludueña, R. F. (1993) *Mol. Biol. Cell* 4, 445–457.
- Burkhardt, C. A., Kavallaris, M., and Horwitz, S. B. (2001) *Biochim. Biophys. Acta* 1471, 1–9.
- He, L., Yang, C.-P. H., and Horwitz, S. B. (2001) *Mol. Cancer Ther.* 1, 3–10.
- Giannakakou, P., Gussio, R., Nogales, E., Downing, K. H., Zaharevitz, D., Bollbuck, B., Poy, G., Sackett, D., Nicolaou, K. C., and Fojo, T. (2000) *Proc. Natl. Acad. Sci. U.S.A.* 97, 2904–2909.
- Gonzalez-Garay, M. L., Chang, L., Blade, K., Menick, D. R., and Cabral, F. (1999) *J. Biol. Chem.* 274, 23875–23882.
- Giannakakou, P., Sackett, D. L., Kang, Y. K., Zhan, Z., Buters, J. T., Fojo, T., and Poruchynsky, M. S. (1997) *J. Biol. Chem.* 272, 17118–17125.
- Cleveland, D. W. (1988) *Trends Biochem. Sci.* 13, 339–343.
- Verdier-Pinard, P., Kepler, J. A., Pettit, G. R., and Hamel, E. (2000) *Mol. Pharmacol.* 57, 180–187.
- Singer, W. D., and Himes, R. H. (1992) *Biochem. Pharmacol.* 43, 545–551.
- Thrower, D., Jordan, M. A., and Wilson, L. (1991) *J. Immunol. Methods* 136, 45–51.
- Kavallaris, M., Kuo, D. Y., Burkhardt, C. A., Regl, D. L., Norris, M. D., Haber, M., and Horwitz, S. B. (1997) *J. Clin. Invest.* 100, 1282–1293.
- Rao, S., Aberg, F., Nieves, E., Horwitz, S. B., and Orr, G. A. (2001) *Biochemistry* 40, 2096–2103.
- Vallee, R. B. (1982) *J. Cell Biol.* 92, 435–442.
- Castellanos-Serra, L., Vallin, A., Proenza, W., Le Caer, J. P., and Rossier, J. (2001) *Electrophoresis* 22, 1677–1685.
- Towbin, H., Ozbey, O., and Zingel, O. (2001) *Electrophoresis* 22, 1887–1893.
- Williams, R. C., Jr., Shah, C., and Sackett, D. (1999) *Anal. Biochem.* 275, 265–267.
- Shah, C., Xu, C. Z., Vickers, J., and Williams, R. (2001) *Biochemistry* 40, 4844–4852.
- Martello, L. A., Verdier-Pinard, P., Shen, H. J., He, L., Torres, K., Orr, G. A., and Horwitz, S. B. (2003) *Cancer Res.* 63, 1207–1213.
- Banerjee, A., Roach, M. C., Wall, K. A., Lopata, M. A., Cleveland, D. W., and Ludueña, R. F. (1988) *J. Biol. Chem.* 263, 3029–3034.
- Wiesen, K., Xia, S., and Horwitz, S. B. (2002) in *AACR 93rd Annual Meeting Proceedings*, pp 788, American Association for Cancer Research, San Francisco.
- Gygi, S. P., Rochon, Y., Franza, B. R., and Aebersold, R. (1999) *Mol. Cell. Biol.* 19, 1720–1730.
- Chen, G., Gharib, T. G., Huang, C. C., Taylor, J. M., Misek, D. E., Kardias, S. L., Giordano, T. J., Iannettoni, M. D., Orringer, M. B., Hanash, S. M., and Beer, D. G. (2002) *Mol. Cell. Proteomics* 1, 304–313.
- Regnard, C., Desbruyeres, E., Denoulet, P., and Eddé, B. (1999) *J. Cell Sci.* 112, 4281–4289.
- Yvon, A. M., Wadsworth, P., and Jordan, M. A. (1999) *Mol. Biol. Cell* 10, 947–959.
- Ranganathan, S., Benetatos, C. A., Colarusso, P. J., Dexter, D. W., and Hudes, G. R. (1998) *Br. J. Cancer* 77, 562–566.
- Ranganathan, S., Dexter, D. W., Benetatos, C. A., and Hudes, G. R. (1998) *Biochim. Biophys. Acta* 1395, 237–245.
- Nicoletti, M. I., Valoti, G., Giannakakou, P., Zhan, Z., Kim, J. H., Lucchini, V., Landoni, F., Mayo, J. G., Giavazzi, R., and Fojo, T. (2001) *Clin. Cancer Res.* 7, 2912–2922.
- Carles, G., Braguer, D., Dumontet, C., Bourgaire, V., Gonçalves, A., Sarrazin, M., Rognoni, J. B., and Briand, C. (1999) *Br. J. Cancer* 80, 1162–1168.
- Banerjee, A., Roach, M. C., Trcka, P., and Ludueña, R. F. (1990) *J. Biol. Chem.* 265, 1794–1799.
- Panda, D., Miller, H. P., Banerjee, A., Ludueña, R. F., and Wilson, L. (1994) *Proc. Natl. Acad. Sci. U.S.A.* 91, 11358–11362.
- Schwarz, P. M., Liggins, J. R., and Ludueña, R. F. (1998) *Biochemistry* 37, 4687–4692.
- Banerjee, A., Roach, M. C., Trcka, P., and Ludueña, R. F. (1992) *J. Biol. Chem.* 267, 5625–5630.
- Roach, M. C., Boucher, V. L., Walss, C., Ravdin, P. M., and Ludueña, R. F. (1998) *Cell Motil. Cytoskeleton* 39, 273–285.
- Arai, K., Shibutani, M., and Matsuda, H. (2002) *Cell Motil. Cytoskeleton* 52, 174–182.
- Gu, W., Lewis, S. A., and Cowan, N. J. (1988) *J. Cell Biol.* 106, 2011–2022.
- Rosell, R., Fossella, F., and Milas, L. (2002) *Lung Cancer* 38, 43–49.

39. Dumontet, C., Isaac, S., Souquet, P. J., Bejui-Thivolet, F., Pacheco, Y., Peloux, N., Frankfurter, A., Ludueña, R. F., and Perol, M. (2002) *Electron. J. Oncol.* 1, 58–64.
40. Garcia, M. L., and Cleveland, D. W. (2001) *Curr. Opin. Cell Biol.* 13, 41–48.
41. Vijayan, S., El-Akkad, E., Grundke-Iqbal, I., and Iqbal, K. (2001) *FEBS Lett.* 509, 375–381.
42. Sato, K., and Abe, K. (2001) *Brain Res.* 904, 157–160.
43. Schuller, E., Gulesserian, T., Seidl, R., Cairns, N., and Lube, G. (2001) *Life Sci.* 69, 263–270.
44. Baumann, M. H., Wisniewski, T., Levy, E., Plant, G. T., and Ghiso, J. (1996) *Biochem. Biophys. Res. Commun.* 219, 238–242.
45. Parvari, R., HersHKovitz, E., Grossman, N., Gorodischer, R., Loeys, B., Zecic, A., Mortier, G., Gregory, S., Sharony, R., Kambouris, M., Sakati, N., Meyer, B. F., Al Aqeel, A. I., Al Humaidan, A. K., Al Zahrani, F., Al Swaid, A., Al Othman, J., Diaz, G. A., Weiner, R., Khan, K. T., Gordon, R., and Gelb, B. D. (2002) *Nat. Genet.* 32, 448–452.

BI027293O

# Direct Analysis of Tubulin Expression in Cancer Cell Lines by Electrospray Ionization Mass Spectrometry<sup>†</sup>

Pascal Verdier-Pinard,<sup>†,‡</sup> Fang Wang,<sup>§,‡</sup> Berta Burd,<sup>‡</sup> Ruth Hogue Angeletti,<sup>§</sup> Susan Band Horwitz,<sup>‡</sup> and George A. Orr<sup>\*,‡</sup>

Department of Molecular Pharmacology and Laboratory for Macromolecular Analysis and Proteomics,  
Albert Einstein College of Medicine, Bronx, New York 10461

Received June 13, 2003; Revised Manuscript Received August 14, 2003

**ABSTRACT:** Differential expression of tubulin isotypes, mutations, and/or post-translational modifications in sensitive and Taxol-resistant cell lines suggests the existence of tubulin-based mechanisms of resistance. Since tubulin isotypes are defined by their C-terminal sequence, we previously described a matrix-assisted laser desorption/ionization time-of-flight mass spectrometry-based analysis of tubulin diversity in human cell lines by analysis of their CNBr-released C-terminal peptides [Rao, S., Aberg, F., Nieves, E., Horwitz, S. B., and Orr, G. A. (2001) *Biochemistry* 40, 2096–103]. We now describe the liquid chromatography/electrospray ionization mass spectrometry analysis of native tubulins in Taxol-stabilized microtubules from parental and Taxol/epothilone-resistant human cancer cell lines. This method allows the direct determination of tubulin isotype composition, including post-translational modifications and mutations occurring throughout the entire protein. Four major isotypes,  $\beta$ I-,  $\beta$ IVb-,  $\alpha$ 1-, and  $\alpha$ 6-tubulin, were detected in two human carcinoma cell lines, A549 and HeLa.  $\beta$ III-Tubulin represented a minor species, as did  $\alpha$ 4-tubulin which was detected for the first time in both cell lines. The three  $\alpha$ -tubulins were almost totally tyrosinated, and post-translational modifications were limited to low levels of monoglutamylation of  $\alpha$ 1-,  $\beta$ I-, and  $\beta$ III-tubulin.  $\beta$ II- and  $\beta$ IVa-tubulins were not detected in either parental or drug-resistant cell lines, in contrast to previous RNA-based studies. Since mutations can occur in a single tubulin allele, the question as to whether the wild-type and mutant transcripts are both translated, and to what levels, is important. Heterozygous expression of  $\alpha$ 1- or  $\beta$ I-tubulin mutants that introduced mass changes as small as 26 Da was readily detected in native tubulins isolated from Taxol- and epothilone-resistant cell lines.

Microtubules composed of  $\alpha/\beta$ -tubulin heterodimers are involved in a diverse range of cellular functions including motility, morphogenesis, intracellular trafficking of macromolecules and organelles, and mitosis and meiosis (1–3). This functional diversity is achieved through the association of structural and motor MAPs<sup>1</sup> with microtubules. MAPs have the ability to regulate the dynamic organization and stability of microtubules and also to recruit other proteins to the microtubule cytoskeleton. The multiple  $\alpha$ - and  $\beta$ -tubulin isotypes (each ~450 amino acids), although highly conserved, display extensive sequence variations at their

C-termini which participate in the binding of MAPs to microtubules (4). Additionally, tubulins are post-translationally modified by polyglutamylation, polyglycylation, and phosphorylation on both  $\alpha$ - and  $\beta$ -subunits, and by acetylation, detyrosination/tyrosination, and removal of the penultimate glutamic acid residue on  $\alpha$ -tubulins (4, 5). The functional significance of this structural diversity remains unclear, except that specific isotypes are incorporated into microtubule-based organelles, such as centrioles, and that differential expression of tubulin isotypes has been observed between tissues and during development (4). The highly divergent C-termini may provide a mechanism for isotype-specific MAP binding. Although MAPs generally regulate their binding affinity for microtubules by phosphorylation, there is an increasing body of evidence suggesting that post-translational modifications of  $\alpha/\beta$ -tubulin can also regulate the association of MAPs with microtubules (6, 7).

The microtubule cytoskeleton has emerged as an effective target for cancer chemotherapy (8), as demonstrated by the clinical effectiveness of Taxol that has been approved by the FDA for the treatment of ovarian, breast, and non-small-cell lung carcinomas. Taxol is an anti-mitotic agent that has the capacity to stabilize microtubules against depolymerization. As with many cancer chemotherapeutic agents, resistance remains a significant problem in the treatment of

<sup>†</sup> This work was supported in part by USPHS Grants CA 39821 and CA 77263, by the National Foundation for Cancer Research (S.B.H.), AI49749, and by Grant DAMD17-01-0123 from the Department of Defense Breast Cancer Program (G.A.O.).

\* To whom correspondence should be addressed. Tel.: (718) 430-3742. Fax: (718) 430-8922. E-mail: orr@aecom.yu.edu.

<sup>‡</sup> Department of Molecular Pharmacology.

<sup>§</sup> Laboratory for Macromolecular Analysis and Proteomics.

<sup>‡</sup> These authors contributed equally to this work.

<sup>1</sup> Abbreviations used: Da, dalton; ESI-MS, electrospray ionization mass spectrometry; FTICR, Fourier transform ion cyclotron resonance; IEF, isoelectric focusing; LC-MS, liquid chromatography-mass spectrometry; MALDI-TOF MS, matrix-assisted laser desorption/ionization time-of-flight; MAPs, microtubule-associated proteins; MS/MS, tandem mass spectrometry; RT-PCR, reverse transcriptase-polymerase chain reaction; SDS-PAGE, sodium dodecyl sulfate-polyacrylamide gel electrophoresis; TFA, trifluoroacetic acid.

malignancies with Taxol (9, 10). It is not known by what mechanisms human tumors become resistant to Taxol, but it is probable that there is more than one mechanism involved in most tumors.

Microtubules are dynamic, not static, polymers and the precise regulation of this dynamicity is important for many cellular processes (1, 11, 12). Alterations in microtubule dynamics that occur in the development of resistance to Taxol and other microtubule-stabilizing drugs have become an emerging theme in drug resistance literature (9, 10, 13, 14). The dynamics of individual rhodamine-labeled microtubules in Taxol-sensitive and -resistant A549 cell lines, derived from a human lung carcinoma, have been quantified by digital time-lapse microscopy (15). The A549-T12 and -T24 cell lines, 9- and 17-fold resistant to Taxol, respectively, were selected by continual exposure of the parental drug-sensitive cell line to increasing concentrations of drug (23). The microtubules from both resistant cell lines exhibited increased dynamic instability compared with the parental, drug-sensitive cell line. There are several potential mechanisms by which microtubule dynamics could be modulated in a Taxol-resistant cell line: altered tubulin isotype expression, mutations to tubulin that affect either longitudinal/lateral interactions or binding of regulatory proteins, alterations in post-translational modifications of tubulin that modify regulatory protein binding, and altered expression or post-translational modifications to microtubule regulatory proteins.

Altered expression of tubulin isotypes and mutated tubulins has been detected in cancer cell lines resistant to microtubule-interacting agents. Microtubules consisting of one particular  $\beta$ -tubulin isotype display differential dynamics and exhibit differential sensitivity to the suppressive effects of Taxol on microtubule dynamics (16–19). There have been numerous reports of altered expression of individual  $\beta$ -tubulin isotypes in cells that have been selected for resistance to antimetabolic agents (20–29). These studies suggest that altered expression of  $\beta$ -tubulin isotypes, especially classes III and IVa, may be correlated with Taxol sensitivity. Mutations in  $\beta$ 1-tubulin either within the Taxol-binding pocket or in domains involved in microtubule assembly have been detected in cell lines resistant to microtubule agents (30–33).

There is a need for rapid, sensitive, and accurate methods for assessing tubulin composition, modifications, and mutations in human cell lines and tissues. We previously reported on the tubulin structural diversity in human cancer cell lines by utilizing negative ion MALDI-TOF MS to analyze the highly acidic C-terminal human tubulin peptides generated by CNBr digestion (34). However, this method does not allow the detection of modifications or mutations occurring outside of the extreme C-terminal domain. More recently, we used isoelectric focusing combined with MALDI mass mapping to resolve and characterize tubulin isotypes in human cell lines (35). This method allows the analysis of post-translational modifications but limits the detection of mutations to those introducing a change in charge. In this paper, we describe the direct analysis of native tubulin isotypes by LC-MS analysis of microtubules isolated from cell lines sensitive or resistant to Taxol and epothilones.

## MATERIAL AND METHODS

**Chemicals.** Taxol was obtained from the Drug Development Branch of the National Cancer Institute (Bethesda,

MD), dissolved in sterile DMSO, and stored at  $-20^{\circ}\text{C}$ . Trypsin was obtained from Promega (Madison, WI). All other chemicals were obtained from Sigma (St. Louis, MO), except where noted.

**Cell Culture.** A549, a human non-small-cell lung line, and HeLa, a human cervical carcinoma cell line, were maintained as described previously (23, 36).

**Isolation of Tubulin from Cell Lines.** Taxol-stabilized microtubule pellets were isolated from cytosolic extracts following the method of Vallee (37) as described previously (35).

**LC-MS.** Taxol-stabilized microtubules ( $\sim 10\ \mu\text{g}$ ) were dissolved in 70% formic acid and immediately loaded onto a  $1.0 \times 150\text{-mm}$  Vydac  $\text{C}_4$  column (Vydac, Hesperia, CA) at a flow rate of  $50\ \mu\text{L}/\text{min}$ . The mobile phases used for protein separations were 5% acetonitrile containing 0.1% TFA (solvent A) and 95% (v/v) acetonitrile containing 0.1% TFA (solvent B). The protein samples were initially desalted with 5% solvent B for 45 min and then separated using either 0.2%/min or 0.05%/min solvent B gradients. For the 0.2%/min gradient, the initial 5% solvent B was increased to 40% over 3 min, followed by 40–60% (100 min) and 60–95% (7 min) gradients. The 0.05%/min gradient was generated by a 5–30% gradient (3 min), followed by 30–45% (17 min), 45–51% (120 min), and 51–75% B (5 min) gradients. The column effluent was delivered directly to a LCQ quadrupole ion trap mass spectrometer (ThermoFinnigan, Riviera Beach, FL). The mass spectrometer was operated in normal MS scan mode to detect ions in the  $m/z$  range of 900–1300.

**"In Solution" Trypsin Digestion of HPLC Fractions.** Proteins were separated as described above using the 0.05%/min solvent B gradient, except that the column effluent flow ( $50\ \mu\text{L}/\text{min}$ ) was split for fraction collection ( $35\ \mu\text{L}/\text{min}$ ) and for delivery to the ion trap mass spectrometer ( $15\ \mu\text{L}/\text{min}$ ). The appropriate HPLC fractions were pooled and centrifuged by a SpeedVac concentrator to evaporate solvents and to reduce the volume to ca.  $10\ \mu\text{L}$ . Twenty microliters of 200 mM ammonium bicarbonate, pH 8.1, was added to each tube, followed by the addition of  $6\ \mu\text{L}$  of trypsin ( $0.05\ \mu\text{g}/\mu\text{L}$ ) dissolved in ammonium bicarbonate. Incubations were performed overnight at  $37^{\circ}\text{C}$  with constant shaking. The digests were desalted by Millipore C18 ZipTip, and the tryptic peptides were eluted with 50% acetonitrile/ $\text{H}_2\text{O}$  solution containing 0.1% TFA ( $4\ \mu\text{L}$ ).

**Analysis of Tubulin C-Terminal Peptides.** Tubulin was isolated from cells as described previously (35). Taxol-stabilized microtubule pellets were solubilized in Laemmli sample buffer, and proteins were separated by SDS-PAGE using running conditions that separate  $\alpha$ -tubulin from  $\beta$ -tubulin (38). Gels were transferred to nitrocellulose and stained with Ponceau Red, and regions containing either  $\alpha$ - or  $\beta$ -tubulin were cut and processed for CNBr digestion and negative-mode MALDI-TOF MS analysis as described previously (34).

**Protein Identification.** MALDI spectra were recorded in the positive or the negative mode on a Voyager-DE STR MALDI-TOF mass spectrometer (PerSeptive Biosystems, Framingham, MA), equipped with a 2.0-m flight tube and a 337-nm nitrogen laser. Saturated  $\alpha$ -cyano-4-hydroxycinnamic acid was used as the matrix. Protein identification was accomplished through database searching (Swiss-Prot and

NCBI) using MS-Fit and ProFound programs (*Homo sapiens*/*Mus musculus*, mass tolerance of 1 Da, partially oxidized methionine, average and/or monoisotopic masses, and a maximum of two miscleavages). The mass value for each tubulin isotype was calculated using the Compute MW/pI tool from the ExPaSy website.

## RESULTS AND DISCUSSION

Alterations in tubulin isotype composition and mutations have been proposed as potential mechanisms of resistance toward microtubule-interacting cytotoxic drugs. However, the structural diversity of mammalian tubulins, involving multiple isotypes with assorted post-translational modifications, makes comparative analysis between sensitive and resistant cell lines difficult. Both RT-PCR product quantitation and sequencing or antibody-based approaches with tubulin isotype-specific antibodies have been exploited to study the tubulin composition in drug-sensitive and -resistant cell lines. However, there is often a poor correlation between mRNA and translated protein levels (39, 40). This is of special relevance when a mutation occurs in a single allele of a specific tubulin gene, since it is important to know whether both wild-type and mutant alleles are expressed and at what levels. No  $\alpha$ -tubulin isotype-specific antibodies are readily available, except for those directed against specific post-translational modifications i.e., acetylated, tyrosinated, and non-tyrosinated  $\alpha$ -tubulins. Antibodies are available that recognize glutamylated and glycylation  $\alpha/\beta$ -tubulins, but these antibodies give no insight into the length of the appended side chain. This is important information since it has been proposed that tubulin polyglutamylation regulates the binding of both structural and motor MAPs as a function of the length of the polyglutamyl side chain (6, 7).

**Analysis of Tubulins by Mass Spectrometry.** In recent years, mass spectrometry-based approaches have gained in popularity for the analysis of tubulins across distinct phyla, from lower protozoa to mammals (41–50). These studies have focused largely on the analysis of the C-terminal peptides in order to define the post-translational modifications that occur to this domain of tubulin. In mammalian brain tubulin, polyglutamylation of  $\alpha$ - and  $\beta$ -tubulin (47), phosphorylation of  $\beta$ III-tubulin (41), reversible tyrosination of  $\alpha$ -tubulin (47), removal of penultimate glutamate from detyrosinated  $\alpha$ -tubulin, and more recently polyglycylation of  $\Delta$ 2-tubulin (51) were demonstrated by mass spectrometry. In contrast, studies of mammalian tubulin from non-neuronal sources by mass spectrometry are very few. We recently developed a strategy for the analysis of tubulin isotype composition and their post-translational modifications in A549, a non-small-cell lung cancer cell line, and in MDA-MB-231, a breast carcinoma cell line (34). Tubulins present in total cell extracts from these cell lines were analyzed by SDS-PAGE and transferred to nitrocellulose, followed by excision of the tubulin region of the membrane and CNBr digestion. The released peptides were analyzed by negative ion mode MALDI-TOF mass spectrometry to detect selectively the highly acidic C-terminal tubulin peptide ions (34, 52). In these cancer cell lines, the major tubulin isotypes detected were K $\alpha$ 1- and  $\beta$ I-tubulin, as well as  $\beta$ IVb-tubulin and, at that time, a new human  $\alpha$ -tubulin that was named  $\alpha^*$ . Subsequent work (see below) established that this isotype was the human homologue of mouse  $\alpha$ 6. In contrast to brain

Table 1: Calculated Masses of Human Tubulin Isoforms

accession no. <sup>a</sup>	tubulin isotype	mass, Da
<b><math>\alpha</math>-Tubulin</b>		
CAA25855	$\alpha$ 1/b $\alpha$ 1	50 157.7
I77403	$\alpha$ 1/K $\alpha$ 1	50 151.6
AAC31959	$\alpha$ 1/K $\alpha$ 1	50 151.6
AAD33871	$\alpha$ 1/K $\alpha$ 1	50 135.6
Q13748	$\alpha$ 3	49 959.5
A25873	$\alpha$ 4	49 924.4
Q9BQE3	$\alpha$ 6	49 895.3
Q9NY65	$\alpha$ 8	50 093.5
<b><math>\beta</math>-Tubulin</b>		
AAD33873	$\beta$ I	49 670.8
P07437	$\beta$ I	49 759.9
AAH01352	$\beta$ II	49 953.1
NP_001060	$\beta$ II	49 907.0
AAH00748	$\beta$ III	50 432.7
NP_006077	$\beta$ III	50 517.8
P04350	$\beta$ IVa	49 630.9
NP_006078	$\beta$ IVa	49 585.8
P05217	$\beta$ IVb	49 831.0
NP_115914	$\beta$ V	49 857.1
NP_110400	$\beta$ VI	50 326.9

<sup>a</sup> NCBI protein database.

tubulin, K $\alpha$ 1- and  $\beta$ I-tubulin were only monoglutamylated, and no other post-translational modifications were detected. However, our inability to detect the C-terminal peptides of  $\beta$ II-,  $\beta$ III-, and  $\beta$ IVa-tubulin isotypes, given that these isotypes were previously identified in A549 cells by Western blotting and/or RT-PCR, revealed a potential limitation to this approach (23). With no separation of C-terminal peptides prior to MALDI-TOF mass spectrometry analysis, ions for minor tubulin species could have been suppressed by the presence of other, more abundant C-terminal tubulin peptides. Moreover, the method gave no information regarding potential modifications or mutations outside the C-terminal domains. More recently, we developed a combined isoelectric focusing/mass mapping approach to analyze tubulin isotypes in Taxol-stabilized microtubule preparations (35).

**Native Tubulin Isotype Masses.** Except for two K $\alpha$ 1-tubulin variants, the calculated masses of the human tubulin isotypes found in the databases are all distinct (Table 1). We have used reversed-phase chromatography in line with ESI mass spectrometry analysis to determine the masses of native tubulin isotypes in human cancer cell lines. Prior to analysis, the  $\alpha/\beta$ -tubulins were isolated from cell extracts by a Taxol-dependent polymerization process originally developed by Vallee (37). We have recently established that there is no selective loss of specific tubulin isotypes during this process (35). Therefore, the isolated tubulins are representative of tubulins in cells. The determination of native tubulin masses is important for relating sequences entered in databases to the proteins expressed in human cell lines. This is particularly important in a protein family like tubulin, where nomenclatures and annotations remain confusing and multiple sequence variants of a single tubulin isotype can be found in databases (Table 1). Native mass determinations could eliminate erroneous entries or validate some that could represent true polymorphisms.

**Tubulin Isotypes in A549 and HeLa Cell Lines.** Proteins present in Taxol-stabilized microtubule pellets from A549 and HeLa cells were analyzed by LC-MS using a microbore C4 reversed-phase column and a 0.2%/min acetonitrile

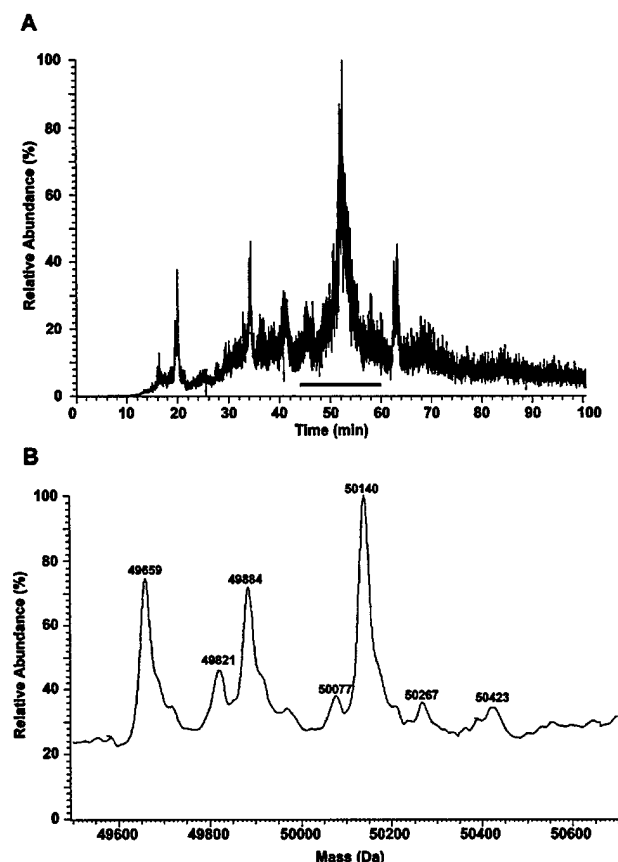


FIGURE 1: Analysis of Taxol-stabilized microtubules from A549 cells by LC-MS. A pellet of A549 Taxol-stabilized microtubules was resuspended in 70% formic acid, and proteins were separated on a microbore C4 reversed-phase column with a 0.2%/min solvent B gradient and detected by ESI-MS. (A) Total ion current profile. (B) Deconvoluted mass obtained by averaging scans in the retention time range indicated by a horizontal black bar in A.

gradient. The total ion chromatograms from both cell lines were similar, although the relative intensities of the signals differed (Figures 1A and 2A). All the masses in the range of human tubulins (see Table 1) were found between 44 and 60 min of the gradient, which includes the largest ion peak. This result was expected, as tubulin represented the major protein component in the Taxol-stabilized microtubule pellets. After averaging the scans between 44 and 60 min, we obtained overall profiles of the deconvoluted mass peaks for the different tubulin proteins in both cell lines (Figures 1B and 2B). The observed masses matched closely those of  $\beta$ I-,  $\beta$ IVb-,  $\alpha$ 6-, tyr  $\alpha$ 4-, K $\alpha$ 1-, glu K $\alpha$ 1-, and  $\beta$ III-tubulin, respectively (Table 2).

To confirm the identity of these tubulin isotypes, tryptic mass mapping of the C4-resolved isotypes present in A549 tubulins was performed. For these experiments, tubulin isotypes were separated using a 0.05%/min acetonitrile gradient to increase the separation between tubulin isotypes, and the column effluent was split for fraction collection and for delivery to the ion trap mass spectrometer. With this shallower gradient, the tubulin isotypes eluted between 54 and 96 min. The total ion current was deconvoluted in 1-min segments across the gradient, and fractions that contained the same protein masses were pooled. After removal of solvents, tryptic digestion was performed and the resulting peptides were analyzed by MALDI-TOF MS, searching for

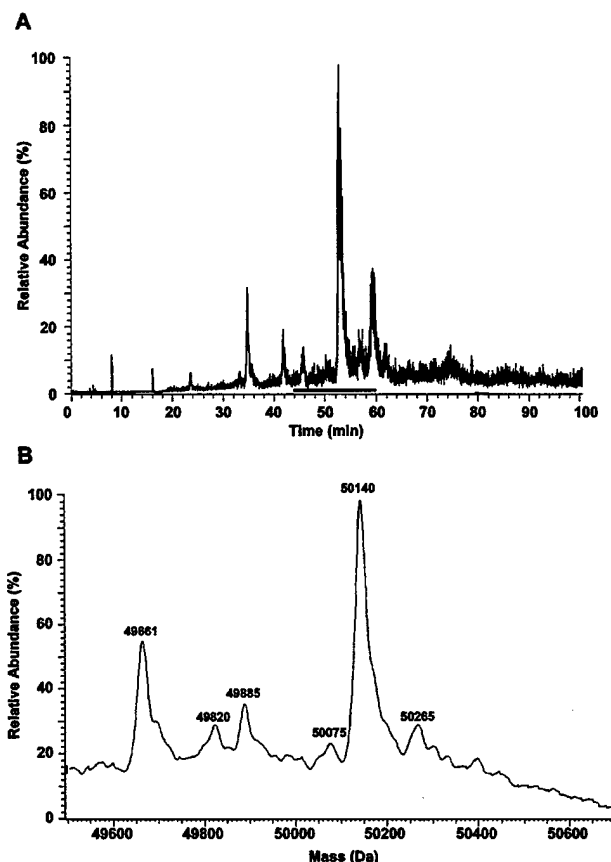


FIGURE 2: Analysis of Taxol-stabilized microtubules from HeLa cells by LC-MS. A pellet of HeLa Taxol-stabilized microtubules was resuspended in 70% formic acid, and proteins were separated on a microbore C4 reversed-phase column with a 0.2%/min solvent B gradient and detected by ESI-MS. (A) Total ion current profile. (B) Deconvoluted mass obtained by averaging scans in the retention time range indicated by a horizontal black bar in A.

Table 2: Comparison of Experimental and Calculated Masses of Human Tubulin Isoforms

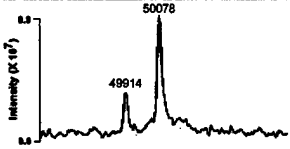
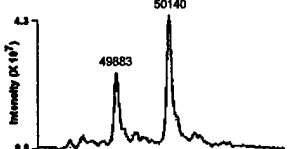
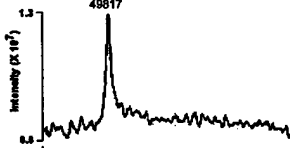
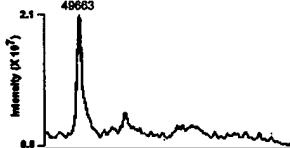
tubulin	mass, Da		$\Delta$ mass
	calcd <sup>a</sup>	measd <sup>b</sup>	
K $\alpha$ 1	50 151.6	50 142.2 $\pm$ 2.2	-9.4
K $\alpha$ 1 glu <sub>1</sub>	50 280.7	50 266.0 $\pm$ 2.0	-14.0
K $\alpha$ 1 Ser <sub>379</sub> Arg	50 220.7	50 209.5 $\pm$ 3.5	-11.2
$\alpha$ 6	49 895.3	49 885.6 $\pm$ 1.3	-9.7
$\alpha$ 4	49 924.4	49 913.3 $\pm$ 1.1	-11.1
$\alpha$ 4 tyr	50 087.6	50 077.0 $\pm$ 1.7	-10.6
$\beta$ I	49 670.8	49 661.6 $\pm$ 0.5	-9.2
$\beta$ IVb	49 831.0	49 821.2 $\pm$ 2.5	-9.8
$\beta$ III	50 432.7	50 422.0 $\pm$ 3.5	-10.7
$\beta$ III glu <sub>1</sub>	50 561.8	50 551.0 $\pm$ 3.5	-10.8

<sup>a</sup> Calculated from sequences in NCBI protein database (see Table 1). <sup>b</sup> Average of four independent experiments with microtubules isolated from A549 and A549-T12 cell lines  $\pm$  standard deviation.

tubulin isotype-specific tryptic peptides. The native tubulin masses (Table 3 and Figure 3) and the detected isotype-specific tryptic peptides (Table 3) present in these pooled fractions are as follows:

**Pool 1.** The 54–56-min segment of the gradient contained a very small peak with an average mass of 49 914 Da and a larger peak with an additional mass of 163 Da. These masses were close to the calculated values for  $\alpha$ 4- and tyrosinated  $\alpha$ 4-tubulins, respectively (Table 2). MALDI mass mapping

Table 3: Peptide Mass Mapping of HPLC-Resolved Tubulin Isoforms from A549 Cells

Retention time range (min)	Mass in HPLC fraction (Da)	Isotype-specific tubulin peptides <sup>a</sup>	Measured mass	Calculated mass	$\Delta$ mass (Da)	Database matched tubulin	Sequence coverage <sup>b</sup> (%)
Pool 1 54-56		115 EIIDPVLDLR <sub>121</sub>	1068.5	1068.6	0.1	$\alpha$ 4	40
		431 DYEEVGIDSYEDEGE <sub>448</sub> <sup>c</sup>	2122.1	2122.0	-0.1		
		431 DYEEVGIDSYEDEGE <sub>448</sub> <sup>c</sup>	2285.0	2285.2	0.2	$\alpha$ 4 Tyr	
Pool 3 70-79		423 EDMAALEKDYEEVGADSDGE <sub>449</sub> <sup>c</sup>	2966.4	2967.0	0.6	$\alpha$ 6	42
		423 EDMAALEKDYEEVGSDVEGE <sub>451</sub> <sup>c</sup>	3237.3	3237.3	0.0	K $\alpha$ 1	52
		423 EDMAALEKDYEEVGSDVEGE <sub>451</sub> (MSO) <sup>c</sup>	3253.5	3253.3	-0.2		
Pool 4 79-89		63 AVLVDLEPGTMD <sub>57</sub>	1601.9	1601.8	-0.1	$\beta$ IVb	53
		47 INVYYNEATGGK <sub>58</sub>	1327.6	1327.6	0.0		
Pool 5 92-96		283 ALTVPELTQQV <sub>297</sub>	1659.4	1659.2	-0.2	$\beta$ I	54
		363 MAVTFIGNSTAIQEL <sub>379</sub> (MSO)	1886.6	1886.2	-0.4		
		20 FWEVISDEHGIDPTGYH <sub>46</sub>	3103.0	3103.3	0.3		

<sup>a</sup> Peptides specific to a tubulin isotype that were detected. MSO: oxidized methionine. <sup>b</sup> Sequence coverage was calculated on the basis of all the tryptic peptides detected, i.e., isotype-specific and shared peptides. <sup>c</sup> Detection of these peptides was greatly improved in negative mode.

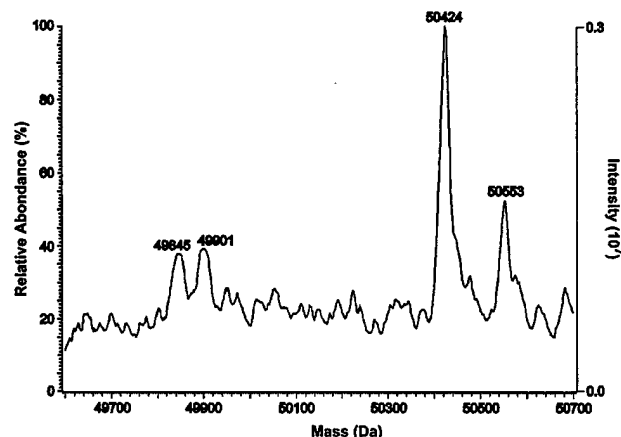


FIGURE 3: Deconvoluted mass spectrum of minor tubulin isoforms. A pellet of A549 Taxol-stabilized microtubules was resuspended in 70% formic acid, and proteins were separated on a microbore C4 reversed-phase column with a 0.05%/min solvent B gradient and detected by ESI-MS. Proteins eluting from 64 to 66 min of retention time (pool 2) were examined for their tubulin isoform content by averaging scans. Two minor mass peaks were tentatively assigned to  $\Delta$ 2 K $\alpha$ 1-tubulin and its monoglycylated isoform. The major peak had a mass matching  $\beta$ III-tubulin, and an associated peak corresponding to its monoglutamylated isoform was present.

identified the isotype-specific C-terminal tryptic peptides from both forms, in addition to an internal  $\alpha$ 4-specific peptide. This is the first evidence of the expression of the  $\alpha$ 4-tubulin isotype in A549 cells.  $\alpha$ 4-Tubulin is the only isotype not to have a tyrosine or phenylalanine residue as the last encoded amino acid. However,  $\alpha$ 4-tubulin is a substrate for tubulin tyrosine ligase, and, once tyrosinated,

it can undergo tyrosination/detyrosination cycles like the other  $\alpha$ -tubulin isotypes (5). We found that the majority of  $\alpha$ 4-tubulin in A549 and HeLa cells was tyrosinated.

**Pool 2.** The 64–66-min segment of the gradient contained several minor peaks (Figure 3). First, two peaks that differed in mass by approximately 56 Da were tentatively identified as detyrosinated/deglutamylated ( $\Delta$ 2)-K $\alpha$ 1-tubulin and its monoglycylated counterpart.  $\Delta$ 2- $\alpha$ -Tubulin is unable to undergo the reversible tyrosination cycle (53) but has been shown to be glycylated in brain tubulin (51). Two other mass peaks that differed by 129 Da were tentatively identified as the  $\beta$ III-isotype and its monoglutamylated counterpart. Unfortunately, we could not detect tryptic peptides specific for either  $\Delta$ 2- $\alpha$ - or  $\beta$ III-tubulin in this pool, presumably because of their low level of abundance. However, by immunoblot analysis, antibodies reportedly specific for  $\Delta$ 2- $\alpha$ -tubulin cross-reacted weakly with a protein of the correct size in the A549 cell line.<sup>2</sup> We have also detected nonmodified  $\beta$ III-tubulin, and a minor more acidic variant, in this cell line by an isoelectric focusing/MALDI mass mapping approach (35). This is consistent with the presence of two  $\beta$ III-tubulin mass peaks detected by LC-MS.

**Pool 3.** The 70–79-min segment of the gradient contained two major peaks corresponding to  $\alpha$ 6- and K $\alpha$ 1-tubulins. The C-terminal tryptic peptide for each isotype was detected. The amino acid sequence obtained previously for the C-terminal peptide of  $\alpha$ \*-tubulin by MS/MS (34) matches the C-terminal sequence of a recently cloned human  $\alpha$ 6-tubulin. In the present study, a protein having the expected

<sup>2</sup> L. Martello and S. B. Horwitz, unpublished observation.



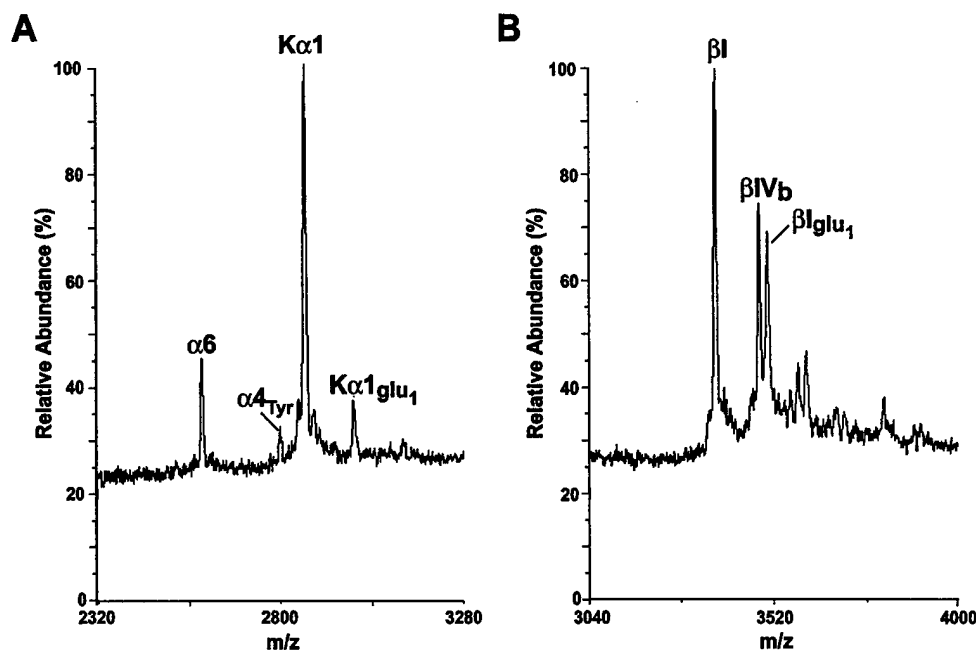


FIGURE 4: Negative ion mode MALDI-TOF analysis of tubulin C-terminal peptides from Taxol-stabilized microtubules isolated from HeLa cells.  $\alpha$ -Tubulin and  $\beta$ -tubulin were separated by SDS-PAGE and transferred to nitrocellulose, and the  $\alpha$ -tubulin band (A) and the  $\beta$ -tubulin band (B) were independently CNBr-digested;  $m/z$  peaks were assigned on the basis of the calculated  $m/z$  values for CNBr-generated C-terminal peptides from human tubulin isotypes (34).

mass for human  $\alpha 6$ -tubulin was detected and confirmed as being  $\alpha 6$ -tubulin by tryptic mass mapping. The observed mass for  $K\alpha 1$ -tubulin is close to the three complete sequence variants present in the databases (Table 1). We did not find a tryptic peptide that was specific for any of these  $K\alpha 1$  variants in our mass mapping experiments. However, the  $K\alpha 1$ -tubulin nucleotide sequence in A549 deduced by cDNA sequencing (36) matches the protein with the accession number AAC31959. Moreover, in our IEF mass mapping study of human tubulins (35), we found two tryptic peptides (residues 230–243,  $m/z$  1487.7 and residues 340–352,  $m/z$  1527.5) that are unique to this particular  $K\alpha 1$ -tubulin variant. Like the  $\alpha 4$  isotype, both  $K\alpha 1$ - and  $\alpha 6$ -tubulins in the A549 and HeLa cell lines are present in their tyrosinated forms.

**Pool 4.** The 79–89-min segment of the gradient contained a single peak with a mass close to that of  $\beta IVb$ -tubulin. Two isotype-specific peptides for this tubulin were detected after tryptic digestion.

**Pool 5.** The 92–96-min segment of the gradient contained a single peak that was shown by mass mapping to be  $\beta I$ -tubulin. In our previous studies, we tentatively attributed a low-abundance C-terminus CNBr peptide to monoglutamylated  $\beta I$ -tubulin (34). Although we did not detect the presence of this modified isotype in A549 by LC-MS, an ion matching monoglutamylated  $\beta I$ -tubulin was observed in Taxol-stabilized microtubules from HeLa cells (Figure 6A, below).

A systematic average difference of  $-10$  Da between measured and calculated masses was observed in our data (Table 2). There are 8–12 cysteine residues present in human tubulins, but only two natural disulfide bonds per native  $\alpha/\beta$  tubulin heterodimer have been reported, i.e., one disulfide bond per subunit (54, 55). This would account for a 2-Da decrease in mass per  $\alpha$ - or  $\beta$ -tubulin chain. However, reduction with DTT or tris[2-carboxyethyl]phosphine prior

to LC-MS did not alter the observed masses (data not shown). Therefore, the observed mass differences are likely to be due to a systematic calibration error for proteins of this mass range or to disulfide bond interchange during the LC separation stage. To unambiguously address these issues in future studies, it may be helpful to alkylate cysteine residues, before and after reduction, prior to mass analysis.

Unlike mammalian neuronal tubulin, the tubulin isolated from the A549 and HeLa cell lines was not extensively post-translationally modified. However, all of the identified  $\alpha$ -tubulin isotypes were mainly tyrosinated. This is consistent with our previous study using MALDI-TOF MS analysis of the C-terminal tubulin peptides from A549 and MDA-MB-231 cell lines (34). Acetylation of Lys<sub>40</sub> is a modification that is also specific to  $\alpha$ -tubulins, but none of the  $\alpha$  isotypes identified in both cell lines were acetylated, on the basis of their experimentally determined masses and the detection of tryptic peptides with N-terminal Thr<sub>41</sub> residues in the mass mapping experiments (data not shown). Glutamylation was limited to one residue and was present in a very small fraction of tubulin.

In cells, both detyrosinated and acetylated tubulins are normally associated with stable microtubules (56). However, under in vitro assembly conditions, tubulin isolated from HeLa cells was shown to be significantly less dynamic than brain tubulin, which is extensively post-translationally modified (57). This suggests that the post-translational status of tubulin has no direct impact on microtubule dynamics and that these modifications are a consequence and not a cause of microtubule stability in vivo. Nevertheless, it is possible that post-translational modifications may affect interactions with regulatory proteins, thus indirectly altering microtubule dynamics (56).

**Relative Quantitation of Tubulin Isotypes.** Although RT-PCR data indicated the presence of  $\beta II$ - and  $\beta IVa$ -tubulin

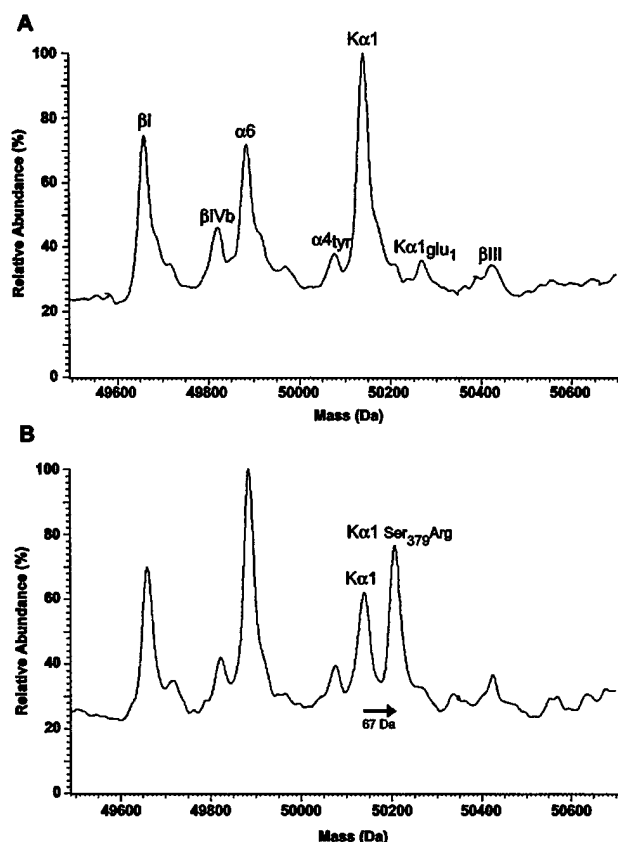


FIGURE 5: Comparison of deconvoluted mass spectra of tubulin isotypes present in A549 and A549-T12. Taxol-stabilized microtubules isolated from A549 (see Figure 1B) and A549-T12 cell lines were analyzed by LC-MS. Mass peaks were assigned on the basis of peptide mapping (Table 3) and calculated values for human tubulin isotypes (Table 2 and Figure 3). Deconvoluted mass profiles were obtained by averaging scans in the retention time range from 44 to 60 min for (A) A549 and (B) A549-T12, where an horizontal arrow indicates a mass shift for a portion of K $\alpha$ 1-tubulin.

mRNA transcripts in the A549 cell line (23), the translated proteins were not expressed at detectable levels. Similar results were obtained by MALDI-MS analysis of either the released C-terminal CNBr peptides (34) or IEF-resolved tubulin isotypes (35). Likewise,  $\beta$ II- and  $\beta$ IVa-tubulins were below the level of detection in HeLa cells. There is no obvious explanation for the discrepancy between tubulin isotype mRNA and protein expression levels, but such absence of correlation has been observed for other proteins (39, 40). Since tubulin was quantitatively recovered from cells by the Taxol-driven polymerization procedure (35), either there is an unknown bias in the RT-PCR results or there is a still unknown silencing mechanism for translation of  $\beta$ II- and  $\beta$ IVa-tubulin mRNA.

It is known from previous studies that the ratio of total  $\alpha$ - to total  $\beta$ -tubulin is close to one (35). Inspection of the ion intensities in Figures 1B and 2B would suggest, however, that the  $\alpha$ -tubulin isotypes are present in considerable excess over the  $\beta$ -tubulin isotypes in these cell lines. However, quantitation of relative protein expression levels by comparison of ion intensities is problematic due to differential ionization efficiencies. Nevertheless, if we estimate the relative amounts of individual  $\alpha$ - or  $\beta$ -tubulin isotypes within each isotype class, we find that K $\alpha$ 1-,  $\alpha$ 6-, and  $\alpha$ 4-tubulin or  $\beta$ I-,  $\beta$ IVb-, and  $\beta$ III-tubulin represent approximately 55%,

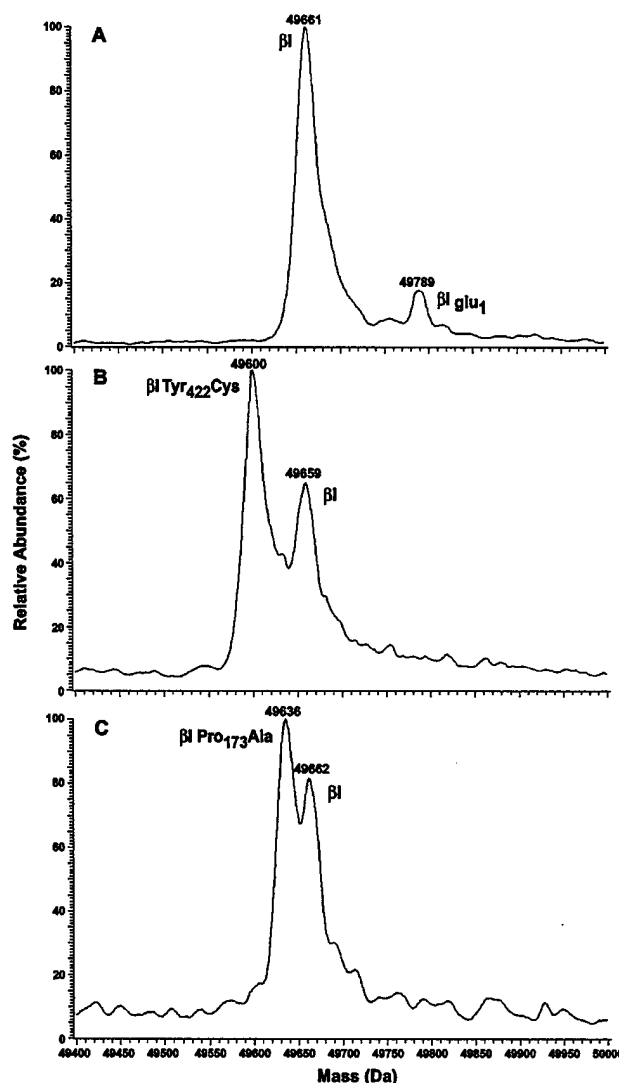


FIGURE 6: Expression of  $\beta$ I-tubulin mutations. Taxol microtubules isolated from parental HeLa cells and drug-resistant HeLa cell lines selected with epothilone B (HeLa.EpoB1.8) or with epothilone A (HeLa.EpoA9) were analyzed by LC-MS as described for A549 cell lines.  $\beta$ I-Tubulin-deconvoluted mass spectrum from (A) HeLa, (B) HeLa.EpoB1.8, and (C) HeLa.EpoA9 are presented.

31%, and 14%, respectively, of total  $\alpha$ -tubulin or total  $\beta$ -tubulin. These percentages are very similar to those obtained by Coomassie blue staining of the tubulin isotypes resolved by isoelectrofocusing (35). It would appear, therefore, that in these human cell lines, K $\alpha$ 1- and  $\beta$ I-tubulin,  $\alpha$ 6- and  $\beta$ IVb-tubulin, and  $\alpha$ 4- and  $\beta$ III-tubulin are apparently present in comparable amounts. Because of this trend, we speculate that there may be a sorting mechanism of tubulin isotypes during  $\alpha/\beta$ -tubulin heterodimer formation. As stated above, our previous MALDI-TOF MS analysis of tubulin CNBr C-terminal peptides from total cell extracts may have under-represented certain tubulin isotypes due to ion suppression effects. In that study, the C-terminal peptides of  $\beta$ II,  $\beta$ III, and  $\beta$ IVa were not observed, and  $\beta$ IVb peptide ion was minor compared to  $\beta$ I. We re-evaluated this approach by reducing the complexity of the sample prior to CNBr. In this study, tubulin was purified by the Taxol-based method from HeLa cells, followed by the separation of  $\alpha$ -tubulin and  $\beta$ -tubulin on SDS-PAGE gels prior to transfer to the nitrocellulose membrane. The region of the blot containing

either  $\alpha$ -tubulin or  $\beta$ -tubulin was CNBr-digested, and MALDI-TOF MS analysis was performed. The  $m/z$  peaks' intensities corresponding to  $\beta$ IVb- and monoglutamylated  $\beta$ I-tubulin C-terminal peptides were increased significantly (Figure 4B). Very low levels of the tyrosinated  $\alpha$ 4-tubulin C-terminal peptide were also detected (Figure 4A), but  $\beta$ III-tubulin C-terminal peptide was still undetectable (data not shown), indicating a particularly strong suppression of this peptide. Similar results were obtained with A549 tubulin (data not shown). Our results are also consistent with the Western blot analysis of purified HeLa tubulin by Newton et al. (57), where  $\beta$ I- and  $\beta$ IV-tubulin isotypes represented 80% and 20% of  $\beta$ -tubulin, respectively, and no  $\beta$ III-tubulin was detected.

**Mutations in  $\alpha$ 1- and  $\beta$ I-Tubulins.** Mutations to the primary drug target are a recurring theme in drug resistance. However, DNA sequence analysis of the multiple tubulin genes in human cell lines and tissues is not straightforward since they are so highly conserved. A recent study identified  $\beta$ -tubulin mutations in serum DNA isolated from 33% of patients with non-small-cell lung cancer (58). This finding was considered extremely significant, since it was thought to validate in vitro data from numerous laboratories documenting the acquisition of mutations in Taxol- and epothilone-resistant cell lines that correlated with increasing levels of resistance. Several groups sought to confirm this initial study (59–61); however, the presence of mutations has not been corroborated in these prospective studies, although silent polymorphisms have been reported. The study by Monzo et al. (58), which utilized genomic DNA that was extracted from circulating tumor DNA, isolated from patient serum samples, and the existence of tubulin pseudogenes, makes it difficult to analyze the precise nucleotide sequence of  $\beta$ -tubulin using genomic DNA.

Since the drug-binding site for the microtubule-stabilizing drugs resides in  $\beta$ -tubulin, the search for tubulin mutations in Taxol/epothilones-resistant cell lines has been largely restricted to the major  $\beta$ I-tubulin transcript (30–33). However, recent studies have shown that mutations to  $\alpha$ -tubulin may also occur in some drug-resistant cell lines (36). The complete sequencing of all tubulin isotypes in drug-selected cell lines, although feasible, would be very time-consuming. Moreover, sequencing of the  $\alpha/\beta$ -tubulin genes from resistant cell lines has shown that mutations introduced often occur to a single tubulin allele (30). Therefore, the question as to whether both the wild-type and mutant transcripts are translated, and to what levels, is important, since the ratio of wild-type to mutant protein could affect resistance levels.

A549-T12, a Taxol-resistant cell line, was reported to have a heterozygous mutation at amino acid 379 of  $\alpha$ 1-tubulin, resulting in a serine-to-arginine substitution (36). The mass spectrum of tubulins isolated from this resistant cell line clearly shows a new protein peak approximately 67 Da greater than that of the parental  $\alpha$ 1 isotype (Figure 5). The difference in mass is very close to the expected 69.1 Da due to the Ser-to-Arg substitution at position 379. We also analyzed Taxol-stabilized microtubules from two HeLa cell lines that are resistant to epothilones. Both cell lines were shown to harbor different heterozygous mutations in  $\beta$ I (33). The  $\beta$ I-tubulins from these cell lines, HeLa.EpoB1.8 with a Tyr422Cys mutation and HeLa.EpoA9 with a Pro173Ala mutation, were predicted to have masses 60 and 26 Da,

respectively, lower than the wild-type isotype. These mass losses were clearly detected in the deconvoluted mass spectra of regions of the gradient at which  $\beta$ I-tubulin elutes (Figure 6). In the parental HeLa cells, we observed only the wild-type  $\beta$ I-tubulin and a small amount of monoglutamylated  $\beta$ I-tubulin (Figure 6A). In the resistant cell lines, the expression of the mutant  $\beta$ I-tubulins was clearly evident (Figure 6B,C), in both cases at levels that appeared higher than the wild-type  $\beta$ I-tubulin.

What is the smallest mass difference between specific tubulin isotypes that can be detected using a mass spectrometer? In this study, we were able to discriminate mutant and wild-type  $\beta$ I isotypes that differed by 26 Da, even though they were incompletely (30%) resolved. Theoretically, the peak width at 50% of maximum peak height is about 15 Da for an  $\sim$ 50 kDa protein, as estimated by calculating the width of the isotopic distribution using the IsoPro program (<http://members.aol.com/msmssoft/>). Therefore, two 50-kDa proteins of equal abundance must differ in mass by more than 15 Da to be resolved. It is likely that the use of quadrupole TOF or FTICR mass spectrometers would permit the detection of tubulin mutants displaying even smaller mass differences. Moreover, the presence of a broad or asymmetrical peak, in which the peak full width at 50% of maximum peak height exceeds 15 Da by FTICR MS, would indicate that incompletely resolved tubulin isotypes/mutants were present. In that case, the protein can be collected off-line for enzymatic digestion and amino acid sequence analysis by LC-MS/MS. In studies performed so far, we have achieved almost complete sequence coverage of the major tubulin isotypes by MS/MS analysis of pepsin-derived overlapping peptide fragments.<sup>3</sup>

The ability to perform simultaneous analysis of the expression of tubulin isotypes in human cell lines will have a major impact on microtubule biology. As noted in Table 1, multiple tubulin sequences are present in the databases. By using the present LC-MS approach and/or the IEF-MS methodology described previously, human tubulin sequences that are expressed should be identifiable. This will improve the annotation of tubulin sequences in databases and provide a reference for the detection of potential mutations and polymorphisms in humans. For example, in A549 and HeLa cell lines, we have unambiguously identified expression of  $\alpha$ 1,  $\beta$ I, and  $\beta$ III with accession numbers AAC31959, AAD33873, and AAH00748, respectively. Likewise, although alterations in tubulin isotype mRNA levels have been noted in cell lines resistant to anti-microtubule agents, our proteomic strategies will afford the opportunity to directly determine the tubulin isotype composition of these cell lines to ascertain whether the mRNA alterations are actually reflected at the protein level. Finally, comparative analysis of tubulin isotype expression and associated post-translational modifications in diseased and normal tissue would provide greater insight into pathologies where the microtubule cytoskeleton appears to be involved (62–66).

#### ACKNOWLEDGMENT

We thank Dr. Alan G. Marshall (National High Magnetic laboratory, Florida State University, Tallahassee, FL) for helpful discussions.

<sup>3</sup> F. Wang, unpublished observation.

## REFERENCES

- Desai, A., and Mitchison, T. J. (1997) *Annu. Rev. Cell Dev. Biol.* 13, 83–117.
- Oakley, B. R. (2000) *Trends Cell Biol.* 10, 537–542.
- Sharp, D. J., Rogers, G. C., and Scholey, J. M. (2000) *Nature* 407, 41–47.
- Ludueña, R. F. (1998) *Int. Rev. Cytol.* 178, 207–275.
- MacRae, T. H. (1997) *Eur. J. Biochem.* 244, 265–278.
- Boucher, D., Larcher, J. C., Gros, F., and Denoulet, P. (1994) *Biochemistry* 33, 12471–12477.
- Bonnet, C., Boucher, D., Lazereg, S., Pedrotti, B., Islam, K., Denoulet, P., and Larcher, J. C. (2001) *J. Biol. Chem.* 276, 12839–12848.
- He, L., Orr, G. A., and Horwitz, S. B. (2001) *Drug Discovery Today* 6, 1153–1164.
- Dumontet, C., and Sikic, B. I. (1999) *J. Clin. Oncol.* 17, 1061–1070.
- Drukmán, S., and Kavallaris, M. (2002) *Int. J. Oncol.* 21, 621–628.
- Wilson, L., and Jordan, M. A. (1995) *Chem. Biol.* 2, 569–573.
- Jordan, M. A., and Wilson, L. (1998) *Curr. Opin. Cell Biol.* 10, 123–130.
- Cabral, F. R., Brady, R. C., and Schibler, M. J. (1986) *Ann. N.Y. Acad. Sci.* 466, 745–756.
- Cabral, F., and Barlow, S. B. (1989) *FASEB J.* 3, 1593–1599.
- Gonçalves, A., Braguer, D., Kamath, K., Martello, L., Briand, C., Horwitz, S., Wilson, L., and Jordan, M. A. (2001) *Proc. Natl. Acad. Sci. U.S.A.* 98, 11737–11742.
- Lu, Q., and Ludueña, R. F. (1993) *Cell Struct. Funct.* 18, 173–182.
- Lu, Q., and Ludueña, R. F. (1994) *J. Biol. Chem.* 269, 2041–2047.
- Panda, D., Miller, H. P., Banerjee, A., Ludueña, R. F., and Wilson, L. (1994) *Proc. Natl. Acad. Sci. U.S.A.* 91, 11358–11362.
- Derry, W. B., Wilson, L., Khan, I. A., Ludueña, R. F., and Jordan, M. A. (1997) *Biochemistry* 36, 3554–3562.
- Carles, G., Braguer, D., Dumontet, C., Bourgaire, V., Gonçalves, A., Sarrazin, M., Rognoni, J. B., and Briand, C. (1999) *Br. J. Cancer* 80, 1162–1168.
- Dumontet, C., Duran, G. E., Steger, K. A., Beketic-Oreskovic, L., and Sikic, B. I. (1996) *Cancer Res.* 56, 1091–1097.
- Haber, M., Burkhart, C. A., Regl, D. L., Madafoglio, J., Norris, M. D., and Horwitz, S. B. (1995) *J. Biol. Chem.* 270, 31269–31275.
- Kavallaris, M., Kuo, D. Y., Burkhart, C. A., Regl, D. L., Norris, M. D., Haber, M., and Horwitz, S. B. (1997) *J. Clin. Invest.* 100, 1282–1293.
- Ranganathan, S., Dexter, D. W., Benetatos, C. A., Chapman, A. E., Tew, K. D., and Hudes, G. R. (1996) *Cancer Res.* 56, 2584–2589.
- Ranganathan, S., Benetatos, C. A., Colarusso, P. J., Dexter, D. W., and Hudes, G. R. (1998) *Br. J. Cancer* 77, 562–566.
- Kyu-Ho Han, E., Gehrke, L., Tahir, S. K., Credo, R. B., Cherian, S. P., Sham, H., Rosenberg, S. H., and Ng, S. (2000) *Eur. J. Cancer* 36, 1565–1571.
- Nicoletti, M. I., Valoti, G., Giannakakou, P., Zhan, Z., Kim, J. H., Lucchini, V., Landoni, F., Mayo, J. G., Giavazzi, R., and Fojo, T. (2001) *Clin. Cancer Res.* 7, 2912–2922.
- Burkhart, C. A., Kavallaris, M., and Horwitz, S. B. (2001) *Biochim. Biophys. Acta* 1471, O1–O9.
- Banerjee, A. (2002) *Biochem. Biophys. Res. Commun.* 293, 598–601.
- Giannakakou, P., Sackett, D. L., Kang, Y. K., Zhan, Z., Buters, J. T., Fojo, T., and Poruchynsky, M. S. (1997) *J. Biol. Chem.* 272, 17118–17125.
- Giannakakou, P., Gussio, R., Nogales, E., Downing, K. H., Zaharevitz, D., Bollbuck, B., Poy, G., Sackett, D., Nicolaou, K. C., and Fojo, T. (2000) *Proc. Natl. Acad. Sci. U.S.A.* 97, 2904–2909.
- Poruchynsky, M. S., Giannakakou, P., Ward, Y., Bulinski, J. C., Telford, W. G., Robey, R. W., and Fojo, T. (2001) *Biochem. Pharmacol.* 62, 1469–1480.
- He, L., Yang, C. P., and Horwitz, S. B. (2001) *Mol. Cancer Ther.* 1, 3–10.
- Rao, S., Aberg, F., Nieves, E., Horwitz, S. B., and Orr, G. A. (2001) *Biochemistry* 40, 2096–2103.
- Verdier-Pinard, P., Wang, F., Martello, L., Burd, B., Orr, G. A., and Horwitz, S. B. (2003) *Biochemistry* 42, 5349–5357.
- Martello, L. A., Verdier-Pinard, P., Shen, H. J., He, L., Torres, K., Orr, G. A., and Horwitz, S. B. (2003) *Cancer Res.* 63, 1207–1213.
- Vallee, R. B. (1986) *Methods Enzymol.* 134, 104–115.
- Rao, S., Krauss, N. E., Heerding, J. M., Swindell, C. S., Ringel, I., Orr, G. A., and Horwitz, S. B. (1994) *J. Biol. Chem.* 269, 3132–3134.
- Gygi, S. P., Rochon, Y., Franza, B. R., and Aebersold, R. (1999) *Mol. Cell Biol.* 19, 1720–1730.
- Chen, G., Gharib, T. G., Huang, C. C., Taylor, J. M., Misek, D. E., Kardis, S. L., Giordano, T. J., Iannettoni, M. D., Orringer, M. B., Hanash, S. M., and Beer, D. G. (2002) *Mol. Cell Proteomics* 1, 304–313.
- Alexander, J. E., Hunt, D. F., Lee, M. K., Shabanowitz, J., Michel, H., Berlin, S. C., MacDonald, T. L., Sundberg, R. J., Rebhun, L. I., and Frankfurter, A. (1991) *Proc. Natl. Acad. Sci. U.S.A.* 88, 4685–4689.
- Bre, M. H., Redeker, V., Vinh, J., Rossier, J., and Levilliers, N. (1998) *Mol. Biol. Cell* 9, 2655–2665.
- Mary, J., Redeker, V., Le Caer, J. P., Rossier, J., and Schmitter, J. M. (1996) *J. Biol. Chem.* 271, 9928–9933.
- Mary, J., Redeker, V., Le Caer, J. P., Rossier, J., and Schmitter, J. M. (1997) *J. Protein Chem.* 16, 403–407.
- Redeker, V., Levilliers, N., Schmitter, J. M., Le Caer, J. P., Rossier, J., Adoutte, A., and Bre, M. H. (1994) *Science* 266, 1688–1691.
- Redeker, V., Rusconi, F., Mary, J., Promé, D., and Rossier, J. (1996) *J. Neurochem.* 67, 2104–2114.
- Redeker, V., Rossier, J., and Frankfurter, A. (1998) *Biochemistry* 37, 14838–14844.
- Rudiger, A., Rudiger, M., Weber, K., and Schomburg, D. (1995) *Anal. Biochem.* 224, 532–537.
- Rudiger, M., Plessmann, U., Rudiger, A. H., and Weber, K. (1995) *FEBS Lett.* 364, 147–151.
- Vinh, J., Langridge, J. I., Bre, M. H., Levilliers, N., Redeker, V., Loyaux, D., and Rossier, J. (1999) *Biochemistry* 38, 3133–3139.
- Banerjee, A. (2002) *J. Biol. Chem.* 277, 46140–46144.
- Jai-nhuknan, J., and Cassidy, C. J. (1998) *Anal. Chem.* 70, 5122–5128.
- Lafanèchère, L., and Job, D. (2000) *Neurochem. Res.* 25, 11–18.
- Chaudhuri, A. R., Khan, I. A., and Ludueña, R. F. (2001) *Biochemistry* 40, 8834–8841.
- Ikeda, Y., and Steiner, M. (1978) *Biochemistry* 17, 3454–3459.
- Palazzo, A., Ackerman, B., and Gundersen, G. G. (2003) *Nature* 421, 230.
- Newton, C. N., DeLuca, J. G., Himes, R. H., Miller, H. P., Jordan, M. A., and Wilson, L. (2002) *J. Biol. Chem.* 277, 42456–42462.
- Monzo, M., Rosell, R., Sanchez, J. J., Lee, J. S., O'Brate, A., Gonzalez-Larriba, J. L., Alberola, V., Lorenzo, J. C., Nunez, L., Ro, J. Y., and Martin, C. (1999) *J. Clin. Oncol.* 17, 1786–1793.
- Kelley, M. J., Li, S., and Harpole, D. H. (2001) *J. Natl. Cancer Inst.* 93, 1886–1888.
- Sale, S., Oefner, P. J., and Sikic, B. I. (2002) *J. Natl. Cancer Inst.* 94, 776–777; discussion 777.
- Tsurutani, J., Komiya, T., Uejima, H., Tada, H., Syunichi, N., Oka, M., Kohno, S., Fukuoka, M., and Nakagawa, K. (2002) *Lung Cancer* 35, 11–16.
- Sato, K., and Abe, K. (2001) *Brain Res.* 904, 157–160.
- Schuller, E., Gulesserian, T., Seidl, R., Cairns, N., and Lube, G. (2001) *Life Sci.* 69, 263–270.
- Vijayan, S., El-Akkad, E., Grundke-Iqbal, I., and Iqbal, K. (2001) *FEBS Lett.* 509, 375–381.
- Garcia, M. L., and Cleveland, D. W. (2001) *Curr. Opin. Cell Biol.* 13, 41–48.
- Parvari, R., Hershkowitz, E., Grossman, N., Gorodischer, R., Loeys, B., Zecic, A., Mortier, G., Gregory, S., Sharony, R., Kambouris, M., Sakati, N., Meyer, B. F., Al Aqeel, A. I., Al Humaidan, A. K., Al Zahrani, F., Al Swaid, A., Al Othman, J., Diaz, G. A., Weiner, R., Khan, K. T., Gordon, R., and Gelb, B. D. (2002) *Nat. Genet.* 32, 448–452.

# Mechanisms of Taxol resistance related to microtubules

George A Orr<sup>1</sup>, Pascal Verdier-Pinard<sup>1</sup>, Hayley McDaid<sup>1</sup> and Susan Band Horwitz<sup>\*,1</sup>

<sup>1</sup>Department of Molecular Pharmacology, Albert Einstein College of Medicine, 1300 Morris Park Avenue, Bronx, NY 10461, USA

Since its approval by the FDA in 1992 for the treatment of ovarian cancer, the use of Taxol has dramatically increased. Although treatment with Taxol has led to improvement in the duration and quality of life for some cancer patients, the majority eventually develop progressive disease after initially responding to Taxol treatment. Drug resistance represents a major obstacle to improving the overall response and survival of cancer patients. This review focuses on mechanisms of Taxol resistance that occur directly at the microtubule, such as mutations, tubulin isotype selection and post-translational modifications, and also at the level of regulatory proteins. A review of tubulin structure, microtubule dynamics, the mechanism of action of Taxol and its binding site on the microtubule are included, so that the reader can evaluate Taxol resistance in context.

*Oncogene* (2003) 22, 7280–7295. doi:10.1038/sj.onc.1206934

**Keywords:** resistance; Taxol; microtubule

## Introduction

The microtubule cytoskeleton is an effective and validated target for cancer chemotherapeutic drugs. A diverse range of structurally dissimilar compounds can interact with the tubulin/microtubule system and function as antimetabolic agents. These antimetabolic agents can be divided into two major classes: those that bind preferentially to  $\alpha/\beta$ -tubulin heterodimers and inhibit polymer assembly, and those with a binding site on the polymer that stabilizes microtubules. The first class is exemplified by the vinca alkaloids. The prototypic microtubule-stabilizing drug is Taxol (Figure 1). More recently, other mechanistically similar but structurally unrelated natural products, including the epothilones, eleutherobin and discodermolide, have been developed, and are in various stages of preclinical/clinical development.

As with many cancer therapeutic agents, resistance remains a significant problem when using Taxol to treat malignancies. Chemotherapeutic failure may be related either to the tumor being inherently resistant to the drug and/or to the acquisition of resistance during treatment. Although Taxol has demonstrated antitumor activity against several cancers, the emergence of clinical drug resistance is a major limitation to its success. Resistance

is often a multifactorial process that may originate through a series of modifications. In the case of Taxol, several potential mechanisms can be proposed to account for the resistance observed in human tumors and tumor cell lines. These include overexpression of the multidrug transporter P-glycoprotein (Gottesman, 2002), altered metabolism of the drug, decreased sensitivity to death-inducing stimuli (Blagosklonny and Fojo, 1999), alterations in microtubule dynamics and altered binding of Taxol to its cellular target, the microtubule (Dumontet and Sikic, 1999; Druksman and Kavallaris, 2002). This review will focus exclusively on potential mechanisms of resistance at the level of the microtubule.

## Structure and function of the microtubule cytoskeleton

### Microtubule dynamics and function

In eucaryotes, microtubules are involved in a diverse range of cellular functions including mitosis and meiosis, motility, maintenance of cell shape and intracellular trafficking of macromolecules and organelles (Desai and Mitchison, 1997; Oakley, 2000; Sharp *et al.*, 2000). Microtubules are hollow cylindrical tubes formed primarily by the self-association of  $\alpha/\beta$ -tubulin heterodimers into polymers (Downing and Nogales, 1998; Nogales, 2000). The tubulin heterodimers (Figure 2) are associated in a head-to-tail fashion to form protofilaments, which associate in a lateral manner to form hollow microtubules. There is considerable flexibility in the number of protofilaments within a microtubule. *In vivo*, the cylinder is usually composed of 13 protofilaments with an overall diameter of 25 nm. After *in vitro* assembly of bovine brain tubulin, the number of protofilaments is usually 14, but can vary from 10 to 15. Since the lateral associations between protofilaments involve interactions between subunits of the same type, that is, the so-called B-type lattice, the protofilaments are arranged in a parallel array, thereby imparting polarity to the structure. Consequently, the  $\beta$ -chains of the tubulin dimer are exposed at one end (plus) of the polymer, and the  $\alpha$ -chains at the other end (minus). In cells, microtubules are usually organized with their minus ends associated with the microtubule-organizing center (MTOC) near the nucleus, and radiate outward so that the plus ends are near the periphery of the cell.  $\gamma$ -Tubulin, a protein highly homologous to the  $\alpha/\beta$ -tubulins, is

\*Correspondence: SB Horwitz; E-mail: shorwitz@aecom.yu.edu

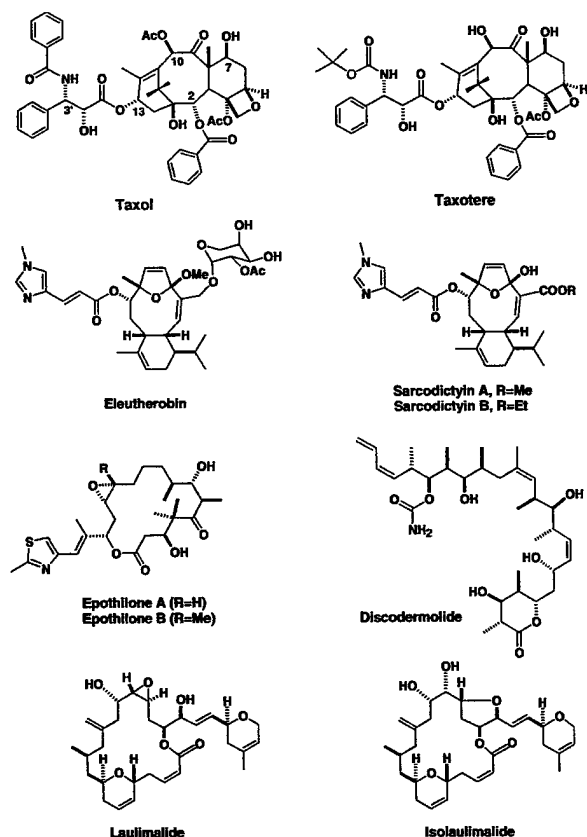


Figure 1 Structures of microtubule-stabilizing agents

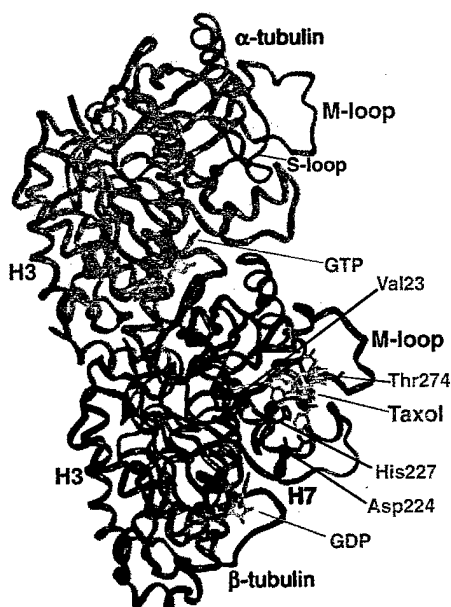


Figure 2 Three-dimensional model of  $\alpha/\beta$ -tubulin heterodimer. Domains of  $\beta$ -tubulin that are discussed in the text, as well as the stabilizing loop (S-loop) unique to  $\alpha$ -tubulin, are colored in red. Helix 3 (H3) and microtubule loop (M-loop) in  $\alpha$ -tubulin are labeled in blue. Amino-acid residues close to Taxol are indicated in gray

localized at the MTOC, and plays an important role in microtubule nucleation by interacting with  $\alpha$ -tubulin (Oakley, 2000).

Microtubules are highly dynamic, and exhibit a nonequilibrium behavior termed dynamic instability (Desai and Mitchison, 1997). In this process, microtubules undergo rapid stochastic transitions between growth and shrinkage, due to the association and dissociation, respectively, of tubulin dimers from the microtubule ends. The transition from growing to shrinking is termed a catastrophe, whereas the reverse behavior is referred to as a rescue. The orchestration of this dynamic instability is related to GTP binding and hydrolysis at the exchangeable or E-site of  $\beta$ -tubulin. GTP binds to both  $\alpha$ - and  $\beta$ -tubulin, but in the case of  $\alpha$ -tubulin, GTP is found at the nonexchangeable or N-site (Figure 2). Microtubule assembly requires  $\beta$ -tubulin to be charged with GTP, which is hydrolysed upon addition of the tubulin dimer to the elongating microtubule. After hydrolysis, the guanine nucleotide becomes nonexchangeable, and so microtubules are mostly composed of  $(\text{GTP}:\alpha\text{-tubulin}/\text{GDP}:\beta\text{-tubulin})_n$ , with the growing end capped with GTP (or  $\text{GDP}\cdot\text{P}_i$ );  $\beta$ -tubulin. In the GTP-cap model, microtubules, which are inherently unstable, are stabilized by GTP (or  $\text{GDP}\cdot\text{P}_i$ )-tubulin at the growing ends. When the GTP cap is lost, the microtubules rapidly depolymerize, with the protofilaments peeling outward. After depolymerization, the released dimers can exchange GTP for GDP at the E-site, and are thus primed for another cycle of polymerization. In contrast, microtubules containing non-hydrolysable GTP analogs are significantly more stable.

Numerous proteins that interact with microtubules and/or free tubulin dimers also have the potential to regulate both catastrophe and rescue rates (Nogales, 2000). The best characterized of these regulatory proteins are the microtubule-associated proteins (MAPs), which stabilize microtubules by decreasing catastrophes and/or increasing rescues. However, other proteins, such as stathmin, may regulate microtubule dynamics by increasing the catastrophe rate. Stathmin appears to bind exclusively to tubulin dimers and not to microtubules. The activities of many of these microtubule-stabilizing/-destabilizing proteins are themselves regulated by phosphorylation/dephosphorylation in a cell cycle-dependent manner.

The tubulin sequence/structure contains the necessary information for self-assembly of tubulin dimers into protofilaments and microtubules. The  $\alpha$ - and  $\beta$ -tubulins (each ~450 amino acids), although highly conserved, display extensive molecular heterogeneity at their C-termini. This structural diversity is a consequence of both the expression of several  $\alpha$ - and  $\beta$ -tubulin isotypes (Sullivan and Cleveland, 1986; Stanchi et al., 2000), the products of distinct genes, and of numerous post-translational modifications occurring to both subunits (MacRae, 1997; Luduena, 1998). These modifications include polyglutamylation and polyglycylation of both subunits, acetylation, reversible tyrosination and excision of the C-terminal glutamate in nontyrosinable  $\alpha$ -tubulin and phosphorylation of the class III  $\beta$ -tubulin.

Significantly, the majority of primary sequence divergence in the various tubulin isotypes and all of the post-translational modifications, except acetylation of lys<sub>40</sub> of  $\alpha$ -tubulin, occur within the C-terminal 20 amino acids of  $\alpha$ - and  $\beta$ -tubulin subunits. While these C-terminal regions are highly variable among the isotypes within a species, the same regions are highly conserved within a single isotype, among species as diverse as human, mouse and chicken. The highly divergent C-termini may provide a mechanism for isotype-specific MAP binding. Moreover, each  $\beta$ -tubulin isotype has a unique pattern of expression ranging from highly specific expression for classes III, IVa and VI to constitutive expression for classes I and IVb. While the class II  $\beta$ -tubulin is predominately expressed in the brain, this isotype is also expressed at low levels in a variety of other tissues. The tissue distribution of the  $\alpha$ -tubulin isotypes is less well established, primarily due to the lack of isotype-specific antisera. We have recently shown by mass spectrometry that  $\alpha$ -1 and  $\alpha$ -6 are the predominant  $\alpha$ -tubulin isotypes expressed in the human breast and lung carcinoma cell lines. The issue of functional specificity of the multiple tubulin isotypes remains unresolved and somewhat controversial. However, the C-terminal isotype sequence conservation and their differential tissue expression strongly imply functional significance.

### Molecular structure of tubulin

Nogales *et al.* (1998, 1999) have obtained, by electron crystallography, a model of the  $\alpha/\beta$ -tubulin dimer fitted to a 3.7 Å density map using zinc-induced tubulin sheets stabilized by Taxol. This model is supported by a 2.8 Å X-ray diffraction map of FtsZ, a bacterial GTP-binding protein with some homology (~10%) to tubulin (Lowe and Amos, 1998). FtsZ also has the propensity to form protofilaments and sheets. Although  $\alpha$ - and  $\beta$ -tubulin monomers share only 40% sequence homology, their overall folding patterns are very similar (Figure 2). Recently, models with improved resolution have been published (Lowe *et al.*, 2001; Meurer-Grob *et al.*, 2001). Each monomer structure can be divided into three major structural domains (Figure 3). The N-terminal domain (residues 1–206) is involved in nucleotide binding, and has a Rossman fold with alternating parallel  $\beta$ -strands (S1–S6) and helices (H1–H6). The central domain (residues 207–384) is involved in both longitudinal/lateral contacts between  $\alpha$ - and  $\beta$ -tubulin monomers present in protofilaments, and is formed by an arrangement of mixed  $\beta$  sheets (S7–S10) and three helices (H8–H10). Taxol binds to a hydrophobic pocket within this central domain (see below). The C-terminal domain is formed by two antiparallel helices (H11 and H12)

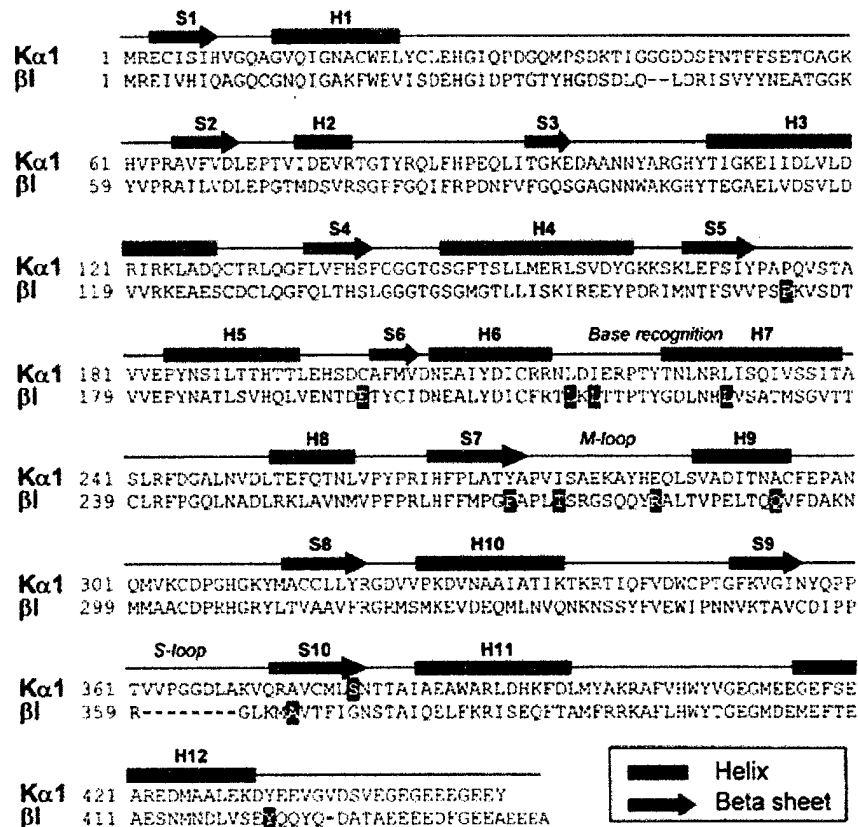


Figure 3 Primary sequences and secondary structure of the major human  $\alpha$ - and  $\beta$ -tubulin isotypes. Helices (H1–H12) are represented as red rectangles and  $\beta$ -sheets (S1–S10) are represented as blue arrows. Mutations detected in Taxol-resistant cell lines are highlighted in black.

that fold across the other two domains. However, the C-terminal 10 residues in  $\alpha$ -tubulin and 18 residues in  $\beta$ -tubulin, which are highly charged, are not visible in this model. This C-terminal domain has been implicated in the binding of several regulatory and motor proteins including tau, MAP-2 and kinesin.

The inter- and intradimer contacts along the protofilaments were readily deduced, since the longitudinal dimer packing in zinc sheets and microtubules is the same. These longitudinal interactions are extensive, and are similar in both inter- and intradimer contacts. The model also provides a rationale for explaining the nonexchangeability/exchangeability of the guanine nucleotide-binding sites on each monomer. In the case of the N-site in  $\alpha$ -tubulin, it is buried at the intradimer interface, thus accounting for the lack of exchange at this site. The guanine nucleotide at the E-site of  $\beta$ -tubulin, in contrast, is at the surface of the dimer allowing for exchange (Figure 2). After polymerization, the E-site becomes nonexchangeable, since it is buried at the interdimer interface.

A major difference between the two polymer types, that is, zinc sheets and microtubules, is the orientation of the protofilaments. In zinc sheets they are aligned antiparallel, whereas in microtubules they are parallel. This implies that the lateral contacts between protofilaments are different in the two polymer types. To visualize the lateral contacts in microtubules, the zinc sheet protofilament structure was docked into a 20 Å resolution map of microtubules obtained by cryoelectron microscopy. In the resulting model, the E-site of  $\beta$ -tubulin was exposed at the plus end of the microtubule and the N-site of  $\alpha$ -tubulin at the minus end, in agreement with previous studies on the orientation of  $\alpha/\beta$ -tubulin heterodimers in microtubules. The model of Nogales *et al.* suggests that the major lateral contacts between  $\alpha$ - $\alpha$  and  $\beta$ - $\beta$  monomers between protofilaments involve interactions between the microtubule loop (M-loop; residues 271–286) and the helix H3 and loop H1-S2 (Figure 2). The M-loop comprises part of the Taxol-binding site in  $\beta$ -tubulin (see below). Although the B-lattice is the predominant protofilament arrangement, many microtubules also contain a seam, in which the lateral contacts involve interactions between  $\alpha$ - and  $\beta$ -tubulin monomers. Whether this seam plays a dynamic role in microtubule function is unclear.

#### *In vitro and in vivo mechanisms of taxol action*

Our research group was the first to examine the mechanism of action of Taxol, and although it became obvious that the drug was an antimitotic agent, it was also clear that Taxol was not a typical antimitotic drug, such as colchicine or the *vinca* alkaloids (Schiff *et al.*, 1979; Schiff and Horwitz, 1980; Horwitz *et al.*, 1986; Horwitz, 1992). These latter drugs bind primarily to tubulin dimers and prevent microtubule assembly. There is no evidence that Taxol can bind to the tubulin dimer. *In vitro*, Taxol binds to the microtubule polymer, enhancing the polymerization of tubulin (Parness and Horwitz, 1981; Manfredi *et al.*, 1982). Microtubules

formed in the presence of the drug possess unusual stability, and resist depolymerization by  $\text{Ca}^{2+}$ , cold temperature and dilution (Schiff *et al.*, 1979). Taxol has the ability to polymerize tubulin in the absence of GTP, which under normal conditions is an absolute requirement for microtubule polymerization. The drug binds to the  $\beta$ -tubulin subunit in microtubules specifically and reversibly, with a stoichiometry, relative to the tubulin heterodimer, approaching one (Parness and Horwitz, 1981; Diaz and Andreu, 1993). Binding is reversible, since unlabeled Taxol can displace [ $^3\text{H}$ ]Taxol from polymerized microtubules. *In vitro*, Taxol alters the kinetics of microtubule assembly. The overall effect of Taxol is to decrease the critical concentration of microtubule protein necessary for microtubule assembly. At a Taxol concentration of 5  $\mu\text{M}$ , the critical concentration of tubulin required for assembly decreases by a factor of 20 from 0.2, to less than 0.01 mg/ml. Taxol also affects the structure of the microtubule polymer by reducing the number of protofilaments from a normal average of 13 to 12 (Diaz *et al.*, 1998).

In cells, high concentrations of Taxol increase polymer mass, and also induce microtubule bundle formation in interphase cells, a phenomenon that has become a hallmark of Taxol binding (Schiff and Horwitz, 1980). However, microtubule bundle formation is a phenotypic consequence of Taxol binding that has a threshold effect. Therefore, at lower concentrations of Taxol, where only a fraction of the total Taxol-binding sites are occupied, the principal effect of the drug is suppression of microtubule dynamics without altering the polymer mass (Jordan *et al.*, 1993; Derry *et al.*, 1995). Interestingly, low concentrations of vinblastine, a microtubule-destabilizing drug, have similar effects on polymer dynamics as Taxol, suggesting that both drugs block mitosis by stabilizing spindle microtubule dynamics. However, we have shown recently that the two major classes of microtubule-based antimitotic agents, that is, the stabilizing and destabilizing drugs, exhibit different mitotic effects at low concentrations (Chen and Horwitz, 2002). Microtubule-stabilizing drugs, including Taxol, the epothilones and discodermolide, produced aneuploid populations of cells in the absence of a sustained mitotic block. In contrast, colchicine, vinblastine and nocodazole, all destabilizing drugs, did not induce aneuploidy at comparable concentrations. Exit from an aberrant mitosis appeared to be responsible for the aneuploidy, since multipolar spindles were induced by stabilizing, but not destabilizing, drugs. These studies imply that Taxol exerts its mitotic effects by alternate mechanisms, depending on the concentration of the drug utilized (Torres and Horwitz, 1998).

#### *Taxol-binding site on the microtubule*

In the absence of a high-resolution structure of tubulin, we used photoaffinity labeling to address the nature of the interaction between Taxol and its target protein (Rao *et al.*, 1992, 1994, 1995; Orr *et al.*, 1998; Rao *et al.*, 1999, 2001). Initially, direct photoaffinity-labeling studies using [ $^3\text{H}$ ]Taxol demonstrated that Taxol binds



specifically to the  $\beta$ -subunit of tubulin (Rao *et al.*, 1992). However, the low extent of photoincorporation precluded a detailed analysis of the Taxol-binding site. The availability of a series of Taxol analogs, bearing photoreactive groups at defined positions around the taxane nucleus, afforded the opportunity to define the contact sites between the drug and  $\beta$ -tubulin. Photoaffinity labeling of microtubules using analogs with photoreactive groups at the C-2, C-3' or C-7 positions also showed exclusive and specific photoincorporation into the  $\beta$ -tubulin monomer. By chemical/enzymatic digestion, and subsequent N-terminal amino-acid sequencing, it was possible to assign the residues in close proximity to the Taxol-binding site. Studies with [ $^3\text{H}$ ]3'-(*p*-azidobenzamido)Taxol, where the arylazide was incorporated into the C-13 side chain, resulted in the isolation of a photolabeled peptide containing amino-acid residues 1–31 in  $\beta$ -tubulin (Rao *et al.*, 1994). Studies with [ $^3\text{H}$ ]2-(*m*-azidobenzoyl)Taxol, where the photoreactive group was attached to the B ring of the taxoid nucleus, demonstrated that a peptide containing amino-acid residues 217–233 of  $\beta$ -tubulin was involved in interacting with the 2-benzoyl group (Rao *et al.*, 1995). Finally, when a benzophenone (BzDC) substituent was attached to the C-7 hydroxyl group of the C ring, specific photocrosslinking to Arg<sub>282</sub> was observed (Rao *et al.*, 1999).

In the electron crystallographic model obtained by Nogales and collaborators, the Taxotere-binding site is located at one side of the  $\beta$ -tubulin monomer that is believed to reside within the microtubule lumen. Although the tubulin model is derived from an unnatural polymer, there was excellent agreement between the binding site, as determined by photoaffinity labeling and electron crystallography. Using the three contact sites obtained through our photoaffinity-labeling studies, we proposed a model for the binding of Taxol to  $\beta$ -tubulin, based on the electron crystallographic model of  $\alpha/\beta$ -tubulin (Rao *et al.*, 1999). The composite model was developed using Taxol containing nitrenes at the *para* position of the C-3' benzamido (labeling residues  $\beta$  1–31) and the *meta* position of the C-2 benzoyl moieties (labeling residues  $\beta$  217–233), and the BzDC group at the C-7 hydroxyl position (labeling  $\beta$ -Arg<sub>282</sub>), and is based on the energy-minimized conformation of 7-BzDC Taxol, derived from the X-ray structure of Taxol. In this model, the nitrene on the C-3' benzamido group is close to Val<sub>23</sub>, in good agreement with the photoaffinity-labeling result, while the nitrene at the *meta* position of the C-2-benzoyl group fits into a pocket formed by the imidazole ring of His<sub>227</sub> and the side chain of Asp<sub>224</sub> (Figure 2). Finally, the photoreactive oxygen atom of the 7-BzDC group can be located at  $\sim 3$  Å distance from the  $\alpha$ -carbon of Arg<sub>282</sub> in  $\beta$ -tubulin.

More recently, two additional models for the Taxol: microtubule interaction have been proposed. Based on data derived from a combination of fluorescence energy transfer (FRET) spectroscopy and solid-state rotational echo double-resonance (REDOR) NMR, Li *et al.* (2000) proposed an orientation for the microtubule-bound Taxol, which differs from that suggested by electron

crystallography and photoaffinity-labeling studies. In this alternate model, Taxol is rotated 180° in its binding site compared to our model. An additional model proposed by Snyder *et al.* (2001) is based on docking individual conformers of Taxol, derived from X-ray crystal structures and NMR studies, into the experimental density map of the tubulin–Taxotere complex. In this model, the C-3' benzamido and the 2-benzoyl groups are positioned as depicted in the earlier model of Rao *et al.* (1999). The C-7 hydroxyl group of Taxol is in close proximity to Thr<sub>274</sub> (Figure 2).

The Taxol-binding site is close to the M-loop, which participates in lateral interactions with the H3 helix of the adjacent  $\beta$ -tubulin monomer in the microtubule (Figure 2). It has been proposed that Taxol-induced stabilization of microtubules is mediated via strengthening of lateral contacts between protofilaments, via a conformational change in the M-loop (Nogales, 2000). Our finding that 7-BzDC Taxol photoincorporates into Arg<sub>282</sub> of the M loop may account for the unusual microtubule-binding properties of this Taxol analog. We observed that 7-BzDC Taxol did not promote tubulin polymerization; yet the analog can stabilize GTP-induced microtubules against cold-induced depolymerization (Rao *et al.*, 1999). Based on our model of the 7-BzDC Taxol:tubulin interaction, it is likely that the analog can bind to small tubulin oligomers, but the presence of the bulky BzDC group in the vicinity of the M-loop prevents free tubulin dimers from associating with these stabilized nucleation centers. The M-loop has also been implicated in the unusual cold stability of Antarctic fish tubulin (Detrich *et al.*, 2000). It has been suggested that two amino-acid substitutions within the M-loop of each  $\alpha$ - and  $\beta$ -monomer (A278T/S287T in  $\alpha$  and S280G/A285S in  $\beta$ ) strengthens the lateral interactions between adjacent protofilaments by increasing the M-loop flexibility. It should be noted that the region of  $\alpha$ -tubulin corresponding to the hydrophobic Taxol-binding pocket of  $\beta$ -tubulin is occupied by an eight-amino-acid loop, the S loop (residues 362–369, Figure 2) (Nogales *et al.*, 1998, 1999; Downing, 2000; Nogales, 2000). It has been suggested that this segment of  $\alpha$ -tubulin acts as an endogenous microtubule-stabilizing factor by promoting the lateral association between protofilaments. We had proposed, a number of years ago, that Taxol was a mimetic of a naturally occurring microtubule-stabilizing factor (Horwitz *et al.*, 1986).

#### Binding site for non-taxane-based microtubule-stabilizing drugs

Several natural products, all with unique structures unrelated to that of Taxol, have been reported to have similar mechanisms of action as Taxol (Figure 1; He *et al.*, 2001). Epothilones A and B, isolated from a *Myxobacterium* fermentation broth, were found to induce tubulin polymerization, arrest cells in mitosis and cause the formation of microtubule bundles (Bollag *et al.*, 1995). Epothilone B was reported to be more potent than Taxol and epothilone A in promoting microtubule assembly *in vitro*. Discodermolide was

isolated from a marine sponge and reported to induce the assembly of microtubules *in vitro* more rapidly than Taxol, and to cause mitotic arrest and microtubule bundling (Hung *et al.*, 1996; ter Haar *et al.*, 1996; Kowalski *et al.*, 1997). Interestingly, the combination of Taxol and discodermolide exhibited a synergistic cytotoxic interaction in human carcinoma cell lines (Martello *et al.*, 2000). A fourth microtubule-stabilizing agent, eleutherobin, was isolated from a marine soft coral and shown to have activity comparable to that of Taxol (Long *et al.*, 1998; Hamel *et al.*, 1999). The epothilones, discodermolide and eleutherobin, are all competitive inhibitors of the binding of [<sup>3</sup>H]-Taxol to microtubules, suggesting that these drugs interact at the same or an overlapping binding domain on  $\beta$ -tubulin (He *et al.*, 2001). The laulimalides are another group of natural products that display microtubule-stabilizing activity (He *et al.*, 2001). However, it appears that laulimalide binds at a site on the tubulin polymer that is distinct from the taxane-binding site (Pryor *et al.*, 2002).

We discovered that 2-*m*-azido baccatin III, a Taxol analog lacking the C-13 side chain but with a *meta* azido benzoyl group at the C-2 position, possesses all of the activities that are characteristic of Taxol (He *et al.*, 2000). Although not as active as Taxol, it does promote microtubule assembly in the absence of GTP, stabilizes microtubules and competitively inhibits the binding of [<sup>3</sup>H]-Taxol to the microtubule protein. The observation that the C-13 side chain is not an absolute requirement for biological activity in a taxane molecule allowed us to propose a new common pharmacophore model between Taxol and epothilone (He *et al.*, 2000). In this model, the thiazole side chain of epothilone corresponds to the C-2 side chain of 2-*m*-azido baccatin III, and binds in the pocket formed by His227 and Asp224. The macrolide ring system of the epothilones overlaps with the taxane ring system. This model of the epothilone:tubulin interaction is essentially equivalent to one of the two models proposed by Fojo's group, based on  $\beta$ -tubulin mutations identified in epothilone-resistant cells (Gianakakou *et al.*, 2000).

Although Taxol does not promote the *in vitro* assembly of yeast tubulin, it has been recently demonstrated that the epothilones do (Bode *et al.*, 2002). Comparison of the primary sequences of mammalian and yeast tubulins show sequence variations at several positions known to be important for Taxol binding. These include K19A, V23T and D26G substitutions in the N-terminal domain of  $\beta$ -tubulin, residues that make contact with the 3'-benzamido-phenyl group of Taxol. In our proposed model (He *et al.*, 2000), the epothilones do not make contact with the N-terminal domain of  $\beta$ -tubulin, potentially explaining their ability to interact with yeast tubulin.

## Resistance to taxol in cell lines

### Alterations in microtubule dynamics

Since the Taxol-binding site is present only on polymerized tubulin, and not on tubulin dimers, selection of

a less stable polymer, that is, a polymer with increased microtubule dynamics, could potentially offer a survival advantage for a tumor challenged with a microtubule-stabilizing drug such as Taxol. Two potential models describing the relationship between resistance to microtubule-active drugs and cellular microtubule dynamics have been proposed. According to Cabral and co-workers, Taxol-resistant cell lines contain 'hypostable' microtubules in which the equilibrium between the dimer and polymer is shifted towards the former (Cabral *et al.*, 1986; Cabral and Barlow, 1989; Minotti *et al.*, 1991). As such, these cells will display increased resistance to polymer-binding drugs like Taxol, and increased sensitivity towards tubulin dimer-specific agents, such as vinblastine and colchicine. In addition, this model offers a potential explanation for the intriguing observation that some Taxol-resistant cell lines have an absolute requirement for low concentrations of Taxol for normal cell growth. In these drug-dependent cells, the stability of the polymer is apparently perturbed to such an extent that normal cell function is compromised, and the cells require low concentrations of Taxol for survival. Based on the observation that low concentrations of microtubule-stabilizing and -destabilizing drugs inhibit microtubule dynamics without altering polymer mass, Wilson and Jordan have suggested that in Taxol-resistant cell lines, the equilibrium between weakly and highly dynamic microtubules has been shifted towards the latter (Derry *et al.*, 1995; Wilson and Jordan, 1995; Jordan and Wilson, 1998; Goncalves *et al.*, 2001).

The dynamics of individual rhodamine-labeled microtubules in Taxol-sensitive and -resistant A549 cell lines, derived from a human lung carcinoma, have been quantified by digital time-lapse microscopy (Goncalves *et al.*, 2001). The A549-T12 and -T24 cell lines, nine- and 17-fold resistant, respectively, to Taxol were selected by continual exposure of the parental drug-sensitive, cell line to increasing concentrations of drug. Significantly, both resistant cell lines are also dependent on low concentrations of Taxol (2 nM) for growth, and become blocked in the G<sub>2</sub>/M phase of the cell cycle if the drug is removed. Both resistant cell lines exhibited increased dynamic instability compared with the parental, drug-sensitive, cell line. Several potential mechanisms can be envisaged by which microtubule dynamics could be modulated in a Taxol-resistant cell line, and include altered tubulin isotype expression, mutations to tubulin that affect either longitudinal/lateral interactions or binding of regulatory proteins, alterations to tubulin through post-translational modifications that modify regulatory protein binding, and altered expression or post-translational modifications to tubulin/microtubule-regulatory proteins.

### Altered expression of $\beta$ -tubulin isotypes

Inherent differences in the assembly properties, microtubule dynamics and drug interactions among some of the  $\beta$ -tubulin isotypes have been revealed by *in vitro* analysis of immunoaffinity-purified isotypes prepared

from bovine brain tubulin (3% class I, 58% class II, 25% class III and 13% class IV  $\beta$ -tubulin) (Banerjee *et al.*, 1990, 1992; Lu and Luduena, 1993, 1994; Panda *et al.*, 1994; Derry *et al.*, 1997). It was reported that microtubules assembled from  $\beta$ III-tubulin had distinct assembly properties compared to  $\beta$ II-,  $\beta$ IV- or unfractionated tubulin (Banerjee *et al.*, 1990; Lu and Luduena, 1993, 1994).  $\beta$ III-tubulin required the highest critical concentration of tubulin for assembly, exhibited a distinct delay in nucleation and proceeded at a slower rate compared to other isotypes. Since the differences in assembly occurred in the absence of MAPs, this would suggest that the various tubulin isotypes, by themselves, can modulate microtubule dynamics (Panda *et al.*, 1994). In fact, microtubules containing only  $\beta$ III-tubulin exhibited a dynamicity more than double that of  $\beta$ II- and  $\beta$ IV-derived microtubules (Panda *et al.*, 1994). As a result, microtubules composed exclusively of  $\beta$ III-tubulin are less stable than microtubules composed of either  $\beta$ II- or  $\beta$ I-tubulin. Nevertheless, when  $\beta$ II-microtubules were spiked with  $\beta$ III-tubulin, the resulting microtubules exhibited decreased, not increased dynamicity. Derry *et al.* (1997) demonstrated that microtubules composed of either  $\beta$ III- or  $\beta$ IV-tubulin were considerably less sensitive to the suppressive effects of Taxol on microtubule dynamics, than microtubules assembled from  $\beta$ II or unfractionated tubulin. Collectively, these *in vitro* studies suggest that microtubule dynamics, and the effects of Taxol on this process, can be modulated by the  $\beta$ -tubulin isotype composition. Such studies have formed the basis for the idea that altered cellular expression of  $\beta$ -tubulin isotypes, especially  $\beta$ III and  $\beta$ IV, could be an important determinant in cellular resistance towards Taxol. However, there are two major caveats to these *in vitro* studies. First, the  $\alpha$ -tubulin isotype composition of the immunoaffinity-purified  $\beta$ -tubulin isotypes has not been determined. Bovine brain tubulin has three major  $\alpha$ -tubulin isotypes,  $\alpha$ 1,  $\alpha$ 2, and  $\alpha$ 4, all of which are extensively post-translationally modified. Preferential association between specific  $\alpha$ - and  $\beta$ -isotypes could complicate the analysis of any *in vitro* studies. Second,  $\beta$ I, not  $\beta$ II, is the major  $\beta$ -tubulin isotype in non-neuronal cells, and the influence of  $\beta$ III- and  $\beta$ IV-tubulins on  $\beta$ I-microtubule dynamicity has not been determined. So, although mammalian brain tubulin is a rich and readily available source of tubulin for *in vitro* studies, its tubulin composition is probably not representative of many human cancer cell lines and tumors.

There have been numerous reports of altered expression of individual  $\beta$ -tubulin isotypes in cells that have been selected for resistance to antimetabolic agents (see Table 1). Analysis of  $\beta$ -tubulin isotypes in Taxol-resistant cells has been performed by utilizing isotype-specific primers for RT-PCR analysis, as well as isotype-specific antibodies for Western blot analysis and/or immunofluorescence. In the Taxol-resistant non-small lung carcinoma cell lines A549-T12 and A549-T24, described above, RT-PCR analysis demonstrated that the class III and IVa isotypes, which were barely detectable in the parental cell line, increased ~2–3-fold,

in the A549-T12, and ~fourfold in the A549-T24 cell lines (Kavallaris *et al.*, 1997). The increase in  $\beta$ III tubulin in A549-T24 cells was confirmed by immunofluorescence. Likewise, a twofold increase in class IVa  $\beta$ -tubulin mRNA and protein level was noted in a K562 erythroleukemia cell line that was ninefold resistant to Taxol (Jaffrezou *et al.*, 1995). Selection of a human prostate carcinoma cell line, DU-145, with Taxol produced alterations in the expression levels of both class III and IVa (Ranganathan *et al.*, 1998a). The DU-145 cell line, which was fivefold resistant to Taxol, had an ~threefold increase in total  $\alpha$ - and  $\beta$ -tubulin, and a fourfold increase in class III protein with a ninefold increase at the RNA level. Nicoletti *et al.* (2001), using RT-PCR, analysed  $\beta$ -tubulin isotype composition in a subset of 17 cancer cell lines from the National Cancer Institute-Anticancer Drug Screen. In these cell lines,  $\beta$ I was the major tubulin isotype accounting for 85–99% of all the  $\beta$ -tubulin mRNA. Significantly, when the sensitivities of these cell lines towards antimetabolic drugs, including Taxol, vinblastine, vincristine and rhizoxin, were correlated with the absolute levels of mRNA expression for the various  $\beta$ -tubulin isotypes, it was found that sensitivity towards Taxol, but not the three other antimicrotubule drugs, correlated with  $\beta$ III-tubulin levels. After  $\beta$ I, the  $\beta$ III mRNA was the next predominant message expressed in these cell lines, with levels ranging from 0.5 to 14%.

All these studies imply that altered expression of  $\beta$ -tubulin isotypes, especially class III and IVa, may be correlated with Taxol sensitivity. This hypothesis is supported by analysis of tubulin isotypes in cells not selected for drug resistance. A study of brain cell lines with different intrinsic levels of class III  $\beta$ -tubulin showed that all were able to accumulate Taxol to a similar extent (Ranganathan *et al.*, 1998b). However, the two cell lines with elevated levels of class III protein were ~5.5-fold less sensitive to Taxol, compared to the cell line that had no detectable levels of class III. Studies in HT29-D4, a human colon adenocarcinoma cell line, that is used as a model for epithelial cell differentiation, also support a role for  $\beta$ III in determining cellular sensitivity towards Taxol (Carles *et al.*, 1999). Undifferentiated HT29-D4 cells are malignant and proliferate rapidly. After galactose-induced differentiation, the cells take on the appearance of polarized epithelial cells. Interestingly, the cytotoxicity of Taxol towards HT29-D4 cells depends upon their differentiation status. Although bundling of microtubules occurred in undifferentiated cells in the presence of Taxol, the microtubules of the differentiated cells failed to bundle even though they accumulated twofold more drug than the undifferentiated cells. RT-PCR and immunoblot analyses have demonstrated that the class I, II, III, IVa and IVb  $\beta$ -tubulin isotypes were expressed in HT29-D4 cells. However, a selective increase in class III  $\beta$ -tubulin mRNA and protein occurred upon differentiation. In other studies, cell lines overexpressing EGFRvIII and HER2 oncogenic growth factors had decreased sensitivity to Taxol (Montgomery *et al.*, 2000). Significantly, Taxol-induced polymerization was suppressed in these

**Table 1** Alterations in tubulin composition associated with resistance to Taxol

Cell line <sup>a</sup>	Alteration in tubulin content <sup>b</sup>		Fold resistance to Taxol <sup>c,d</sup>	Reference
	Tubulin (fold increase) <sup>d</sup>	Detection method		
<i>Taxol-selected</i>				
NCIH460/T800 (lung)	$\alpha$ -Tubulin ( $\uparrow$ )	WB	1000 <sup>e</sup>	Kyu-Ho <i>et al.</i> (2000)
A549-T12 (lung)	$\beta$ III (2)	RT-PCR	9	Kavallaris <i>et al.</i> (1997)
A549-T24 (lung)	$\beta$ IVa (3)	RT-PCR	17f	Kavallaris <i>et al.</i> (1997)
	$\beta$ III (4)	RT-PCR		
	$\beta$ III ( $\uparrow$ )	NB IF		
	$\beta$ IVa (4)	RT-PCR		
H69/Tx1 (lung)	Acet $\alpha$ -tubulin ( $\uparrow$ )	WB	4.7	Ohta <i>et al.</i> (1994)
MCF-7-PTX30 (breast)	Tyr $\alpha$ -tubulin (2)	WB	ND	Banerjee (2002)
	$\beta$ III (2)	WB		
	$\beta$ IV (1.5)	WB		
	$\beta$ II (2.4)	RT-PCR		
S2/TXT (pancreas) <sup>g</sup>	$\beta$ III (2.3)	RT-PCR	9.5 <sup>e</sup>	Liu <i>et al.</i> (2001)
	$\alpha$ - and $\beta$ -tubulin (3)	IF IF		
	$\beta$ III (4)	WB		
	$\beta$ III (9)	RT-PCR		
DU-145-Pac10 (prostate)	$\beta$ IVa (5)	RT-PCR	24	Giannakakou <i>et al.</i> (1997)
	$\beta$ I (1.8)	RT-PCR		
	$\beta$ IVa (0.03)	RT-PCR		
	$\beta$ IVa (2)	RT-PCR		
1A9PTX22 (ovary)	$\beta$ IV ( $\uparrow$ )	WB	9	Jaffrezou <i>et al.</i> (1995)
	$\beta$ I (1.9)	RT-PCR		
	$\beta$ II (21)	RT-PCR		
	$\beta$ I (3.6)	RT-PCR		
Taxol-resistant ovarian tumor samples	$\beta$ III (4.4)	RT-PCR	NA	Kavallaris <i>et al.</i> (1997)
	$\beta$ IVa (7.6)	RT-PCR		
	$\beta$ IVa (2.5)	RT-PCR		
	$\beta$ IVb (3.1)	RT-PCR		
<i>Not drug-selected</i>				
NIH3T3-HC2 (murine fibroblast)	$\beta$ III (1.7)	RT-PCR	1000	Carles <i>et al.</i> (1999)
HT29-D4 (colon)	$\beta$ III ( $\uparrow$ )	WB	5.5	Ranganathan <i>et al.</i> (1998b)
	Tyr $\alpha$ -tubulin ( $\downarrow$ )	WB		
	$\beta$ III ( $\uparrow$ )	WB		
	$\beta$ III ( $\uparrow$ )	WB		
SF 295 vs SF 539 (glioblastoma)	$\beta$ III ( $\uparrow$ )	WB	5.5	Ranganathan <i>et al.</i> (1998b)
SNB75 vs SF539 (glioblastoma)	$\beta$ III ( $\uparrow$ )	WB	5.5	Ranganathan <i>et al.</i> (1998b)
17 Human cancer cell lines	$\beta$ III ( $\uparrow$ )	RT-PCR	$\uparrow$	Nicoletti <i>et al.</i> (2001)

<sup>a</sup>Human cell lines except where noted. <sup>b</sup>WB, Western blotting; RT-PCR, reverse transcriptase-polymerase chain reaction; IF, immunofluorescence; NB, Northern blotting; acet, acetylated; tyr, tyrosinated. <sup>c</sup>IC<sub>50</sub>-resistant cell line/IC<sub>50</sub> parental cell line. ND, not determined; NA, not available.

<sup>d</sup>Vertical arrows indicate relative increase or decrease. <sup>e</sup>Expresses high levels of Pgp. <sup>f</sup>Expresses very low levels of Pgp. <sup>g</sup>Selected with Taxotere

cells compared to cells expressing wild-type EGFR. Increases in class IVa  $\beta$ -tubulin were observed in both oncogene-transfected cell lines. Introduction of a mutation into the kinase domain of the receptor, thereby inhibiting EGFRvIII kinase activity, partially reversed resistance to Taxol and decreased expression of the class IVa  $\beta$ -tubulin by 50%. These studies are highly significant since they suggest that certain oncogenes can alter drug sensitivity by modulating  $\beta$ -tubulin isotype levels.

#### Alterations in $\beta$ -tubulin isotype levels by transfection studies

To validate definitively that tubulin isotype composition can modulate Taxol sensitivity, specific isotype levels must be modulated in drug-naïve cells using either protein overexpression or antisense oligonucleotide approaches. In three reported transfection experiments, stable overexpression of class I, II and IVb  $\beta$ -tubulin genes in Chinese hamster ovary (CHO) cells (Blade *et al.*, 1999), the class II  $\beta$ -tubulin gene in NIH 3T3 cells (Burkhart *et al.*, 2001) and  $\beta$ III in a human prostate carcinoma cell line (Ranganathan *et al.*, 2001) failed to

confer resistance to Taxol. However, downregulation of class III  $\beta$ -tubulin by antisense oligonucleotides in Taxol-resistant A549-T24 cells resulted in a 40–50% decrease in both class III mRNA and protein levels, and was associated with a 39% increase in sensitivity to Taxol (Kavallaris *et al.*, 1999).

It is important to consider why overexpression of tubulin isotypes in drug-naïve cells failed to confer a resistant phenotype, while downregulation of  $\beta$ III tubulin in a drug-resistant cell line was modestly effective in altering drug sensitivity. Attempts to modulate specific  $\beta$ -tubulin isotype levels in cells are complicated by compensatory changes in the expression levels of other  $\beta$ -tubulin isotypes. The mechanisms of transcriptional regulation of  $\alpha$ - and  $\beta$ -tubulin synthesis are distinct. Cellular  $\beta$ -tubulin levels are autoregulated by cotranslational degradation of mRNAs. This negative feedback control utilizes a tetrapeptide, MREI, in the N-terminus of  $\beta$ -tubulins, to induce a signal for message degradation.

$\beta$ I-Tubulin is the major isotype in all of the transfected cells and, as discussed previously, is the least

studied of the isotypes in terms of *in vitro* microtubule assembly and dynamics. It has yet to be established whether  $\beta$ III or  $\beta$ IV isotypes can alter the dynamics of microtubules composed predominately of  $\beta$ I tubulin. It is also possible that the levels of overexpression achieved in the above transfection experiments were not sufficient to alter microtubule dynamics and thus produce a resistance phenotype. RT-PCR analysis and isotype-specific antibodies were used in these studies to quantify isotypic changes. Unfortunately, quantitation of tubulin mRNA levels may not accurately reflect the protein profile in transfected cells. Likewise, antibody-based methods can only give relative, not absolute, levels of a specific tubulin isotype in cells. Our research group has recently described a mass spectrometry-based method for analysing human tubulin isotype composition (Rao *et al.*, 2001). By incorporating stable isotope quantitation into this method, we anticipate that we will be able to determine absolute levels of each isotype in cells and tissues.

Finally, altered expression of  $\beta$ -tubulin isotypes may not be directly related to the resistant phenotype, but represents a secondary effect that may require the participation of additional isotype-specific regulatory proteins. Since it is known that some MAPs bind to the highly divergent, but isotype-specific C-terminal regions of tubulin, it would not be unexpected if such regulatory proteins exist and are coordinately expressed along with their respective isotype upon drug selection. This scenario would explain why simple overexpression of tubulin isotypes in drug-sensitive cells cannot produce a resistance phenotype; yet alterations in drug sensitivities of resistant cell lines can be observed using an antisense approach.

### Alterations in $\alpha$ -tubulin isotype composition

The  $\alpha$ -tubulin isotype composition also has the potential to affect the drug sensitivity of cells (Table 1). Under *in vitro* conditions, tubulin enriched by immunoaffinity purification in the tyrosinated  $\alpha$ 1,  $\alpha$ 2 isotypes was shown to assemble three times faster than the nontyrosinated forms (Banerjee and Kasmala, 1998). At the cellular level, the lung carcinoma cell line, NCI-H460/T800, an MDR-expressing cell which is 1000-fold resistant to Taxol compared to the parental cell line, overexpresses its  $\alpha$ -tubulin protein, but not at the mRNA level (Kyu-Ho Han *et al.*, 2000). Downregulation of  $\alpha$ 1-tubulin in this resistant cell line using an anti-sense DNA construct caused a 45–51% increased sensitivity towards Taxol in three independent clones. Furthermore, overexpression of  $\alpha$ 1-tubulin in the parental H460 cells caused a 2.5-fold increase in resistance towards Taxol. Interestingly, both the antisense and sense clones also displayed altered sensitivities towards vinblastine and colchicine, but not to nocodazole.

### Point mutations in tubulin leading to alterations in microtubule dynamics

Tumor cell lines selected for resistance to Taxol often demonstrated altered migration of  $\alpha$ - and  $\beta$ -tubulin by two-dimensional gel electrophoresis. Several lines of evidence suggest that many of the Taxol-resistant cells contained a less stable microtubule polymer. Some of the selected cell lines were Taxol-dependent, and exhibited lower levels of microtubule assembly than the parental drug-sensitive or the Taxol-independent, but resistant, cell lines (Table 2). Moreover, many of the Taxol-resistant lines were hypersensitive to

Table 2 Tubulin mutations associated with resistance to Taxol

Cell line <sup>a</sup>	Mutation <sup>b</sup>	Fold resistance to drug <sup>c</sup>			Taxol dependence <sup>d</sup>	Impairment of drug-induced polymerization	Reference
		Taxol	Vinblastine	Colchicine			
<i>Taxol</i>							
A549-T12	αSer379Ser/Arg	9	1.5	1.0	++++	Taxol no	Martello <i>et al.</i> (2003)
A549-T24 <sup>e</sup>	αSer379Ser/Arg	17	1.4	1.3	++++	Taxol no	Martello <i>et al.</i> (2003)
1A9PTX10	βPhe270Val	24	0.5	ND <sup>f</sup>	—	Taxol yes; EpoB no	Giannakakou <i>et al.</i> (1997)
1A9PTX22	βAla364Thr	24	0.4	ND	—	Taxol yes; EpoB no	Giannakakou <i>et al.</i> (1997)
CHO-Tax mutants	βLeu215His	2–3	ND	ND	—	Taxol no	Gonzalez-Garay <i>et al.</i> (1999)
	βLeu215Arg	↓	↓	↓	—	↓	↓
	βLeu215Phe	↓	↓	↓	++++	↓	↓
	βLeu217Arg	↓	↓	↓	—	↓	↓
	βLeu228Phe	↓	↓	↓	++++	↓	↓
	βLeu228His	↓	↓	↓	++++	↓	↓
MDA-MB-231/K20T	βGlu198Gly	19	1.0	ND	—	Taxol no	Wiesen <i>et al.</i> (2002) <sup>g</sup>
<i>Epothilone A or B</i>							
A549.EpoB40	βGlu292Glu	22	0.5	0.6	+	EpoB yes	He <i>et al.</i> (2001)
HeLa.EpoA9	βPro173Pro/Ala	6.4	0.9	0.6	+	ND	He <i>et al.</i> (2001)
HeLa.EpoB1.8	βTyr422Tyr/Cys	2.8	1.6	0.4	++	ND	He <i>et al.</i> (2001)
1A9/A8	βThr274Ile	10	ND	ND	—	Taxol yes; EpoA yes	Giannakakou <i>et al.</i> (2000)
1A9/B10	βArg282Gln	6.5	ND	ND	—	Taxol yes; EpoA yes	Giannakakou <i>et al.</i> (2000)

<sup>a</sup>The drug used for selection is indicated. <sup>b</sup>Location of mutation is described in text and Figure 3. <sup>c</sup>IC<sub>50</sub>-resistant cell line/IC<sub>50</sub> parental cell line. <sup>d</sup>++++, total dependence; ++, medium dependence; +, low dependence; —, no dependence. <sup>e</sup>Expresses very low levels of Pgp. <sup>f</sup>Not determined. <sup>g</sup>Proceedings of the AACR 93rd Annual meeting, 2002, Vol. 43, p. 788, #3906

microtubule-destabilizing drugs, such as vinblastine or colchicine, that bind to free tubulin dimers. A detailed analysis of class I  $\beta$ -tubulin mutations in Taxol-resistant CHO cell lines, isolated by single-step selection, revealed a cluster of mutations at leucines 215, 217 and 228 (Gonzalez-Garay *et al.*, 1999). It was concluded that resistance in these cells was due to the mutations that altered microtubule dynamics by affecting the lateral/longitudinal interactions important for microtubule assembly. By destabilizing microtubules, these mutations apparently counteract the stabilizing effects of Taxol. Importantly, using a tetracycline-regulated expression system, it was shown that the low-level expression of  $\beta$ -tubulin containing any one of these mutations conferred Taxol resistance in CHO cells.

Three new epothilone-resistant cell lines have been selected in our laboratory in A549 and HeLa cells. These resistant cell lines are crossresistant to the taxanes and do not express the MDR1 gene. Sequence analysis of the class I  $\beta$ -tubulin from these resistant cell lines revealed that there were single point mutations at  $\beta$ 292 (Gln to Glu),  $\beta$ 173 (Pro to Ala) and  $\beta$ 422 (Tyr to Tyr/Cys), respectively. These mutations are near the M-loop, the nucleotide-binding site and the C-terminus, regions that are involved in stabilizing the lateral contacts between adjacent protofilaments, the hydrolysis of GTP and the binding of MAPs, respectively (Figure 3). It is likely that these mutations decrease the endogenous stability of the microtubule to compensate for the activities of microtubule-stabilizing drugs. Consistent with this hypothesis, it was found that these resistant cell lines became more sensitive to microtubule-destabilizing drugs such as vinblastine and colchicine.

Sequencing of the class I  $\beta$ -tubulin gene in the A549-T12 cells did not reveal any mutations. However, a heterozygous point mutation in K- $\alpha$ 1 tubulin was found at residue 379 (Ser to Ser/Arg) (Martello *et al.*, 2003). The expression of both the wild-type and mutated  $\alpha$ -tubulins in the A549-T12 cell line was confirmed by mass spectrometry (Verdier-Pinard *et al.*, 2003). This region of  $\alpha$ -tubulin is near the C-terminus, and is close to the proposed sites of interaction for both MAP4 and stathmin.

#### Post-translational modifications to tubulin

As mentioned previously, the structural diversity of the tubulin protein family is further increased by extensive post-translational modifications. All of the post-translational modifications, except acetylation, occur within the C-terminal 20 amino acids of  $\alpha$ - and  $\beta$ -tubulin chains. Since several MAPs have been shown to interact with the C-terminal region of tubulin, it is possible that reversible post-translational modifications to this region of tubulin could regulate its interaction with MAPs, thus modulating microtubule dynamics. It is known that the ability of several structural and motor MAPs, including tau, MAP-2 and kinesin, to interact under *in vitro* conditions with the microtubule cytoskeleton is regulated by the level of polyglutamylation of the  $\alpha$ - and  $\beta$ -tubulins (Boucher *et al.*, 1994; Larcher *et al.*, 1996; Bonnet *et al.*, 2001). The levels of tubulin glutamylation

and tubulin polyglutamylase activity were shown to be cell cycle dependent (Bobinnec *et al.*, 1998; Regnard *et al.*, 1999). Although enzymatic activity peaked in G<sub>2</sub> phase, the level of glutamylated tubulins was maximally elevated in mitosis, suggesting a complex regulation involving both polyglutamylase and deglutamylase activities. Removal of phosphate from  $\beta$ III tubulin by protein phosphatase 2A inhibited MAP-2-stimulated *in vitro* microtubule assembly (Khan and Luduena, 1996).

Utilizing 2-D gel electrophoresis, P19 embryonal carcinoma cells demonstrated increased expression of the more acidic isoforms of  $\beta$ III tubulin after Taxol treatment (Laferriere and Brown, 1996). The lack of <sup>32</sup>Pi incorporation into the more acidic  $\beta$ III isoform suggests that glutamylation was responsible for the shift in isoelectric point. In the case of a Taxol-resistant human small lung cell carcinoma, increased acetylation of  $\alpha$ -tubulin was observed (Ohta *et al.*, 1994) (Table 1). However, it is likely that these modifications reflect substrate preference, namely polymer over dimer, of the modifying enzymes, and are not directly associated with Taxol resistance. To date, however, there is little evidence that altered post-translational modifications are a major determinant of cellular sensitivity towards Taxol or any tubulin-directed antimitotic agent.

#### Altered expression/post-translational modifications of tubulin-microtubule-regulatory proteins

Proteins that regulate microtubule dynamics by interacting with tubulin dimers or polymerized microtubules clearly have the potential to modulate the sensitivity of a cell towards Taxol. Stathmin, a microtubule destabilizer, and MAP4, a microtubule stabilizer, represent such proteins that regulate the dynamics of cellular microtubules. Stathmin is a soluble cytoplasmic protein that can bind to tubulin dimers and stimulate microtubule catastrophes (Belmont and Mitchison, 1996; Cassimeris, 2002). This destabilizing activity is regulated by phosphorylation, and is lost when stathmin is fully phosphorylated (Marklund *et al.*, 1996; Horwitz *et al.*, 1997). MAP4 is the predominant human non-neuronal MAP, and the microtubule-stabilizing function of MAP4 is also regulated by phosphorylation (Chapin *et al.*, 1995; Chang *et al.*, 2001). MAP4 alters microtubule dynamics by increasing the rescue frequency, without affecting the catastrophe frequency. Phosphorylation of MAP4 results in a loss of this microtubule-stabilizing activity. The overexpression/activation of stathmin and/or the downregulation/inactivation of MAP4 should increase the dynamicity and decrease the stability of microtubules. Such changes in cancer cells could reduce the microtubule-stabilizing potency of Taxol, and confer a mechanism of resistance to the drug. Inversely, the potency of microtubule-depolymerizing drugs like vinca alkaloids could be enhanced.

Downregulation of stathmin, by a stathmin antisense construct stably transfected into K562 erythroleukemia cells, produced a synergistic inhibition of their growth and clonogenicity when treated with low concentrations of Taxol, and were more resistant to vinblastine

compared to control mock-transfected cells (Iancu *et al.*, 2000, 2001). In contrast, overexpression of stathmin in human lung carcinoma cells sensitized the cells to vindesine and vincristine, but did not significantly decrease their sensitivity to Taxol or Taxotere (Nishio *et al.*, 2001). Moreover, stathmin inhibited *in vitro* Taxol-induced polymerization of microtubules (Larsson *et al.*, 1999). Altogether, these data indicate that overexpression of active stathmin in cancer cells could decrease their sensitivity to Taxol by opposing the microtubule-stabilizing effect of Taxol.

Alterations in expression of various forms of MAP4 are also predicted to modulate cancer cell sensitivity to microtubule-interacting drugs. Inhibition of MAP4 expression by an antisense approach decreased microtubule polymer levels in HeLa cells, whereas overexpression of MAP4 increased microtubule stability. MAP4 expression has been shown to be transcriptionally repressed in the presence of wild-type p53 (Murphy *et al.*, 1996), and Hait and co-workers demonstrated that inactivation of p53 in murine fibroblasts increased their sensitivity to Taxol, but decreased their sensitivity to vinblastine (Zhang *et al.*, 1998). This group confirmed this trend when they induced p53 by treating the same cells with DNA-damaging agents, and observed a decrease in Taxol sensitivity and an increased sensitivity to vinblastine (Zhang *et al.*, 1999). MAP4 phosphorylation and dissociation from microtubules correlated with a decrease in Taxol sensitivity in Taxol-resistant ovarian cell lines (Poruchynsky *et al.*, 2001). In contrast, the expression of nonphosphorylated forms of MAP4 is increased in vinblastine-resistant cells (Kavallaris *et al.*, 2001).

The protein levels of stathmin and MAP-4 have been quantified in the Taxol-sensitive and -resistant A549 cell lines. The stathmin protein levels in the A549-T12 and -T24 resistant cell lines were increased ~twofold compared to the parental drug. Since stathmin activity is regulated by phosphorylation, its phosphorylation status was also evaluated. In the parental A549 cells, exposure to increasing concentrations of Taxol caused a shift from the nonphosphorylated and active form of stathmin to the fully phosphorylated and inactive protein. Significantly, no shift in phosphorylation was observed in the two Taxol-resistant cell lines. With regard to MAP4, the parental cell line expressed exclusively the nonphosphorylated and active form of the microtubule-stabilizing protein, whereas A549-T24 cells predominately expressed the phosphorylated and inactive form. A549-T12 cells that display lower resistance to Taxol than the A549-T24 cell line expressed both forms of MAP4. These changes in the tubulin-/microtubule-regulatory proteins observed in the Taxol-resistant A549 cell lines would be predicted to act in concert, to increase the dynamicity of their microtubules.

The regulation of microtubule dynamics by interacting proteins is complex, and is likely to involve a variety of proteins in addition to stathmin and MAP4. For example, the expression levels of MAP4 and E-MAP-115, another MAP expressed in cells of epithelial origin, were quantified during HT29-D4 cell differentia-

tion. Levels of MAP-4 did not vary during differentiation. However, extremely low levels of E-MAP-115 were present in undifferentiated cells, and the levels were upregulated significantly during the differentiation process. Overexpression of E-MAP-115 in MCF-7 and HeLa cells increased their sensitivity towards Taxol (Gruber *et al.*, 2001).

#### *Altered binding of taxol to the microtubule*

The acquisition of mutations that confer altered binding of a drug to its primary target is a recurring theme in drug resistance. Not unexpectedly, examples of altered drug binding have been identified in cell lines resistant to microtubule-stabilizing drugs. Two independent Taxol-resistant human ovarian carcinoma cell lines, 1A9PTX10 and 1A9PTX22, have been isolated, and are 24-fold resistant to Taxol, but are hypersensitive to vinblastine (Giannakakou *et al.*, 1997) (Table 2). These cell lines were not Taxol dependent, and the resistant phenotype was sustained even after the cells were cultured for 3 years in the absence of drug. The total tubulin contents of both the resistant and the parental cells were similar and all the cells had the same fraction of tubulin in the polymerized state, suggesting that microtubule dynamics in these Taxol-resistant cells was not altered. However, the isolated tubulins from the resistant cells polymerized poorly in the presence of Taxol, suggesting that these mutations abrogated Taxol binding. Interestingly, these Taxol-resistant cells retained sensitivity to epothilone B and to 2-*m*-azido-benzoyl-Taxol, both of which are considerably more potent microtubule-stabilizing drugs than Taxol. Sequence analysis of the major  $\beta$ -tubulin isotype  $\beta$ 1 in these cell lines revealed that the 1A9PTX10 cells had a Phe<sub>270</sub>-to-valine substitution, whereas the 1A9PTX22 cell line had an Ala<sub>364</sub>-to-threonine substitution. From molecular modeling studies, Phe<sub>270</sub> is close to the region of tubulin that makes important contacts with the taxane ring system of Taxol (see above). It is possible that replacing the phenyl ring at this position by the less bulky side chain of valine could disrupt Taxol binding to the mutant tubulin. Epothilone-resistant cell lines were isolated after exposure of the human ovarian carcinoma cell line to epothilone A or epothilone B (Giannakakou *et al.*, 2000). These epothilone-resistant cell lines exhibited impaired epothilone- and Taxol-induced tubulin polymerization (Table 2). One cell line had a mutation leading to a threonine-to-isoleucine change at amino acid 274, and the other had a mutation leading to an arginine-to-glutamine change at amino acid 282. This arginine residue is the site of photoincorporation of 7-BzDC Taxol (see above; Rao *et al.*, 1999). Based on molecular modeling studies, it was suggested that the Thr<sub>274</sub>Ile substitution could disrupt the hydrogen bond between the side chain hydroxyl group of threonine and the C7-hydroxyl of the epothilones (Giannakakou *et al.*, 2000).

#### *Alterations in signaling pathways*

Key proteins that mediate various signaling pathways are often localized to microtubules (Gundersen and



Cook, 1999; Hollenbeck, 2001; Cardone *et al.*, 2002), and microtubule-targeting drugs, such as Taxol, have the potential to modulate these pathways. One well-documented example of a signaling pathway that interacts with microtubules is the extracellular signal-regulated kinase (ERK1 and 2), a component of the mitogen-activated protein kinase (MAPK) family. We and others have documented activation of the ERK-signaling cascade in response to microtubule disruption (Shinohara-Gotoh *et al.*, 1991; Schmid-Alliana *et al.*, 1998; McDaid and Horwitz, 2001). In fact, we have demonstrated additivity between Taxol and MEK inhibition, utilizing a commercially available MEK inhibitor, U0126 (McDaid and Horwitz, 2001). Other groups have demonstrated similar findings with respect to Taxol and other drugs that induce MEK/ERK activation (e.g. UCN-01) (Dai *et al.*, 2001). Our study clearly demonstrated that it is the degree of activation of this signaling pathway that governs whether the interaction between Taxol and MEK inhibition is additive/synergistic, or antagonistic. The mechanism for the enhanced cytotoxic effects of Taxol in the presence of MEK inhibitors may be related to the repression of the survival-signaling function of the ERK/MEK pathway, and to enhanced microtubule polymerization, since it has been proposed that MAPK activation inhibits microtubule stabilization (Shinohara-Gotoh *et al.*, 1991).

Although Taxol has been shown to activate MAPK *in vitro*, there are currently no data available from patients treated with Taxol. However, a recent report has suggested that active MAPK is expressed in approximately 48% of primary human breast cancer tumors, and is potentially a marker of breast cancer metastasis since its expression is elevated in lymph node metastases (Adeyinka *et al.*, 2002). Since Taxol is FDA approved for the treatment of ovarian, breast and lung carcinomas, it may be possible to potentiate clinical responses in these disease types by combining Taxol-based chemotherapy with signal transduction inhibitors, including EGFR inhibitors and farnesyl transferase inhibitors that target oncogenic ras signaling. In this strategy, Taxol-based chemotherapy may have enhanced efficacy in patients who would otherwise respond poorly. This strategy is currently being investigated in current clinical trials (Tolcher, 2001; Esteva *et al.*, 2002; Forero *et al.*, 2002). Indeed, the FDA has approved the use of trastuzumab (the humanized anti-ErbB2 antibody) and Taxol as first-line treatment of ErbB2 (HER2)-overexpressing metastatic breast cancer, based on the results of a randomized phase III clinical trial, showing that this combination produced higher response rates and longer survival duration than treatment with chemotherapy alone (Slamon *et al.*, 2001). It has been demonstrated that ErbB2 overexpression inhibits Cdc2 activation and Taxol-induced cell death in breast cancer cells, via deregulation of the G2/M cell cycle checkpoint (Yu *et al.*, 1998), and more recently that ErbB2-overexpressing breast cancer cells and primary tumors have elevated levels of inhibitory phosphorylation of

Cdc2 on tyrosine (Y)15 (Tan *et al.*, 2002), providing a mechanistic rationale for the association between ErbB2 overexpression and Taxol resistance. As discussed previously, there may exist a novel relationship between oncogenic growth factor signaling, and the modulation of tubulin isotypes (Montgomery *et al.*, 2000), although this hypothesis will require validation in human tumors that express oncogenic forms of receptor tyrosine kinases. Interestingly, overexpression of EGFRvIII, a receptor variant of the EGFR gene that has the most common alteration of the EGFR gene, a deletion encompassing exons 2-7, is associated with constitutive activation of the pERK (Montgomery *et al.*, 1995) and phosphatidylinositol 3-kinase pathways (PI3k/AKT) (Moscatello *et al.*, 1998), consistent with increased cellular survival. It has recently been demonstrated that overexpression of a catalytically active subunit of PI3k in ovarian cancer cells confers Taxol resistance, which is reverted upon inhibition of the PI3k pathway utilizing a selective inhibitor (Hu *et al.*, 2002). Thus, aberrant expression of key signaling molecules required for the control of cellular survival may confer Taxol resistance, and one current focus of future chemotherapy in the treatment of cancer is the circumvention of this type of resistance, utilizing selective inhibitors of these proteins to increase drug sensitivity.

#### Taxol resistance in patients

Taxol, in combination with the platinum agents, has been accepted as the standard chemotherapy in patients with advanced ovarian cancer. This combination has also shown activity in patients with breast and non-small-cell lung cancer. Despite the clinical success of Taxol in treating a number of solid malignancies, several disease types are intrinsically resistant to the drug, notably gastrointestinal tumors, thereby limiting its therapeutic applications. It is thought that the high expression of P-glycoprotein in the gastrointestinal tract mediates Taxol resistance. This supposition has been supported by the observation that patients with advanced colorectal tumors have demonstrated clinical responses to epothilone B, which is not a substrate for P-glycoprotein (Calvert *et al.*, 2001).

The majority of patients with advanced cancer eventually develop progressive disease after initially responding to Taxol treatment. Drug resistance, whether intrinsic or acquired, represents a major obstacle in improving the response and survival of cancer patients, and these problems related to resistance have motivated a search for novel antimitotic agents that have the potential to improve the Taxol prototype. The ideal Taxol prototype would display activity in a broad range of malignancies, have manageable toxicities, a reduced propensity for acquired clinical resistance, and ideally produce an enhanced degree and duration of antitumor response. The epothilones and discodermolide, both of which are being evaluated in clinical trials, fulfill some of these criteria, although their toxicity profiles are



still being assessed and it remains to be seen if they will attain the same clinical success as Taxol.

#### *Alterations in tubulin isotype composition in tumors*

An analysis of  $\beta$ -tubulin isotype expression levels in Taxol-sensitive and-resistant human ovarian epithelial tumors by RT-PCR was undertaken (Kavallaris *et al.*, 1997). Resistance to Taxol was defined as disease progression during treatment, or relapse within 6 months following treatment. Taxol-resistant ovarian tumor samples displayed significant increases in class I (3.6-fold), class III (4.4-fold), and class IVa (7.6-fold)  $\beta$ -tubulin compared to primary untreated ovarian tumors. In contrast, no correlation was observed between  $\beta$ -tubulin mRNA expression and Taxol sensitivity in mouse xenografts established from 12 human ovarian carcinomas taken before or after the initiation of Taxol treatment (Nicoletti *et al.*, 2001).

#### *Tubulin mutations in human tumors*

A recent study identified  $\beta$ -tubulin mutations in serum DNA isolated from 33% of patients with non-small-cell lung cancer (Monzo *et al.*, 1999). This finding was considered extremely significant, since it validated *in vitro* data from numerous laboratories documenting the acquisition of mutations in Taxol- and epothilone-resistant cell lines that correlated with increasing levels of resistance. Moreover, this report suggested a relationship between the location of the mutations on  $\beta$ -tubulin and response to Taxol-based chemotherapy, since patients with and without mutations had dramatic differences in median survival, a finding, which if validated, would have profound implications in determining treatment options for patients with NCSLC. Several groups sought to confirm this initial study; however, the results have not been corroborated in these prospective studies (Kelley *et al.*, 2001; Kohonen-Corish *et al.*, 2002; Sale *et al.*, 2002; Tsurutani *et al.*, 2002), although silent polymorphisms have been reported. A recent study analysing 62 human breast cancer tumors also concluded a lack of  $\beta$ -tubulin mutations in these tumors, and documented the presence of a silent polymorphism at codon 217 (Hasegawa *et al.*, 2002). All of these studies addressed the issue of concomitant amplification of tubulin pseudogenes during the analyses, an artifact that appears to be circumvented by cDNA sequencing (Tsurutani *et al.*, 2002). We have identified a unique polymorphism, utilizing cDNA sequencing, at the extreme C-terminus of  $\beta$ -tubulin in a patient with advanced breast cancer (McDaid *et al.*, 2002). This patient had a partial response to BMS-247550, an epothilone B analog currently in clinical development, although the relevance of this polymorphism to her response is unknown. In addition, a Taxol-resistant cell line that harbors a mutation in  $\alpha$ -tubulin has recently been identified (Martello *et al.*, 2003), suggesting that nucleotide alterations may not be confined to  $\beta$ -tubulin, but may arise in multiple locations, resulting

in perturbation of normal microtubule function. Therefore, the prevalence of sequence variants of tubulin in human tumors, and the relevance, if any, of these variants to response to Taxol-directed chemotherapy is still a subject of debate.

The study by Monzo *et al.* utilized genomic DNA that was extracted from circulating tumor DNA isolated from patient serum samples. The  $\beta$ -tubulin gene has many pseudogenes, seven of which have been reported to date (Wilde *et al.*, 1982a, b; Lee *et al.*, 1983). The existence of pseudogenes makes it difficult to analyse the precise nucleotide sequence of  $\beta$ -tubulin using genomic DNA. One report (Tsurutani *et al.*, 2002) has documented the amplification of nonspecific nucleotide sequences in  $\beta$ -tubulin, depending on whether genomic DNA or cDNA is utilized. There is also the possibility that circulating tumor DNA may have additional nucleotide alterations compared to DNA from a primary tumor, due to the clonal expansion of tumor cells and the metastatic process. However, whether these micrometastases give rise to secondary tumors that may have tubulin alterations remains to be determined. Owing to the potential clinical relevance of sequence variants in tubulin to microtubule-directed chemotherapy, a sensible recommendation for future studies would be to carry out a systematic analysis of the genetic basis of these nucleotide alterations, utilizing rigorous strategies that eliminate the possibility of detecting pseudogenes.

#### *Tubulin-microtubule-regulatory proteins in human cancers*

Stathmin mRNA levels are known to be upregulated in breast carcinoma cells from patients with more aggressive disease, and in acute leukemias, lymphomas and various carcinomas (Hanash *et al.*, 1988; Nylander *et al.*, 1995; Bieche *et al.*, 1998; Curmi *et al.*, 2000). In the case of MAP4, a recent phase I clinical study of sequential doxorubicin/vinorelbine indicated partial correlation with induction of p53 and decreased MAP4 expression in peripheral blood mononuclear cells and in tumors (Bash-Babula *et al.*, 2002).

#### **Summary**

Acquired Taxol resistance may be mediated by a number of putative mechanisms, based on data accrued from the selection of cells with Taxol *in vitro*. These include, but are not limited to, overexpression of P-glycoprotein, alterations in tubulin and aberrant signal transduction pathways and/or cell death pathways. The real contribution of these potential mechanisms is ultimately dependent on the extent of dysregulation of normal cellular integrity in cancer cells. As our knowledge of drug resistance increases, based on *in vitro* models in resistant cells, it is apparent that there are multiple mechanisms responsible for the resistant phenotype in cells cultured *in vitro*. The contribution of the various drug-resistant phenotypes to acquired

Taxol resistance in actual human tumors has yet to be precisely defined.

# Acknowledgements

We thank our many colleagues, who have worked with us over the years, for their interest and contributions to studies on drug resistance. This work was supported in part by USPHS

Grants CA 39821 (SBH), CA 77263 (SBH) and the National Foundation for Cancer Research (SBH), AI49749 (GAO) and Department of Defence Breast Cancer Research Program DAMD17-01-0123 (GAO). H.M.D. was supported by post-doctoral fellowship 99-3054 from the Susan B. Komen foundation.

# References

- Adeyinka A, Nui Y, Cherlet T, Snell L, Watson PH and Murphy LC. (2002). *Clin. Cancer Res.*, **8**, 1747-1753.
- Banerjee A and Kasmala LT. (1998). *Biochem. Biophys. Res. Commun.*, **245**, 349-351.
- Banerjee A, Roach MC, Trcka P and Luduena RF. (1990). *J. Biol. Chem.*, **265**, 1794-1799.
- Banerjee A, Roach MC, Trcka P and Luduena RF. (1992). *J. Biol. Chem.*, **267**, 5625-5630.
- Bash-Babula J, Toppmeyer D, Labassi M, Reidy J, Orlick M, Senzon R, Alli E, Kearney T, August D, Shih W, Yang JM and Hait WN. (2002). *Clin. Cancer Res.*, **8**, 1057-1064.
- Belmont LD and Mitchison TJ. (1996). *Cell*, **84**, 623-631.
- Bieche I, Lachkar S, Becette V, Cifuentes-Diaz C, Sobel A, Lidereau R and Curmi PA. (1998). *Br. J. Cancer*, **78**, 701-709.
- Blade K, Menick DR and Cabral F. (1999). *J. Cell Sci.*, **112** (Part 13), 2213-2221.
- Blagosklonny MV and Fofo T. (1999). *Int. J. Cancer*, **83**, 151-156.
- Bobinnec Y, Moudjou M, Fouquet JP, Desbruyeres E, Edde B and Bornens M. (1998). *Cell Motil. Cytoskeleton*, **39**, 223-232.
- Bode CJ, Gupta Jr ML, Reiff EA, Suprenant KA, Georg GI and Himes RH. (2002). *Biochemistry*, **41**, 3870-3874.
- Bollag DM, McQueney PA, Zhu J, Hensens O, Koupal L, Liesch J, Goetz M, Lazarides E and Woods CM. (1995). *Cancer Res.*, **55**, 2325-2333.
- Bonnet C, Boucher D, Lazereg S, Pedrotti B, Islam K, Denoulet P and Larcher JC. (2001). *J. Biol. Chem.*, **276**, 12839-12848.
- Boucher D, Larcher JC, Gros F and Denoulet P. (1994). *Biochemistry*, **33**, 12471-12477.
- Burkhardt CA, Kavallaris M and Band Horwitz S. (2001). *Biochim. Biophys. Acta*, **1471**, O1-O9.
- Cabral F and Barlow SB. (1989). *FASEB J.*, **3**, 1593-1599.
- Cabral FR, Brady RC and Schibler MJ. (1986). *Ann. N.Y. Acad. Sci.*, **466**, 745-756.
- Calvert PM, O'Neill V, Twelves C, Azzabi A, Hughes A, Bale C, Robinson A, Machan M, Dimitrijevic S, Moss D, Rothermel J, Cohen P, Chen T, Man A and Calvert A. (2001). *Proc. Am. Soc. Clin. Oncol.*, **20** (Abstract 429).
- Cardone L, de Cristofaro T, Affaitati A, Garbi C, Ginsberg MD, Saviano M, Varrone S, Rubin CS, Gottesman ME, Avvedimento EV and Feliciello A. (2002). *J. Mol. Biol.*, **320**, 663-675.
- Carles G, Braguer D, Dumontet C, Bourgarel V, Goncalves A, Sarrazin M, Rognoni JB and Briand C. (1999). *Br. J. Cancer*, **80**, 1162-1168.
- Cassimeris L. (2002). *Curr. Opin. Cell Biol.*, **14**, 18-24.
- Chang W, Gruber D, Chari S, Kitazawa H, Hamazumi Y, Hisanaga S and Bulinski JC. (2001). *J. Cell Sci.*, **114**, 2879-2887.
- Chapin SJ, Lue CM, Yu MT and Bulinski JC. (1995). *Biochemistry*, **34**, 2289-2301.
- Chen JG and Horwitz SB. (2002). *Cancer Res.*, **62**, 1935-1938.
- Curmi PA, Nogues C, Lachkar S, Carelle N, Gonthier MP, Sobel A, Lidereau R and Bieche I. (2000). *Br. J. Cancer*, **82**, 142-150.
- Dai Y, Yu C, Singh V, Tang L, Wang Z, McInistry R, Dent P and Grant S. (2001). *Cancer Res.*, **61**, 5106-5115.
- Derry WB, Wilson L and Jordan MA. (1995). *Biochemistry*, **34**, 2203-2211.
- Derry WB, Wilson L, Khan IA, Luduena RF and Jordan MA. (1997). *Biochemistry*, **36**, 3554-3562.
- Desai A and Mitchison TJ. (1997). *Annu. Rev. Cell Dev. Biol.*, **13**, 83-117.
- Detrich III HW, Parker SK, Williams Jr RC, Nogales E and Downing KH. (2000). *J. Biol. Chem.*, **275**, 37038-37047.
- Diaz JF and Andreu JM. (1993). *Biochemistry*, **32**, 2747-2755.
- Diaz JF, Valpuesta JM, Chacon P, Diakun G and Andreu JM. (1998). *J. Biol. Chem.*, **273**, 33803-33810.
- Downing KH. (2000). *Annu. Rev. Cell Dev. Biol.*, **16**, 89-111.
- Downing KH and Nogales E. (1998). *Eur. Biophys. J.*, **27**, 431-436.
- Drukman S and Kavallaris M. (2002). *Int. J. Oncol.*, **21**, 621-628.
- Dumontet C and Sikic BI. (1999). *J. Clin. Oncol.*, **17**, 1061-1070.
- Esteve FJ, Valero V, Booser D, Guerra LT, Murray JL, Pusztai L, Cristofanilli M, Arun B, Esmaili B, Fritsche HA, Sneige N, Smith TL and Hortobagyi GN. (2002). *J. Clin. Oncol.*, **20**, 1800-1808.
- Forero L, Patnaik A, Hammond LA, Tolcher A, Schwartz G, Hidalgo M, Malik S, Murphy T, Goetz A, Mays T, Kiene A, Hill M, DeBono JS, Beeram M, Forouzes B, Hao D, Zitelli A, Woods D, Nadler P and Rowinsky EK. (2002). *Proc. Am. Soc. Clin. Oncol.* (Abstract 1908).
- Giannakakou P, Gussio R, Nogales E, Downing KH, Zaharevitz D, Bollbuck B, Poy G, Sackett D, Nicolaou KC and Fojo T. (2000). *Proc. Natl. Acad. Sci. USA*, **97**, 2904-2909.
- Giannakakou P, Sackett DL, Kang YK, Zhan Z, Buters JT, Fojo T and Poruchynsky MS. (1997). *J. Biol. Chem.*, **272**, 17118-17125.
- Goncalves A, Braguer D, Kamath K, Martello L, Briand C, Horwitz S, Wilson L and Jordan MA. (2001). *Proc. Natl. Acad. Sci. USA*, **98**, 11737-11742.
- Gonzalez-Garay ML, Chang L, Blade K, Menick DR and Cabral F. (1999). *J. Biol. Chem.*, **274**, 23875-23882.
- Gottesman MM. (2002). *Annu. Rev. Med.*, **53**, 615-617.
- Gruber D, Faire K and Bulinski JC. (2001). *Cell Motil. Cytoskeleton*, **49**, 115-129.
- Gundersen GG and Cook TA. (1999). *Curr. Opin. Cell Biol.*, **11**, 81-94.
- Hamel E, Sackett DL, Vourloumis D and Nicolaou KC. (1999). *Biochemistry*, **38**, 5490-5498.
- Hanash SM, Strahler JR, Kuick R, Chu EH and Nichols D. (1988). *J. Biol. Chem.*, **263**, 12813-12815.
- Hasegawa S, Miyoshi Y, Egawa C, Ishitobi M, Tamaki Y, Monden M and Noguchi S. (2002). *Int. J. Cancer*, **101**, 46-51.

- He L, Jagtap PG, Kingston DG, Shen HJ, Orr GA and Horwitz SB. (2000). *Biochemistry*, **39**, 3972–3978.
- He L, Orr GA and Horwitz SB. (2001). *Drug Discov. Today*, **6**, 1153–1164.
- Hollenbeck P. (2001). *Curr. Biol.*, **11**, R820–R823.
- Horwitz SB. (1992). *Trends Pharmacol. Sci.*, **13**, 134–136.
- Horwitz SB, Lothstein L, Manfredi JJ, Mellado W, Parness J, Roy SN, Schiff PB, Sorbara L and Zeheb R. (1986). *Ann. N.Y. Acad. Sci.*, **466**, 733–744.
- Horwitz SB, Shen HJ, He L, Dittmar P, Neef R, Chen J and Schubart UK. (1997). *J. Biol. Chem.*, **272**, 8129–8132.
- Hu L, Hofmann J, Lu Y, Mills GB and Jaffe RB. (2002). *Cancer Res.*, **62**, 1087–1092.
- Hung DT, Chen J and Schreiber SL. (1996). *Chem. Biol.*, **3**, 287–293.
- Iancu C, Mistry SJ, Arkin S and Atweh GF. (2000). *Cancer Res.*, **60**, 3537–3541.
- Iancu C, Mistry SJ, Arkin S, Wallenstein S and Atweh GF. (2001). *J. Cell Sci.*, **114**, 909–916.
- Jaffrezou JP, Dumontet C, Derry WB, Duran G, Chen G, Tsuchiya E, Wilson L, Jordan MA and Sikic BI. (1995). *Oncol. Res.*, **7**, 517–527.
- Jordan MA, Toso RJ, Thrower D and Wilson L. (1993). *Proc. Natl. Acad. Sci. USA*, **90**, 9552–9556.
- Jordan MA and Wilson L. (1998). *Curr. Opin. Cell Biol.*, **10**, 123–130.
- Kavallaris M, Burkhardt CA and Horwitz SB. (1999). *Br. J. Cancer*, **80**, 1020–1025.
- Kavallaris M, Kuo DY, Burkhardt CA, Regl DL, Norris MD, Haber M and Horwitz SB. (1997). *J. Clin. Invest.*, **100**, 1282–1293.
- Kavallaris M, Tait AS, Walsh BJ, He L, Horwitz SB, Norris MD and Haber M. (2001). *Cancer Res.*, **61**, 5803–5809.
- Kelley MJ, Li S and Harpole DH. (2001). *J. Natl. Cancer Inst.*, **93**, 1886–1888.
- Khan IA and Luduena RF. (1996). *Biochemistry*, **35**, 3704–3711.
- Kohonen-Corish MR, Qin H, Daniel JJ, Cooper WA, Rivory L, McCaughan B, Millward MJ and Trent RJ. (2002). *Int. J. Cancer*, **101**, 398–399.
- Kowalski RJ, Giannakakou P, Gunasekera SP, Longley RE, Day BW and Hamel E. (1997). *Mol. Pharmacol.*, **52**, 613–622.
- Kyu-Ho Han E, Gehrke L, Tahir SK, Credo RB, Cherian SP, Sham H, Rosenberg SH and Ng S. (2000). *Eur. J. Cancer*, **36**, 1565–1571.
- Laferriere NB and Brown DL. (1996). *Cell Motil. Cytoskeleton*, **35**, 188–199.
- Larcher JC, Boucher D, Lazereg S, Gros F and Denoulet P. (1996). *J. Biol. Chem.*, **271**, 22117–22124.
- Larsson N, Segerman B, Gradin HM, Wandzioch E, Cassimeris L and Gullberg M. (1999). *Mol. Cell. Biol.*, **19**, 2242–2250.
- Lee MG, Lewis SA, Wilde CD and Cowan NJ. (1983). *Cell*, **33**, 477–487.
- Li Y, Poliks B, Cegelski L, Poliks M, Gryczynski Z, Piszczek G, Jagtap PG, Studelska DR, Kingston DG, Schaefer J and Bane S. (2000). *Biochemistry*, **39**, 281–291.
- Long BH, Carbone JM, Wasserman AJ, Cornell LA, Casazza AM, Jensen PR, Lindel T, Fenical W and Fairchild CR. (1998). *Cancer Res.*, **58**, 1111–1115.
- Lowe J and Amos LA. (1998). *Nature*, **391**, 203–206.
- Lowe J, Li H, Downing KH and Nogales E. (2001). *J. Mol. Biol.*, **313**, 1045–1057.
- Lu Q and Luduena RF. (1993). *Cell Struct. Funct.*, **18**, 173–182.
- Lu Q and Luduena RF. (1994). *J. Biol. Chem.*, **269**, 2041–2047.
- Luduena RF. (1998). *Int. Rev. Cytol.*, **178**, 207–275.
- MacRae TH. (1997). *Eur. J. Biochem.*, **244**, 265–278.
- Manfredi JJ, Parness J and Horwitz SB. (1982). *J. Cell Biol.*, **94**, 688–696.
- Marklund U, Larsson N, Gradin HM, Brattsand G and Gullberg M. (1996). *EMBO J.*, **15**, 5290–5298.
- Martello LA, McDaid HM, Regl DL, Yang CP, Meng D, Pettus TR, Kaufman MD, Arimoto H, Danishefsky SJ, Smith III AB and Horwitz SB. (2000). *Clin. Cancer Res.*, **6**, 1978–1987.
- Martello LA, Verdier-Pinard P, Shen H-J, He L, Torres K, Orr GA and Horwitz SB. (2003). *Cancer Res.*, **63**, 1207–1213.
- McDaid HM and Horwitz SB. (2001). *Mol. Pharmacol.*, **60**, 290–301.
- McDaid HM, Mani S, Shen HJ, Muggia F, Sonnichsen D and Horwitz SB. (2002). *Clin. Cancer Res.*, **8**, 2035–2043.
- Meurer-Grob P, Kasparian J and Wade RH. (2001). *Biochemistry*, **40**, 8000–8008.
- Minotti AM, Barlow SB and Cabral F. (1991). *J. Biol. Chem.*, **266**, 3987–3994.
- Montgomery RB, Guzman J, O'Rourke DM and Stahl WL. (2000). *J. Biol. Chem.*, **275**, 17358–17363.
- Montgomery RB, Moscatello DK, Wong AJ, Cooper JA and Stahl WL. (1995). *J. Biol. Chem.*, **270**, 30562–30566.
- Monzo M, Rosell R, Sanchez JJ, Lee JS, O'Brate A, Gonzalez-Larriba JL, Alberola V, Lorenzo JC, Nunez L, Ro JY and Martin C. (1999). *J. Clin. Oncol.*, **17**, 1786–1793.
- Moscatello DK, Holgado-Madruga M, Emlet DR, Montgomery RB and Wong AJ. (1998). *J. Biol. Chem.*, **273**, 200–206.
- Murphy M, Hinman A and Levine AJ. (1996). *Genes Dev.*, **10**, 2971–2980.
- Nicoletti MI, Valoti G, Giannakakou P, Zhan Z, Kim JH, Lucchini V, Landoni F, Mayo JG, Giavazzi R and Fojo T. (2001). *Clin. Cancer Res.*, **7**, 2912–2922.
- Nishio K, Nakamura T, Koh Y, Kanzawa F, Tamura T and Saijo N. (2001). *Cancer*, **91**, 1494–1499.
- Nogales E. (2000). *Annu. Rev. Biochem.*, **69**, 277–302.
- Nogales E, Whittaker M, Milligan RA and Downing KH. (1999). *Cell*, **96**, 79–88.
- Nogales E, Wolf SG and Downing KH. (1998). *Nature*, **391**, 199–203.
- Nylander K, Marklund U, Brattsand G, Gullberg M and Roos G. (1995). *Histochem. J.*, **27**, 155–160.
- Oakley BR. (2000). *Trends Cell Biol.*, **10**, 537–542.
- Ohta S, Nishio K, Kubota N, Ohmori T, Funayama Y, Ohira T, Nakajima H, Adachi M and Saijo N. (1994). *Jpn. J. Cancer Res.*, **85**, 290–297.
- Orr GA, Rao S, Swindell CS, Kingston DG and Horwitz SB. (1998). *Methods Enzymol.*, **298**, 238–252.
- Panda D, Miller HP, Banerjee A, Luduena RF and Wilson L. (1994). *Proc. Natl. Acad. Sci. USA*, **91**, 11358–11362.
- Parness J and Horwitz SB. (1981). *J. Cell Biol.*, **91**, 479–487.
- Poruchynsky MS, Giannakakou P, Ward Y, Bulinski JC, Telford WG, Robey RW and Fojo T. (2001). *Biochem. Pharmacol.*, **62**, 1469–1480.
- Pryor DE, O'Brate A, Bilcer G, Diaz JF, Wang Y, Kabaki M, Jung MK, Andreu JM, Ghosh AK, Giannakakou P and Hamel E. (2002). *Biochemistry*, **41**, 9109–9115.
- Ranganathan S, Benetatos CA, Colarusso PJ, Dexter DW and Hudes GR. (1998a). *Br. J. Cancer*, **77**, 562–566.
- Ranganathan S, Dexter DW, Benetatos CA and Hudes GR. (1998b). *Biochim. Biophys. Acta*, **1395**, 237–245.
- Ranganathan S, McCauley RA, Dexter DW and Hudes GR. (2001). *Br. J. Cancer*, **85**, 735–740.
- Rao S, Aberg F, Nieves E, Horwitz SB and Orr GA. (2001). *Biochemistry*, **40**, 2096–2103.

- Rao S, He L, Chakravarty S, Ojima I, Orr GA and Horwitz SB. (1999). *J. Biol. Chem.*, **274**, 37990–37994.
- Rao S, Horwitz SB and Ringel I. (1992). *J. Natl. Cancer Inst.*, **84**, 785–788.
- Rao S, Krauss NE, Heerding JM, Swindell CS, Ringel I, Orr GA and Horwitz SB. (1994). *J. Biol. Chem.*, **269**, 3132–3134.
- Rao S, Orr GA, Chaudhary AG, Kingston DG and Horwitz SB. (1995). *J. Biol. Chem.*, **270**, 20235–20238.
- Regnard C, Desbruyeres E, Denoulet P and Edde B. (1999). *J. Cell Sci.*, **112**, 4281–4289.
- Sale S, Oefner PJ and Sikic BI. (2002). *J. Natl. Cancer Inst.*, **94**, 776–777 (discussion 777).
- Schiff PB, Fant J and Horwitz SB. (1979). *Nature*, **277**, 665–667.
- Schiff PB and Horwitz SB. (1980). *Proc. Natl. Acad. Sci. USA*, **77**, 1561–1565.
- Schmid-Alliana A, Menou L, Manie S, Schmid-Antomarchi H, Millet MA, Giuriato S, Ferrua B and Rossi B. (1998). *J. Biol. Chem.*, **273**, 3394–3400.
- Sharp DJ, Rogers GC and Scholey JM. (2000). *Nature*, **407**, 41–47.
- Shinohara-Gotoh Y, Nishida E, Hoshi M and Sakai H. (1991). *Exp. Cell Res.*, **193**, 161–166.
- Slamon DJ, Leyland-Jones B, Shak S, Fuchs H, Paton V, Bajamonde A, Fleming T, Eiermann W, Wolter J, Pegram M, Baselga J and Norton L. (2001). *N. Engl. J. Med.*, **344**, 783–792.
- Snyder JP, Nettles JH, Cornett B, Downing KH and Nogales E. (2001). *Proc. Natl. Acad. Sci. USA*, **98**, 5312–5316.
- Stanchi F, Corso V, Scannapieco P, Ievolella C, Negrisolo E, Tiso N, Lanfranchi G and Valle G. (2000). *Biochem. Biophys. Res. Commun.*, **270**, 1111–1118.
- Sullivan KF and Cleveland DW. (1986). *Proc. Natl. Acad. Sci. USA*, **83**, 4327–4331.
- Tan M, Jing T, Lan KH, Neal CL, Li P, Lee S, Fang D, Nagata Y, Liu J, Arlinghaus R, Hung MC and Yu D. (2002). *Mol. Cell*, **9**, 993–1004.
- ter Haar E, Kowalski RJ, Hamel E, Lin CM, Longley RE, Gunasekera SP, Rosenkranz HS and Day BW. (1996). *Biochemistry*, **35**, 243–250.
- Tolcher AW. (2001). *Oncologist*, **6**, 40–44.
- Torres K and Horwitz SB. (1998). *Cancer Res.*, **58**, 3620–3626.
- Tsurutani J, Komiya T, Uejima H, Tada H, Syunichi N, Oka M, Kohno S, Fukuoka M and Nakagawa K. (2002). *Lung Cancer*, **35**, 11–16.
- Verdier-Pinard P, Wang F, Martello LA, Orr GA and Horwitz SB. (2003). *Biochemistry*, **42**, 5349–5357.
- Wilde CD, Crowther CE and Cowan NJ. (1982a). *Science*, **217**, 549.
- Wilde CD, Crowther CE, Cripe TP, Gwo-Shu Lee M and Cowan NJ. (1982b). *Nature*, **297**, 83–84.
- Wilson L and Jordan MA. (1995). *Chem. Biol.*, **2**, 569–573.
- Yu D, Jing T, Liu B, Yao J, Tan M, McDonnell TJ and Hung MC. (1998). *Mol. Cell*, **2**, 581–591.
- Zhang CC, Yang JM, Bash-Babula J, White E, Murphy M, Levine AJ and Hait WN. (1999). *Cancer Res.*, **59**, 3663–3670.
- Zhang CC, Yang JM, White E, Murphy M, Levine A and Hait WN. (1998). *Oncogene*, **16**, 1617–1624.